

michigan state university Libraries
3 1293 00908 7648

This is to certify that the

dissertation entitled

$\begin{array}{cccc} \text{VOLTAGE-DEPENDENT} & \text{CURRENTS OF } \underline{\text{SCHISTOSOMA}} & \underline{\text{MANSONI}} \\ & \text{MUSCLE FIBERS} \end{array}$

presented by

Timothy A. Day

has been accepted towards fulfillment of the requirements for

Ph.D. degree in Pharmacology & Toxicology

Date June 25, 1993

MSU is an Affirmative Action/Equal Opportunity Institution

0-12771

LIBRARY Michigan State University

PLACE IN RETURN BOX to remove this checkout from your record. TO AVOID FINES return on or before date due.

DATE DUE	DATE DUE	DATE DUE
		· .

MSU is An Affirmative Action/Equal Opportunity Institution c/circ/datedua.pm3-p.1

VOLTAGE-DEPENDENT CURRENTS OF SCHISTOSOMA MANSONI MUSCLE FIBERS

by

Timothy Allen Day

A DISSERTATION

Submitted to
Michigan State University
in partial fulfillment of requirements
for the degree of

DOCTOR OF PHILOSOPHY

Department of Pharmacology and Toxicology

1993

ABSTRACT

VOLTAGE-DEPENDENT CURRENTS OF SCHISTOSOMA MANSONI MUSCLE FIBERS

by

Timothy Allen Day

Individual muscle fibers acutely dissociated from the human parasite <u>Schistosoma mansoni</u> were studied in order to determine the nature of the voltage-dependent currents of the sarcolemma. These studies were performed on frayed contractile fibers which were morphologically distinct from a number of other types of contractile fibers that could be dispersed from the parasite.

Current clamp experiments revealed that the frayed fibers had a resting potential of \approx -22 mV. The fibers display a marked time-dependent outward rectification that was attenuated by the replacement of intracellular K⁺ with Cs⁺. Under these conditions, the fibers did not produce action potentials in response to depolarizing current injections, even if the outward rectification was blocked.

Voltage clamp experiments revealed that the frayed fibers have at least two distinct voltage-dependent K⁺ currents: a slow current which is in the delayed rectifier class and a fast current which is in the "A" class. The fibers did not show any voltage-dependent inward currents,

even when the outward currents were blocked, the fibers were bathed in high extracellular Ca²⁺ or Ba²⁺, hyperpolarizing prepulses were supplied before depolarization, and a variety of additives were supplied in the intracellular solution.

to my Mother, who instilled in me a love for science

ACKNOWLEDGEMENTS

Many thanks to Dr. Jim Bennett (Department of Pharmacology & Toxicology), my major professor!, for all of his efforts concerning my graduate education and this research. I would also like to express my sincere thanks to Dr. Ralph Pax (Department of Zoology) for all of the guidance that he has provided. Without their training and constant guidance (and patience and equipment and laboratory space, etc...), I would have been completely incapable of performing this research.

I would also like to thank committee members Dr. Peter Cobbett and Dr. Jim Galligan (Department of Pharmacology & Toxicology), each of whom provided important ideas at significant times in the course of this research. A special thanks also to Dr. Kevin Blair, who established much of the foundation on which this project was based. Finally, thanks to Mrs. Mary Lou Pax for all of the many contributions that she made to this project.

TABLE OF CONTENTS

LIST	OF	TABL	ES	•	•	•	•	•	•	•	•	•	•	•	•	•	•	•	•	•	•	•	•	ix
LIST	OF	FIGU	RES	•	•	•	•	•	•	•	•	•	•	•	•	•	•	•	•	•	•	•	•	×
ABBRI	EVI	ATION	s.	•	•	•	•	•		•	•	•	•	•	•	•	•	•	•	•	•	•		xiii
INTRO			•	•	•	•	•	•		•	•	•		•	•	•	•	•	•	•	•	•		1
	I.	Gene	ral	Ва	ac}	(gi	coi	ind	ìc	n	th	1e	Sc	chi	st	COS	501	ne	•		•	•		1
		A.	The	e s	sch	ris	sto	sc	me	a	ıs	а	рa	ara	ısi	ite	3	•		•	•		•	1
		В.	The	e s	sch	nis	sto	osc	me	a	as	a	pı	cin	ait	i	<i>j</i> e							
				inv																				2
	TT.	Bac	kar	our	nd	or	า 5	Sch	nis	sto	sc	ome	. 1	lus	ic]	le	•		_		•	•		5
			Gr																					5
		R.	Ind	div	zić	1112	3 T	mı	160	 ء 1 د		ans	•1 •+	· ·	,	•	•	٠	•	•	•	•	•	5 8
			Mus																					9
	TT1	r mi.	Mui -h-	2C1	. E	bī	1 y z) T C		93		•	.h-		•	•	•	•	•	•	•	•	•	10
	TTI	. Ti	anc.	-56	a I	LI	ec	OI	.uı	ruć	, ,	-ec	:111	ııç	lue	:5	•	•	•	•	•	•	•	10
OBJEC	CTIV	ÆS	• •	•	•	•	•	•	•	•	•	•	•	•	•	•	•	•	•	•	•	•	•	12
MATE	RIAI	LS AN	D M	ETH	IOI	S								•	•					•	•		•	14
	Τ.	Musc	le i	Dis	SDE	ers	sic	'n																14
		Des																						15
	III	Ele	ect	rop	ohy	, si	lol	Log	jic	al	. F	Rec	or	di	ng	, Is		•						23
				_																				
RESUI	LTS	• •	• •	•	•	•	•	•	•	•	•	•	•	•	•	•	•	•	•	•	•	•	•	26
		Pass:																						26
	II.	Cur	rent	t C	la	amp	o E	Exp	er	cin	aer	nts	3	•	•	•	•	•	•	•	•	•	•	30
		A.	Fil	ber	:s	di	sr	olā	١y	ου	itv	var	ď	re	ct	:if	ic	cat	ic	on	•	•		30
			Fil																					30
	TTI	. Vo																						36
			Two																				•	36
		***		1.																				36
				2.																				39
			Bot																					47
		ъ.	DO	111 111	Οι 	1 L V	vai	.u		ILI	. eı	165		TT C	1 :	\ 4	-50	. T.C	30 (1	CT /	<i>/</i> E	•	•	4,
		C.	Vo.																					
				cur																	•	•	•	55
				1.																				55
				2.																				56
		D.	Kir																					63
				1.																				63
			:	2.	ir	ac	ti	va	ıti	.or	ı k	cin	et	ic	s			•	•	•	•	•	•	67
				3																				70

TABLE OF CONTENTS (CONT'D)

RESULTS (cont'd)	
<pre>III. Voltage-Dependent Outward Currents (cont'd)</pre>	
E. Pharmacology of the outward currents	74
1. tetraethylammonium (TEA^+)	74
2. 4-aminopyridine (4-AP)	74
3. dendrotoxin (DTX)	79
IV. Voltage-Dependent Inward Currents	82
DISCUSSION	88
I. Mathematical Modeling	88
II. Classification of the Two Schistosome K+	
Currents	93
A. Delayed rectifier current	93
B. "A" current	94
III. Absence of Voltage-Dependent Inward Currents	94
V. Functions of the Delayed Rectifier Current . 1	02
A. General Delayed Rectifier Current	
	02
1. slow rectification:	
creating plateaus in	
	02
2. repolarization after action	
potential:	
controlling spike duration 1	.03
B. Consideration of the function of the	
delayed rectifier current in the	
schistosome muscle	.04
1. inactivation characteristics:	
the ability to provide	
	.05
2. activation rate:	
the ability to control	
spike duration	05
	.06
A. General "A" current functions 1	.06
1. fast rectification:	
delaying the initiation	
	.06
2. after-spike rectification:	
lengthening the	
	.08
3. repolarization after action	
potential:	
	09

TABLE OF CONTENTS (CONT'D)

DISCUSSION (cont'd)	
VI. Functions of the "A" Current (cont'd) B. Consideration of the function of the "A"	
current in the schistosome muscle 1. relationship between resting potential and V ₅₀ : the ability to provide rectification from the	110
resting potential	111
spike duration	115
SUMMARY	116
APPENDIX IPreparation of Dispersed Muscle Fibers from the Schistosome	119
APPENDIX IIComparison of Voltage-Dependent K ⁺ Current Properties	126
BIBLIOGRAPHY	133

LIST OF TABLES

Table	#		Pag	<u>e#</u>
Table	1.	Passive Properties of the Pipet and the Frayed Muscle Fibers in the Whole-Cell Configuration		27
Table	2.	Properties of the Two Voltage-Dependent K+ Currents of Schistosome Frayed Muscle Fibers		73
Table	3.	Variables Utilized for the Current Model in Figure 26		90
Table	4.	Primary Media Used in Various Isolation Procedures	•	125
Table	5.	Comparison of the Properties of Various Delayed Rectifier Currents	•	129
Table	6.	Comparison of the Properties of Various "A" Currents	•	131

LIST OF FIGURES

Figure #		Pa	ge	#
Figure 1.	Many consider flatworms to be the closest extant relatives of the common ancestor of the protostomes and the dueterostomes	•	•	4
Figure 2.	A syncytial tegument covers a thin layer of circular muscle and a thicker layer of longitudinal muscle in the adult schistosome	•	•	7
Figure 3.	The isolation procedure yields a wide variety of morphological cell types as well as a wide variety of debris	•	•	17
Figure 4.	Three morphological categories of contractile fibers can be reliably distinguished from the others	•	•	20
Figure 5.	Frayed fibers are contractile, very distinctive and can be very prevalent in the cell dispersion	•	•	22
Figure 6.	High resistance seals with the frayed fibers could be obtained routinely	•	•	29
Figure 7.	The frayed fibers display a time-dependent outward rectification .	•	•	32
Figure 8.	The frayed fibers do not display action potentials in response to depolarizing current injections	•	•	35
Figure 9.	Two distinct voltage-dependent outward currents are present in some fibers	•	•	38
Figure 10.	The two outward currents can be separated by manipulation of the prepulse potential	•	•	41

LIST OF FIGURES (CONT'D)

Figure	<u>#</u>		Pa	ge	#
Figure	11.	The larger voltage-dependent outward current activates slowly and inactivates very slowly	•	•	44
Figure	12.	The smaller voltage-dependent outward current activates rapidly and inactivates rapidly		•	46
Figure	13.	The reversal potential of the slow outward current depends on the extracellular $[K^+]$	•	•	49
Figure	14.	The slow outward current is K+-selective	•	•	51
Figure	15.	The reversal potential of the fast outward current coincides with the equilibrium potential for K^+	•	•	54
Figure	16.	The conductance of the slow outward current is dependent on the amplitude of the test potential and the holding potential	•	•	58
Figure	17.	The conductance of the fast outward current is dependent on the amplitude of the test potential and the holding potential	•	•	60
Figure	18.	The rate of activation is voltage-dependent for both the slow and the fast outward currents	•	•	65
Figure	19.	The rate of inactivation is voltage-independent for the slow outward current, but voltage-dependent for the fast outward current	•	•	69
Figure	20.	The rate of relaxation is voltage-dependent for the slow outward current	•	•	72
Figure	21.	The slow outward current is partially blocked by tetraethylammonium or 4-aminopyridine	•	•	76

LIST OF FIGURES (CONT'D)

Figure #		P	ag	e #
Figure 22.	The fast outward current is partially blocked by tetraethylammonium and is completely blocked by high concentrations of 4-aminopyridine	•	•	78
Figure 23.	The slow and fast outward currents are both insensitive to dendrotoxin	•	•	81
Figure 24.	Increased extracellular [Ca ²⁺] does not expose a voltage-dependent inward current nor does it alter the macroscopic outward current	•	•	84
Figure 25.	No voltage-dependent inward currents are evident when the outward currents are partially blocked by extracellular tetraethylammonium or completely attenuated by intracellular Cs ⁺	•	•	87
Figure 26.	The combined equation describing delayed rectifier and "A" current activation and inactivation is sufficient to model the macroscopic current of the fibers	•	•	92
Figure 27.	The frayed fibers contract in response to depolarization by high extracellular K^+	•	•	97

AT BS: DM: DT: ED: EG:

GTI HEF RPM TEA

ABBREVIATIONS

4-AP	4-amino pyridine
ATP	adenosine triphosphate
BSA	bovine serum albumin
DMEM	Dulbecco's Modified Eagle's Medium
DTX	dendrotoxin
EDTA	ethylenediamine tetraacetic acid
EGTA	ethyleneglycol-bis-(\beta-aminoethyl ether) N,N,N',N'-
	tetraacetic acid
GTP	quanosine triphosphate
HEPES	4-(2-hydroxyethyl)-1-piperazine ethanesulfonic acid
RPMI	Roswell Park Memorial Institute
TEA ⁺	tetraethylammonium ion

INTRODUCTION

I. GENERAL BACKGROUND ON THE SCHISTOSOME

A. THE SCHISTOSOME AS A PARASITE

The schistosome is the etiological agent of schistosomiasis, a disease that currently threatens over one-half billion people (Utroska et. al, 1989). Nearly 200 million humans are infected with schistosomes according to current estimates, with almost half of them being under 15 years of age. Between two and four million die as a result of schistosome infection each year, the largest portion of these being children.

The schistosome life cycle involves two parasitic and two free-living life stages, each of which must coordinate a series of complex behaviors. Appropriate muscle function is critical to the schistosome in each stage of its life cycle, including the adult forms which reside in the human mesenteric blood system. The adult schistosome utilizes muscles for migration within the host, for attachment at appropriate locations within the host, for a primitive digestive tract, for reproductive function, as well as other vital processes.

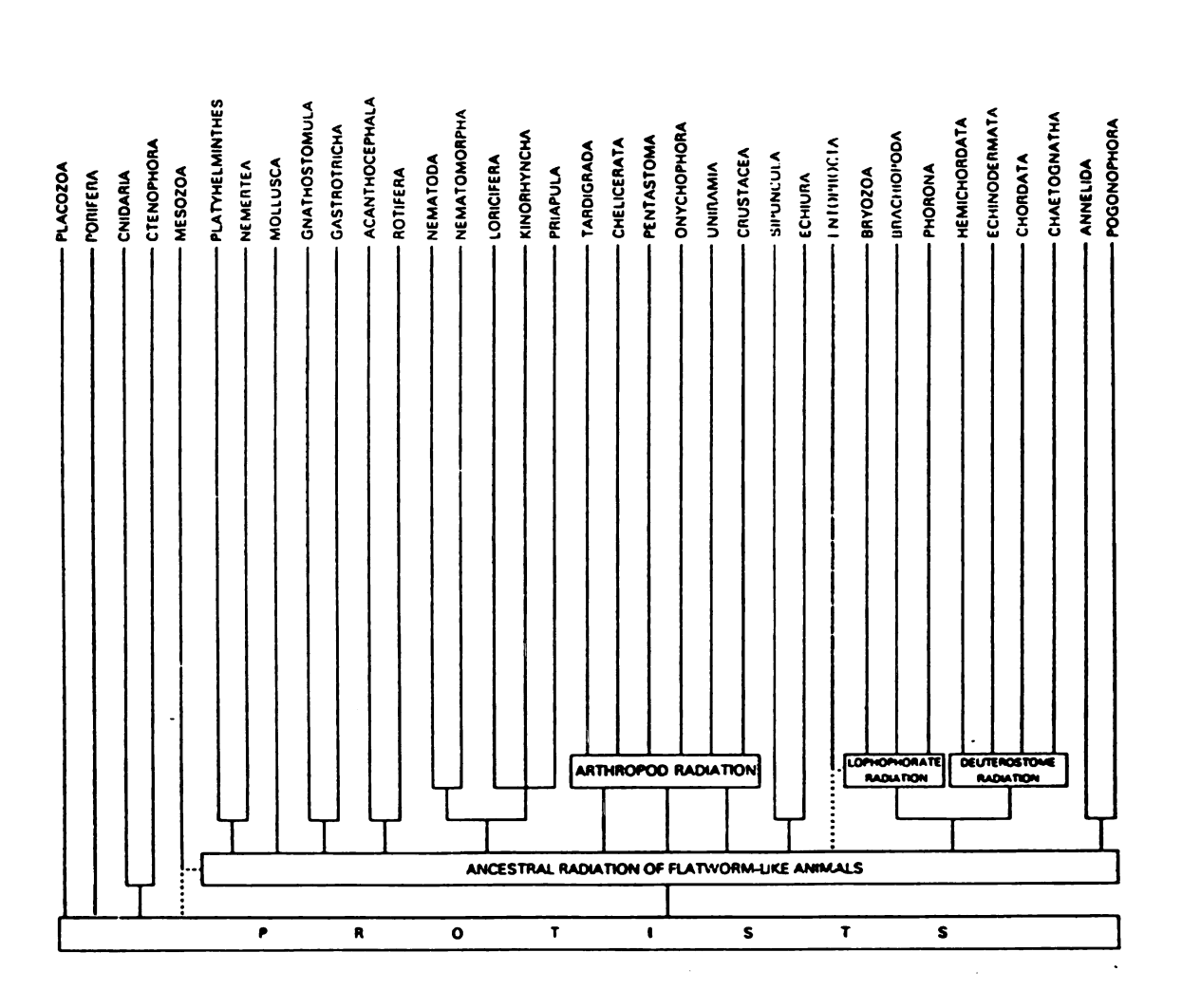
A large number of the anti-schistosomal drugs currently in use produce severe alterations of muscle function, such as metrifonate (Pax et al., 1981) or praziquantel (Fetterer, Pax & Bennett, 1980). The usefulness of these antiparasitic drugs lies, at least in part, in the drug's ability to exert an effect that is somewhat selective for the musculature of the parasite in comparison to the musculature of the host, most directly to the muscle of the vasculature of the host. Although much is known about the mechanisms by which contraction of mammalian vascular muscle is controlled, almost nothing is known about the mechanisms which control schistosome muscle, so the basis of the selectivity is not at all understood.

B. THE SCHISTOSOME AS A PRIMITIVE INVERTEBRATE

The schistosome is a platyhelminth (flatworm) and as such occupies an important position in the phylogenetic scheme. Flatworms are the most primitive animals that display bilateral symmetry, central cerebral ganglia, and neural components condensed into a central nervous system (Bullock & Horridge, 1965). Many consider them to be the closest extant relatives of the common ancestor of the protostomes and the deuterostomes (Figure 1), or the common stock from which all metazoan life evolved (Barnes, Calow & Olive, 1988). Although the details of muscle physiology are currently being elucidated in the more primitive radially

FIGURE 1. Many consider flatworms to be the closest extant relatives of the common ancestor of the protostomes and the dueterostomes. One suggested scheme depicting the radiations which produced the phyla of living animals (Barnes, Calow & Olive, 1988). The authors say, "Multicellular animals may have arisen from within the Protista from three to five or six times, to consider only those groups which have survived through to the present, but it is almost certainly from only one of these lines—the bilaterally symmetrical flatworms—that all other animal phyla have derived."

FIGURE 1



symmetrical coelenterates (Anderson, 1984; Dubas, Stein & Anderson, 1988), almost nothing is known about the muscle physiology of the platyhelminths.

II. BACKGROUND ON SCHISTOSOME MUSCLE

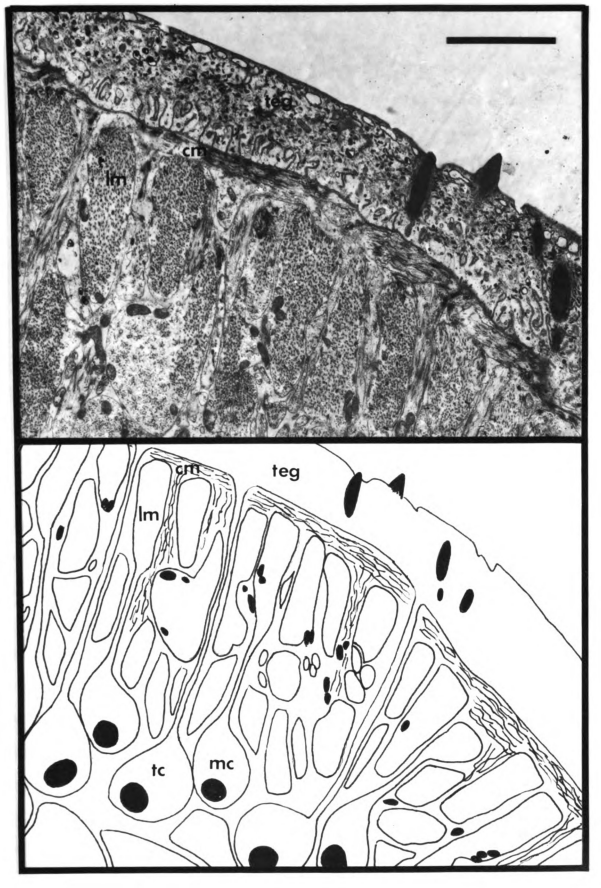
As mentioned, knowledge of how schistosomes, or flatworms in general, control their motor behavior is extremely limited. Direct information about the nature of events occurring at the level of the muscle cell membrane or the neuro-muscular junction does not exist. Even information about the anatomical relationships between nerves and the muscles is very sparse.

A. GROSS MUSCULAR ANATOMY

Several groupings of somatic muscle, such as circular, longitudinal, and oblique, have been identified in the schistosome (Silk & Spence, 1969a). The outermost feature of the schistosome is the tegument, which consists of an outer and an inner lipid bilayer surrounding a cytoplasm that is syncytial about the entire animal (Figure 2). A thin layer of circular muscle lies directly beneath the basement membrane of the tegument. Beneath the circular muscle lies a much thicker layer of longitudinal fibers, which constitute the bulk of the mass of schistosome muscle. A small number of oblique fibers, aligned in neither a circular nor longitudinal fashion, have also been

FIGURE 2. A syncytial tegument covers a thin layer of circular muscle and a thicker layer of longitudinal muscle in the adult schistosome. (Top) A micrograph showing the tegument and the underlying muscle layers. The circular muscle (cm) is the thin band of striations that lie directly beneath the basement membrane of the tegument (teg). longitudinal muscles (lm) lie beneath the circular muscle and are seen cut in cross-section, revealing the filament (Below) A schematic showing the relationship between muscle cytons and tegumental cytons. This schematic represents a wider angle view of the area in the micrograph above. The nuclei of the somatic muscle are not located in the contractile elements, rather in cell bodies called cytons (mc) which are buried deeper in the animal. Similarly, the nuclei which service the tegument are located in tegumental cytons (tc) that are adjacent to the muscle cytons and are coupled to them via gap junctions.

FIGURE 2



identified. Also present are transverse somatic muscles, which traverse the parenchyma, spanning the animal in a plane perpendicular to the dominant somatic muscle layers. The parenchyma, as well as digestive and reproductive structures, underlie the dominant somatic muscle layers.

B. INDIVIDUAL MUSCLE ANATOMY

In adult schistosomes, all muscle lacks the striations and the T-tubule arrangement of mammalian skeletal muscles. The individual longitudinal fibers are small (4-5 µm diameter), often have branching ends and are quite complex in their structure (Silk & Spence, 1969a). The contractile elements of the individual cells are located in the muscle layers as described above and are electrically coupled to the contractile elements of other fibers (Thompson, Pax & Bennett, 1982). However, the nucleus of the cell is contained in a distal cell body (cyton) that is connected to the contractile elements by one or more thin cytoplasmic bridges. The cell bodies are buried deeper in the animal, toward the parenchyma and are electrically coupled to neighboring cytons which serve other muscles and the tegumental cytoplasm. Although some synaptic junctions have been observed on the contractile fibers, they seem very rare (Silk & Spence, 1969b). Nothing is known about the nature of the input to the muscle in the schistosome, but speculation is that the muscles have non-contractile

cytoplasmic arms which extend toward the nervous system, since this has been demonstrated to be the case for other members of this phylum (Webb, 1987).

C. MUSCLE PHYSIOLOGY

Investigation of parasitic flatworm muscle physiology has been hampered by the inability to obtain a muscle preparation free of extraneous and interfering tissues on which controlled experiments can be performed (Pax & Bennett, 1992; Sukhdeo, 1992). As a result, studies of schistosome muscle control have centered on studies of the whole animal (Hillman, 1983; Pax et al., 1983).

In vitro, the schistosome displays fairly continuous, random, slow, rhythmic movements that are superimposed on a resting tone (Sukhdeo & Mettrick, 1987). Although this activity of the longitudinal somatic musculature is much like the spontaneous myogenic activity that is characteristic of many smooth muscles, it is not known if this activity is myogenic in these parasites.

The spontaneous motor activity can be altered by the exogenous application of a wide range of putative neurotransmitters, neurohormones and anthelmintics.

Acetylcholine is abundant in the nervous system of the schistosome and exogenous application of cholinergics or dopaminergics cause an inhibitory or relaxing effect to the longitudinal musculature (Tomosky, Bennett & Bueding, 1974).

Exogenous application of serotonin to the whole parasite increases both the force and the rate of motor activity (Barker, Bueding & Timms, 1966; Fetterer, Pax & Bennett, 1977). Although not synthesized by these parasites, schistosomes have a high-affinity uptake system for serotonin (Bennett & Bueding, 1973) and it is present throughout the nervous system (Bennett & Bueding, 1971).

Such studies involving the application of various compounds to intact worms have provided a wealth of information regarding the control of schistosome muscle in the whole worm, yet they cannot provide any conclusive evidence regarding the site of action of any of these agents nor can they provide any conclusive evidence as to what mechanisms of control are present in the muscles of schistosomes. Any action observed in the whole worm could be mediated by effects on sensory systems, on the central nervous system, on pre-synaptic transmitter release, or directly on the muscle.

III. TIGHT-SEAL RECORDING TECHNIQUES

Many of the limitations of interpretation imposed by these whole-animal studies can be avoided due to the recent development of a procedure for obtaining dispersed cells from schistosomes (Blair et al., 1991). The availability of individual muscle fibers provides the potential for the

dete musc

very micro

tight refer

to st

of io

cell volta

chann

chara

cell

to ide

a wide

cells

cells

Singer (Simmo

cells,

cells.

studie

their

the ph

determination how various treatments directly affect the muscle itself.

The individual schistosome muscle fibers are typically very small—too small for study with conventional microelectrode techniques. However, the development of tight—seal recording techniques (Hamill et al., 1981), often referred to as patch clamp techniques, have made it possible to study the electrophysiological properties and the nature of ion channels in such small cells.

Some of the most important descriptors of smooth muscle cell function are the complement and characteristics of the voltage-gated ion channels present. Voltage-gated ion channels mediate the currents that determine the characteristics of excitability in the fiber. The wholecell configuration of tight-seal recording has been utilized to identify and describe the voltage-gated ionic currents of a wide variety of muscle cells, including comb jelly muscle cells (Dubas, Stein & Anderson, 1988), arthropod muscle cells (Wu & Haugland, 1985), amphibian smooth (Walsh & Singer, 1987), striated (Stein & Palade, 1989) and cardiac (Simmons, Creazzo & Hartzell, 1986; Hume et al., 1986) muscle cells, as well as a wide selection of mammalian muscle cells. In each of these examples, and in every muscle studied to date, voltage-dependent currents are present and their characteristics play an important role in determining the physiology of the fibers.

OBJECTIVES

The general goal of the present study is to gain a better understanding of the physiology of individual schistosome muscle fibers. Such research has previously been limited by an inability to obtain a preparation of individual muscle fibers and the extremely small size of those individual fibers. I will be taking advantage of recent advances in our laboratory that have resulted in a specific protocol for the dispersion of individual contractile fibers from schistosomes (Blair et al., 1991). Further, I will be employing fairly recently-developed techniques for tight-seal, recording that make feasible the electrophysiological study of very small cells (Hamill et al., 1981).

Specifically, my goal will be to identify the major voltage-dependent currents of schistosome muscle fibers. Voltage-dependent currents have been found to be present in every type of muscle thus far examined and are a critical determinant for the function of those muscles. Included in my goals will be the characterization of any currents present in terms of their ionic selectivity, voltage-dependence, kinetic behavior and pharmacology. This will provide us with a better understanding of the possible roles

that

musc.

compa

prese

that these currents may be playing in normal schistosome muscle function, as well as providing a basis for relevant comparisons between the schistosome currents and those present in animals of other phyla.

MATERIALS AND METHODS

I. MUSCLE DISPERSION

The standard incubation medium for the muscles in these studies was a supplemented Dulbecco's Modified Eagle's Medium (DMEM, w/o Na₂HPO₄ or NaHCO₃, catalog no. 3656, Sigma, St. Louis, MO, USA). It consisted of the DMEM reduced to 67% of its usual concentration to which was added the following components: 2.2 mM CaCl₂, 2.7 mM MgSO₄, 0.04 mM Na₂HPO₄, 61.1 mM glucose, 1.0 mM dithiothreitol (DTT), 10 µM serotonin, 10 mg/ml pen-strep and 15 mM 4-(2-hydroxyethyl)-1-piperazine ethanesulfonic acid (HEPES) (pH 7.4); final measured osmolality, 290 mosm. With these modifications, the final concentrations of ions were, 4.1 mM K⁺, 82.6 mM Na⁺, 3.6 mM Ca²⁺, 3.3 mM Mg²⁺, 93.7 mM Cl⁻, 3.3 mM SO₄⁻, and 0.04 mM PO₄⁻ (the complete composition of this medium is listed in Table 4, Appendix I).

The parasites used as the source for the dispersed muscle fibers were adult <u>S. mansoni</u> (Puerto Rican strain) recovered 45-60 days post-infection from the portal and mesenteric veins of female Swiss Webster mice. Once recovered, the parasites were stored in the supplemented DMEM at 37.C. For the enzymatic digestion procedure, 20 to

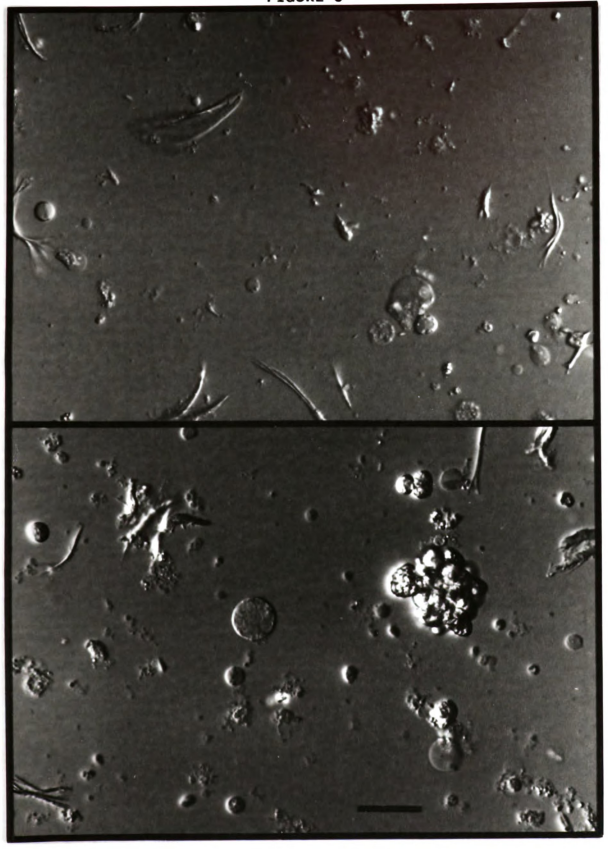
25 paired parasites were first placed on a glass microscope slide and coarsely chopped with a razor blade. resultant pieces were then incubated with gentle agitation on a shaker table for 45 min at 37 °C in the supplemented DMEM to which was added: 1 mM ethyleneglycol-bis-(Baminoethyl ether) N,N,N',N'-tetraacetic acid (EGTA), 1 mM ethylenediamine tetraacetic acid (EDTA), 0.1% bovine serum albumin, and 1 mg/ml papain (Sigma). After 45 min, the enzymatic medium was removed and the worm pieces were washed with three gentle exchanges of enzyme-free incubation medium and then incubated for an additional 10 min in the enzymefree supplemented DMEM. The worm pieces, still intact for the most part, were then broken up by forcing them back and forth through the orifice of a pasteur pipet 75 to 100 This process yielded a cell suspension which was then plated onto glass cover slips and allowed to settle for This resulted in the attachment of a large number of the fibers to the glass surface, at which point the unattached cells and debris were rinsed away with several exchanges of fresh culture medium.

II. DESCRIPTION OF THE PREPARATION

This procedure for the dispersion of <u>S. mansoni</u> cells yields a wide range of cell morphologies as well as cellular debris (Figure 3). Amongst the products of the preparation are numerous fibers which contract when exposed to elevated

FIGURE 3. The isolation procedure yields a wide variety of morphological cell types as well as a wide variety of debris. Two very typical examples of the product of the cell dispersion protocol. Noticeable in the milieu are a number of fibers and a number of more spherically-shaped entities as well as a large amount of debris. The scale bar is 25 μm .

FIGURE 3



extracellular K⁺. From amongst these contractile fibers, three morphological categories have emerged that can be reliably distinguished from the other cell types and from the debris (Figure 4).

In the first category (Figure 4, top) are fibers with bifurcated or fraved endings which are most frequently about 20 um in length (range 15-100 um). This type will be referred to as fraved fibers. Distinct from these are crescent-shaped fibers with concave sides that are characterized by numerous thin projections (Figure 4, middle). Their average length is 60 µm (range 30-200 µm), and they often occur in pairs, with the concave sides facing each other. The third category of contractile fibers are spindle-shaped and average 25 µm in length (range 15-120 um)(Figure 4, bottom). Spindles typically comprise less than 10 per cent of the fibers that can be classified into one of these three categories, and sometimes are not present at all. The frayed fibers and the crescent-shaped fibers are relatively more common, each constituting about 45 per cent of these fiber types. In every preparation there were a variety of contractile fibers that did not fit into any of these three categories.

The studies reported here will focus solely on the frayed fibers. Figure 5 shows a number of the frayed fibers and demonstrates how prevalent they can be in the dispersed cell preparation. Although data on the crescent- and

FIGURE 4. Three morphological categories of contractile fibers can be reliably distinguished from the others. Scanning electron micrograph of a frayed fiber (top) a crescent-shaped fiber (middle) and a spindle-shaped fiber (bottom). The scale bar in each micrograph is 10 μ m. These electron micrographs were supplied by Dr. Nailah Orr.

FIGURE 4

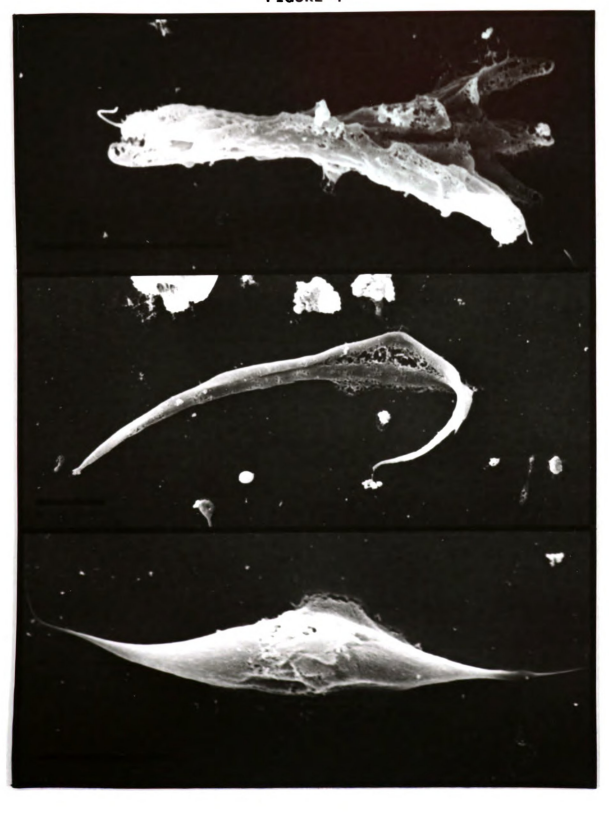
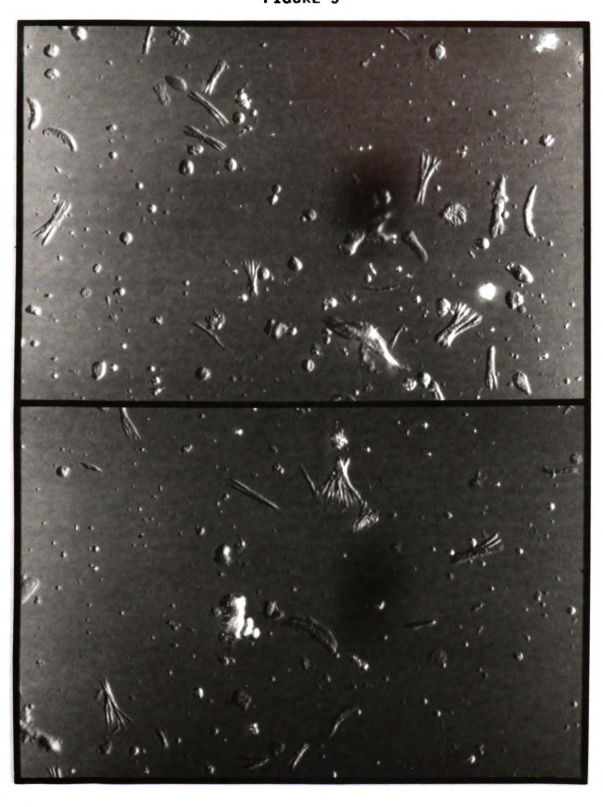


FIGURE 5. Frayed fibers are contractile, very distinctive and can be very prevalent in the cell dispersion. Examples of fields with many frayed fibers. It was not unusual to find many frayed fibers in a single microscopic field. Eight frayed fibers are present in the top example and five are present in the bottom example.

22

FIGURE 5



spindle-shaped contractile fibers is not included here, a general description of the voltage-dependent currents of all three types has been published (Day et al., 1993).

The frayed fibers may not be whole cells. In the intact animal, the contractile portion of the somatic muscles is connected to a distal cell body by a thin cytoplasmic bridge. It is likely that these bridges are severed in the dispersion process and the cell bodies are disconnected from the contractile fibers. Nuclei were not discernable in the frayed fibers with the nuclear stain bizbenzimide (Holy et al., 1989), but they were clearly discernable in many of the unidentified cell types. On rare occasions, the preparation yeilded some frayed fibers which may have been intact, whole cells. These fibers had a thin process which projected from the central portion of the fiber and terminated in a cell body-like structure. Despite the fact that most of the frayed fibers may not be whole cells, they will exclude trypan blue and will retain their morphology and contractility for at least 24 hrs. Further, larger pieces of undigested worm in the preparation contain meshwork of fibers very similar in morphology to the isolated frayed fibers.

III. ELECTROPHYSIOLOGICAL RECORDINGS

The standard extracellular bathing solution for the electrophysiological studies was an inorganic incubation

medium which consisted of 110 mM NaCl, 5.4 mM KCl, 0.4 mM MgCl₂, 2 mM EGTA and 20 mM Na-HEPES (pH=7.4). The standard pipet (intracellular) solution consisted of 120 mM KCl, 1 mM CaCl₂, 10 mM EGTA and 20 mM K-HEPES (pH=7.4). Any variance made from these standard media will be described specifically in the text with the pertinent experiments. All of the experiments were performed at room temperature.

Patch pipets were pulled from 1.2 mm outer diameter borosilicate glass using a two-stage vertical puller (Model PP83, Narashige USA, Inc., Greenvale, NY, USA) and were fire-polished by heated nichrome filament to resistances between 5-15 M Ω . When pipets of this size were used, 75% of attempts resulted in the formation of a high-resistance seals of ≥5 GN. Lower-resistance recording pipets resulted in a clear decrease in the probability of obtaining a highresistance seal with the fibers and higher resistance pipets tended to generate unacceptably high access resistances (see Part I of the Results section). Access resistance values were often high, due in large part to the need to use higher resistance pipets. Since high access resistance can give rise to error in the control of voltage when large currents are flowing, I did not include data from any fibers in which the access resistance value was greater than 30 M Ω or greater than three times the pipet resistance.

For several reasons, -40 mV was utilized as the standard holding potential for all of the fibers in the

volta
the m
peric
probat
studie
near 1982).
potent

Darmsta voltage at 7 kF

Muscle

A

interfa stored

current 5.5 soi

interfa

5.5. tin the

^{digita}]

t stand

voltage clamp experiments. Importantly, attempts to clamp the membrane voltage more negative than -40 mV for long periods of time resulted in a drastic increase in the probability of losing cell and/or seal resistance. Also, studies on intact schistosomes attribute a resting potential near -30 mV to the muscle in situ (Bricker, Pax & Bennett, 1982). Numerous other smooth muscle types report resting potentials near -40 mV, for example rabbit intestinal smooth muscle is -39 mV (Ohya et al., 1986), toad stomach smooth muscle is -40 mV (Singer & Walsh, 1980).

A List EPC-7 patch clamp amplifier (List Electronic, Darmstadt/Eberstadt, Germany) was used for current to voltage conversion and amplification. The data were aquired at 7 kHz and filtered at 3 kHz. The voltage signal was converted from analogue to digital using an Axon TL-1 DMA interface (Axon Instruments, Foster City, CA, USA) and stored directly to computer hard disk. Control voltages and currents were applied to the fibers with the use of pClamp 5.5 software (Axon Instruments) through the Axon TL-1 DMA interface. Data were analyzed with the assistance of pClamp 5.5. Unless otherwise noted, the current traces displayed in the figures are single iterations that have been digitally filtered at 0.5 ms. All statistics given are mean t standard deviation.

I. Pas

record:

0

must b

lower

Whiche

are li

T seal r

resist

genera

to obta

attempt

and/or

The ave

20 MΩ,]

access r

pipets w

RESULTS

I. PASSIVE PROPERTIES OF THE FIBERS

Of the first 85 attempts at tight-seal, whole-cell recording from the frayed fibers, 31 were successful as judged by the following two criteria: 1) seal resistance must be greater than 5 G Ω and 2) access resistance must be lower than 30 M Ω or three times the pipet resistance, whichever is less. Data from these 31 successful attempts are listed in Table 1.

Thirty-three of the initial 85 attempts resulted in seal resistances of less than 5 G Ω . The average pipet resistance for these 33 attempts was 1.5 M Ω , leading to the general conclusion that acceptable seals were more difficult to obtain when the pipets were too large. Twenty-one of the attempts resulted in access resistances greater than 30 M Ω and/or greater than three times the electrode resistance. The average pipet resistance for these 21 attempts was over 20 M Ω , leading to the general conclusion that acceptable access resistances were more difficult to obtain when the pipets were too small.

Passiv

was 10

T

utiliz

same c

were a

these

the fi

area ba

were qu

Üs

the for

became c

Certainl

producti

Penetrate

TABLE 1.

Passive Properties of the Pipet and the Frayed Muscle Fibers in the Whole-Cell Configuration.

Pipet Resistance $10 \pm 4 \text{ M}\Omega$ Seal Resistance $11 \pm 3 \text{ G}\Omega$ Access resistance $14 \pm 5 \text{ M}\Omega$ Cell capacitance $5.7 \pm 1.9 \text{ pF}$

The average pipet resistance for successful attempts was 10 ± 4 M Ω , so pipets ranging between 5-15 M Ω were utilized for the bulk of the remaining experiments and the same criteria regarding seal quality and access resistance were applied. The cell capacitance averaged 5.7 pF for these 33 fibers but, due to the extremely irregular shape of the fibers, it is fruitless to attempt to calculate membrane area based on this data.

Using pipets in the 5-15 M Ω range, the frayed fibers were quite amenable to tight-seal recording techniques and the formation of high-resistance seals with the fibers became quite routine, as detailed in the Figure 6 legend. Certainly, these tight-seal techniques were vastly more productive than my completely unsuccessful attempts to penetrate the fibers with microelectrodes.

FIGURE 6. High resistance seals with the frayed fibers could be obtained routinely. An example of an pipet with a resistance of $\approx\!10$ MN which had formed a seal of >5 GN with a frayed fiber. Such high-resistance seals were successfully obtained in 413 of the first 551 attempts with the frayed fibers, when pipets in the range of 5-15 MN were used. Whole-cell access was gained in approximately 70% of fibers successfully sealed. Of these, 60% remained stable for a sufficient period of time to obtain voltage or current clamp recordings.

FIGURE 6



II. Cų

A. FIB

used t

restin

showed

I

fibers

hyperpo

state d

-117600

membran

steady-

rectifi

the ave

 $ext{depend}\epsilon$

times g

B. FIBE

Th action

[Cd₅₊]

depende:

II. CURRENT CLAMP EXPERIMENTS

A. FIBERS DISPLAY OUTWARD RECTIFICATION

The tight-seal, whole-cell current clamp technique was used to record membrane voltage changes in response to applied currents. When the current was clamped to zero and resting membrane potentials monitored, the frayed fibers showed a resting membrane potential of -22 ± 3 mV (n=33).

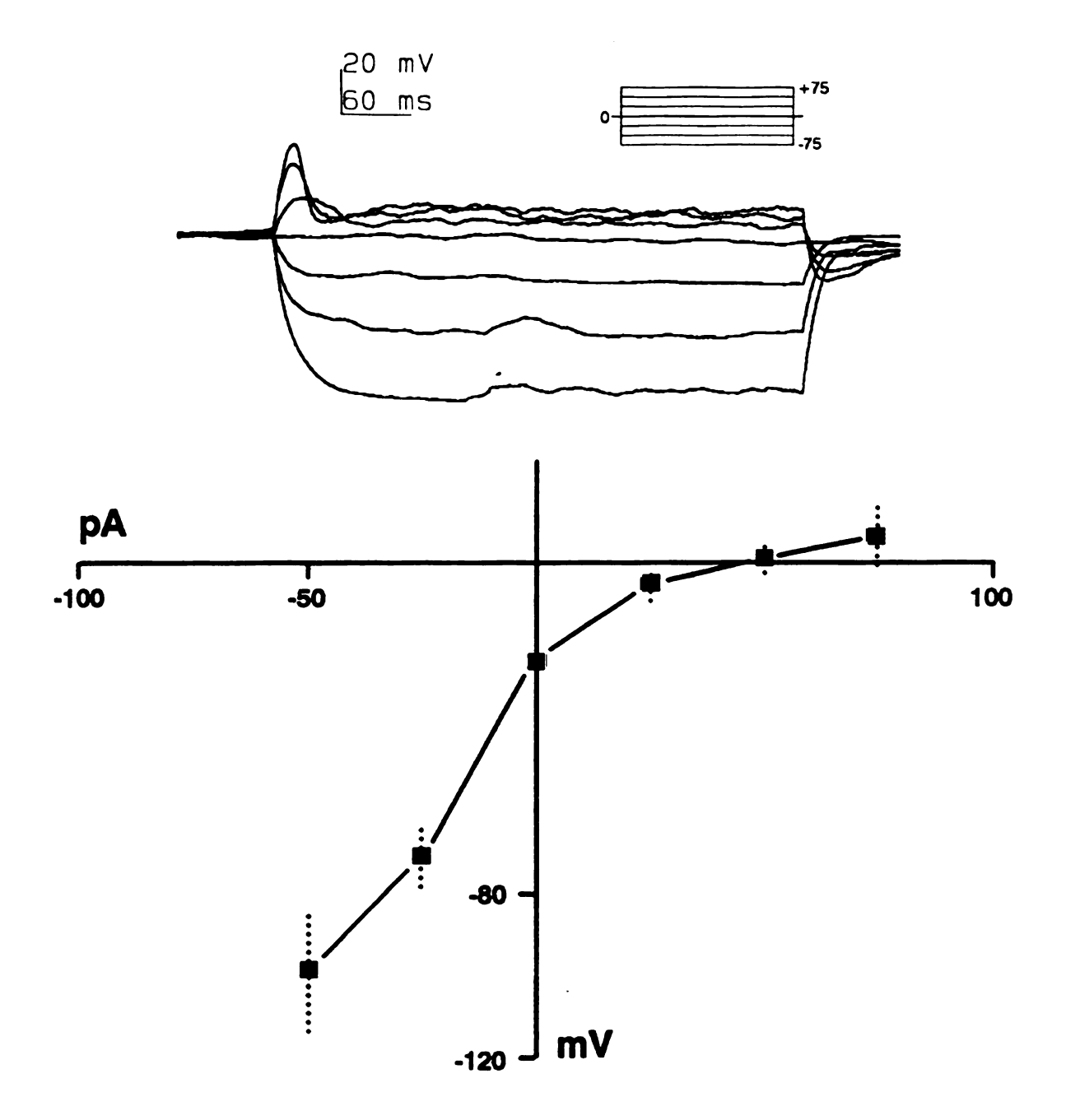
Injected current flowed much more easily out of the fibers than it did into the fibers. The injection of hyperpolarizing current injections produced a linear steady-state change in membrane voltage. Depolarizing current injections were accompanied by a time-dependent increase in membrane conductance and, therefore, produced a smaller steady-state change in voltage (Figure 7). This outward rectification was essentially the same in every fiber, with the average steady-state input conductance (after time-dependent rectification) to positive currents being over six times greater than the input conductance to negative currents (Figure 7).

B. FIBERS DO NOT DISPLAY ACTION POTENTIALS

The injection of depolarizing current did not induce action potentials in any of the fibers tested when the [Ca²⁺] in the extracellular medium was 0.4 mM. The time-dependent outward rectification of the schistosome fibers

FIGURE 7. The fraved fibers display a time-dependent outward rectification. (Above) An example of the voltage responses of a single frayed fiber to current injections. The depolarizing current injections elicited a timedependent decrease in membrane resistance and, therefore, a (Below) The average voltage vs. smaller voltage excursion. current relationship for the fraved fibers. There is no data point displayed for the -75 pA injection, because the membrane typically became rather unstable in response to such current injection, even though that is not the case for the example shown above. Steady-state voltage levels were used for the V-I relationship and were obtained as averages of the values between 250 and 300 ms after the initiation of the current injection. A best fit of the points from 0 to -50 pA yielded a conductance of 0.6 nS (a resistance of 1514 $M\Omega$), while the points from +25 to +75 mV yielded a conductance of 4.1 nS (a resistance of 244 M Ω) (n=13).

FIGURE 7



w:

ar (1

(]

c)

sc (I

ir hy

ms ac

ir

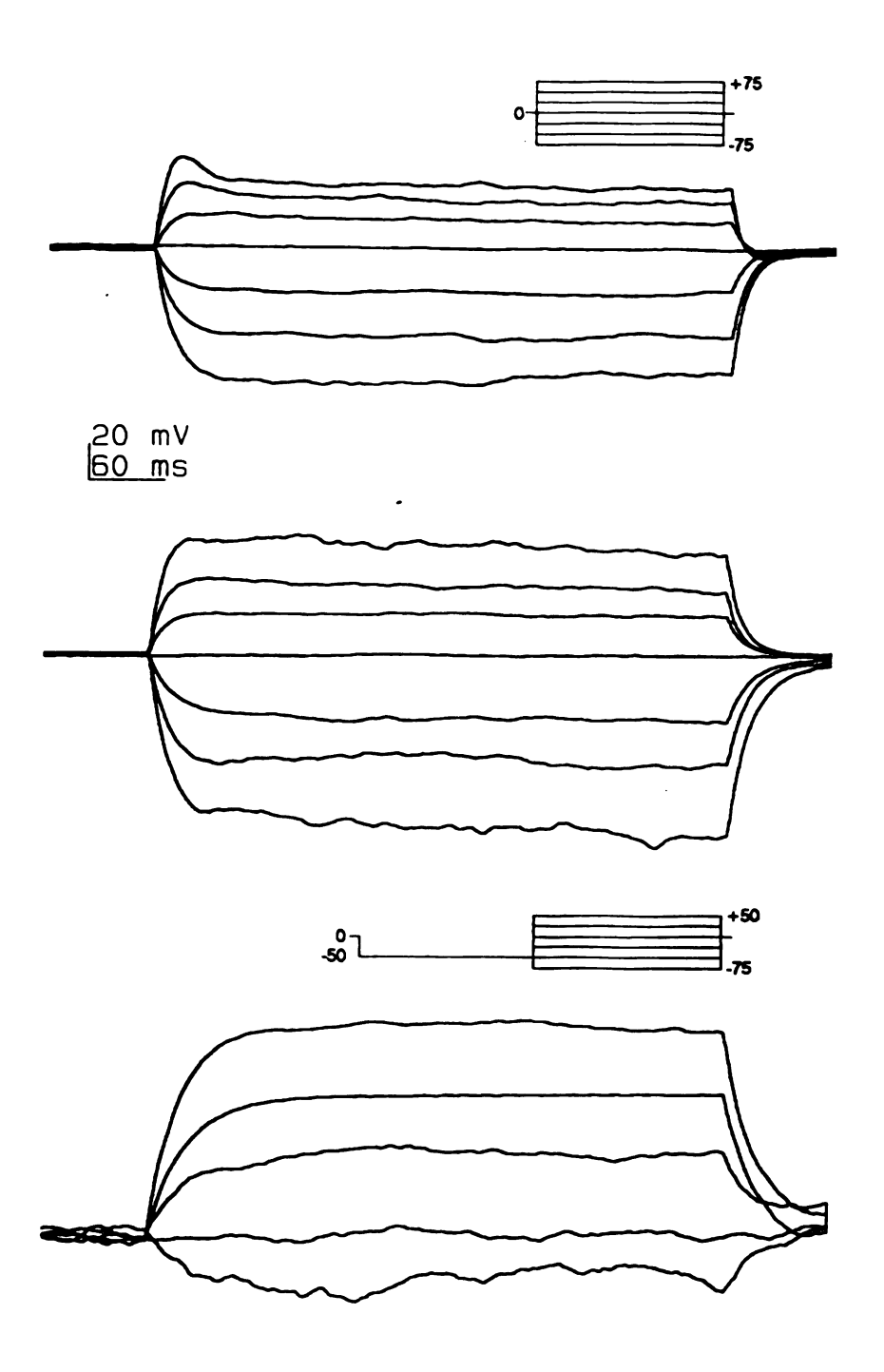
f c

6>

was only partially blocked and no action potentials were evident even when the 110 mM Na+ of the extracellular bath was completely replaced by 110 mM tetraethylammonium (TEA+) (Figure 8), even though TEA+ blocks outward rectification and unmasks action potentials in some muscle cell types (Fatt & Katz, 1953). The outward rectification was almost completely blocked when Cs+, which is impermeant to most K+ channels, was substituted for K+ in the intracellular solution, but action potentials were still not evident (Figure 8). Also, to overcome any possible steady-state inactivation of voltage-gated channels, some fibers were hyperpolarized to potentials near -70 mV by applying a 450 ms, -25 pA prepulse, yet these fibers still did not produce action potentials when depolarized. Additionally, an increase in extracellular Ca2+ concentration of over 100fold (from 0.4 mm to 50 mm) did not elicit action potentials even when applied in combination with any or all the experimental treatments discussed above (Figure 8).

FIGURE 8. The frayed fibers do not display action potentials in response to depolarizing current injections. (Top) An example of voltage responses from a frayed fiber in 120 mM extracellular TEA+. In these experiments, all of the Na in the extracellular medium was replaced with the general K+ channel blocker TEA+. The time-dependent outward rectification was only partially blocked and no action potentials were unmasked. (Middle) An example of voltage responses from a frayed fiber with 130 mM intracellular Cs+. All of the K⁺ in the intracellular medium was replaced with Cs+, which is impermeant to most K+ channels. The timedependent outward rectification was almost completely abrogated, but action potentials were still not elicited. The largest depolarizing current injections produced a depolarization to +40 mV in this fiber. (Bottom) An example of voltage responses from a frayed fiber with 130 mM intracellular Cs+, 70 mm TEA+ and 50 mm Ca2+ in the extracellular medium and a 150 ms, -50 pA hyperpolarizing prepulse. Again, all of the K+ in the intracellular medium was replaced with Cs+, and the Na+ in the extracellular medium was replaced with TEA+ and Ca2+. This fiber had a resting potential of -22 mV under these ionic conditions and the hyperpolarizing prepulse held the potential near -80 mV. Even with outward rectification blocked, increased extracellular Ca2+ and a hyperpolarizing prepulse, no action potentials were generated in response to the depolarizing current injections.

FIGURE 8



III

A.

VO

pc re

fi

ת

С

)

III. VOLTAGE-DEPENDENT OUTWARD CURRENTS

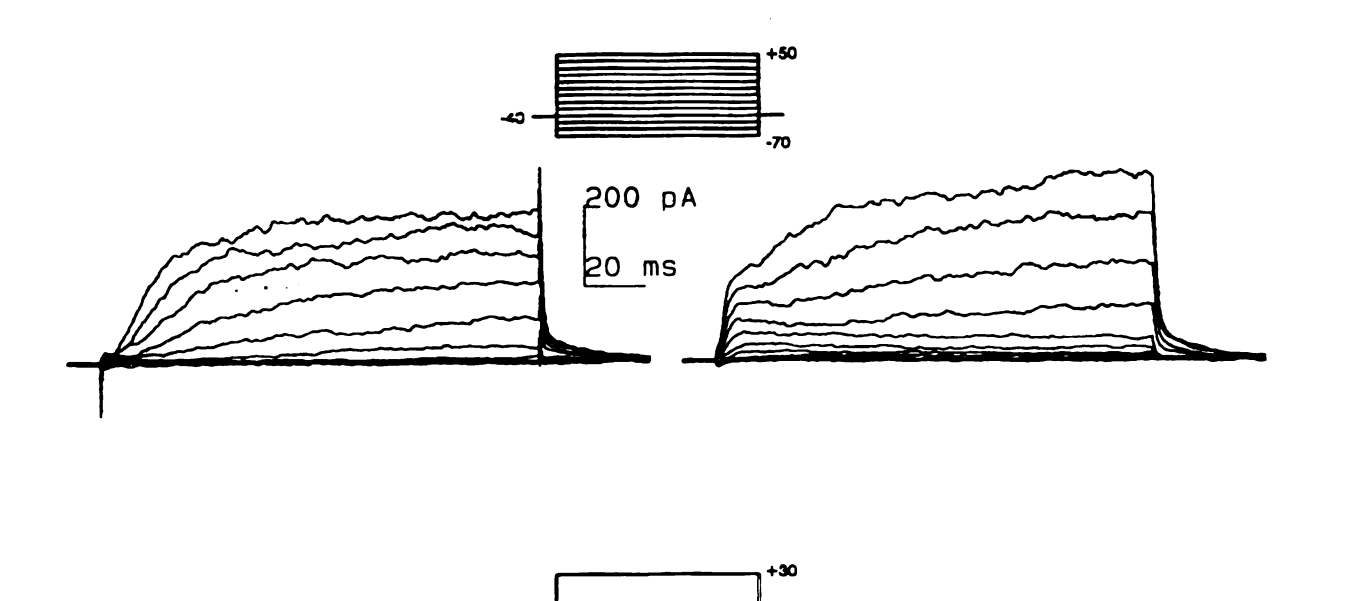
A. Two distinct outward currents are present

1. RECOGNITION OF TWO CURRENTS

The schistosome muscle fibers displayed a profile of voltage-dependent currents which was dominated by a relatively large net outward current that activates at test potentials near -10 mV. When the test pulses were applied from a -40 mV holding potential, some of the fibers had a net outward current which appeared to have only a single component (Figure 9). In these cases, the rising phase of the net outward current was fit very well by Hodgkin-Huxley kinetic equations (see Part D of this section for further elaboration). No inactivation of this net outward current occurred within the span of the 150 ms test pulse. Other fibers, however, had two components to the rising phase of the net outward current. In these examples, the n² power function did not fit the data as well, and a visual inspection of the fit revealed a smaller component of the net outward current which was activating markedly faster than the component that was described by the power function, creating the appearance of a "shoulder" on the rising current (Figure 9).

FIGURE 9. Two distinct voltage-dependent outward currents are present in some fibers. (Top left) An example of the net outward current from a fiber that appeared to have only a single component and (top right) a fiber that had an additional fast-rising "shoulder". The conditions were identical for these two recordings. (Bottom) A direct comparison of the current responses of these two fibers. The respective responses to the +30 mV step are superimposed in order to clarify the difference in the responses of the two fibers. The difference suggests the presence of two outward currents in the fiber with the more complex current profile.

FIGURE 9



100 pA 20 ms

ti p m:

> po in cu

e: d:

d: t:

S

IJ,

w p

a O

n

t

W

Ci

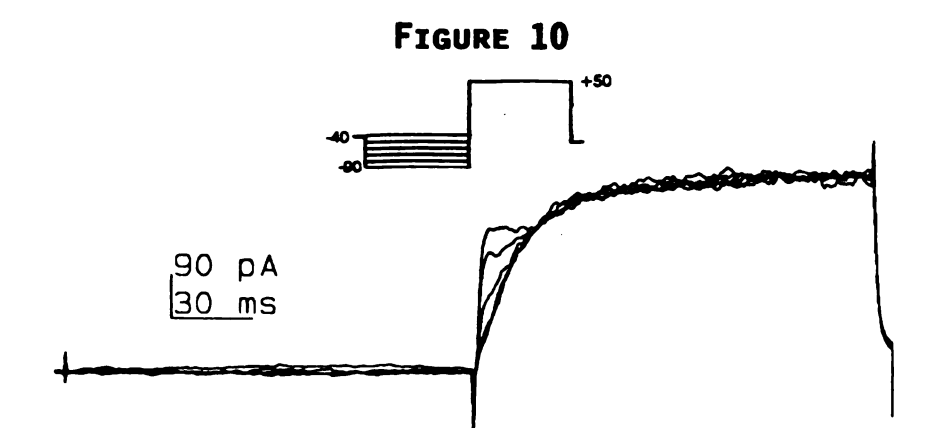
aı

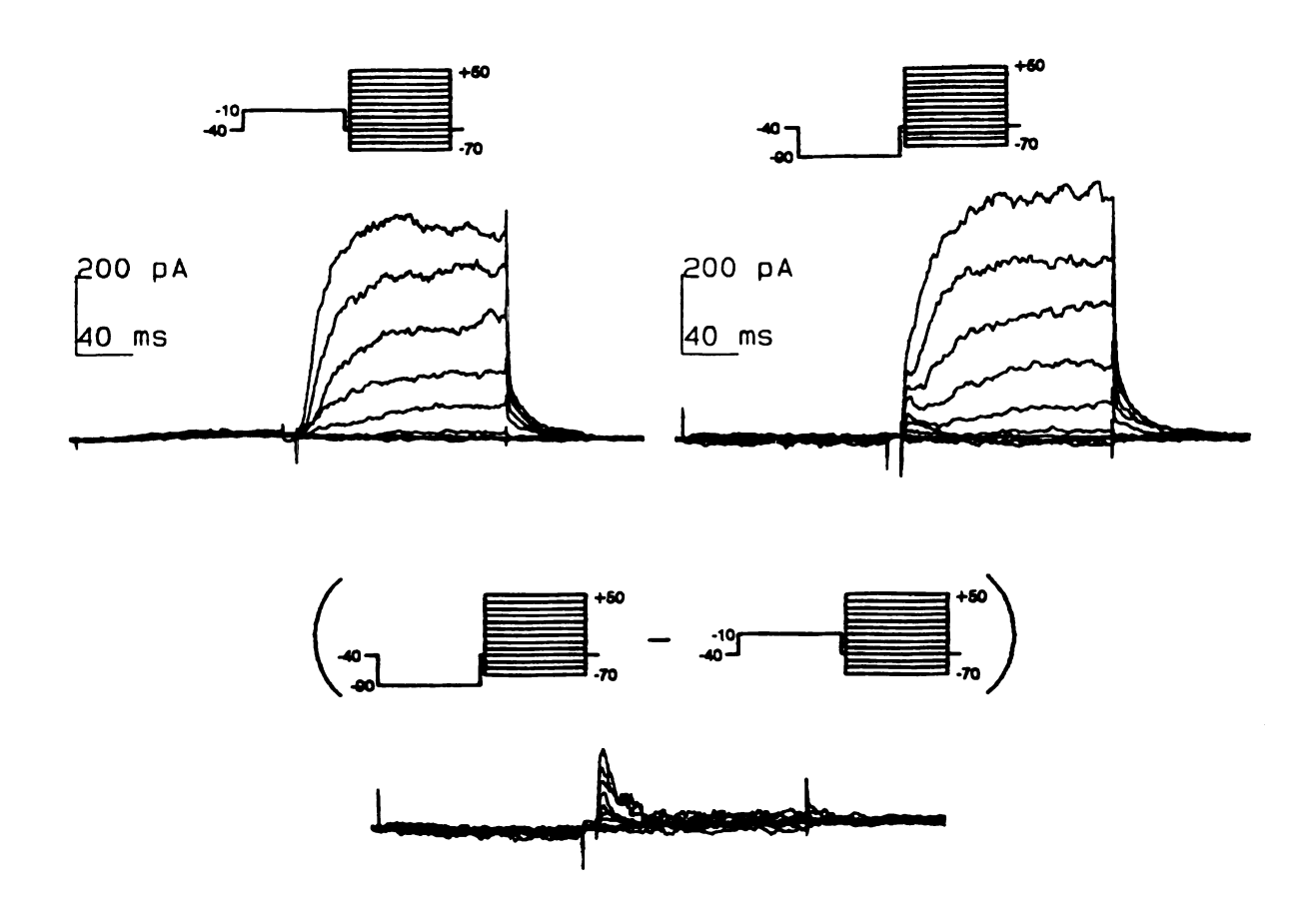
2. SEPARATION OF THE TWO CURRENTS

The shoulder progressively increased in prominence as the fiber was held at potentials more negative than -40 mV prior to the test pulse (Figure 10). When a prepulse of 150 ms to -90 mV was applied before each of a series of test potentials, the amplitude of the fast current dramatically increased, whereas a prepulse to -10 mV minimized the fast current. Since neither of the prepulses had significant effect on the amplitude of the slow outward current, the difference between the current families elicited by these different protocols was simply the presence (the family with the -90 mV prepulse) or the absence (the family with the -10 mV prepulse) of the fast outward current. Therefore, a subtraction of the outward currents elicited in protocols with the -10 mV prepulse from those elicited with the -90 mV prepulse yields a remainder which is the isolated profile of a quickly activating and inactivating voltage-dependent outward current. This fast current had a threshold of -20 mV and completely inactivated within the span of the 150 ms test pulse.

Therefore, for the studies on the slow current, fibers were used in which the fast current was not evident from the -40 mV holding potential, or a prepulse of -10 or -20 mV was utilized to erase the effects of the fast current. The slow voltage-dependent outward current had an amplitude of 413 ± 158 pA (n=21) at +50 mV in the time span

FIGURE 10. The two outward currents can be separated by manipulation of the pre-pulse potential. (Top) An example of a fiber to which hyperpolarizing pre-pulses of various amplitudes were applied before a single test pulse to +50 mV. These hyperpolarizing prepulses of 150 ms increased the amplitude of the fast component of the net outward current. (Middle) An example of a fiber to which was applied a prepulse of (left) -10 mV and (right) -90 mV before each of an entire series of test pulses. The depolarizing prepulse left no evidence of the shoulder on the current profile and the hyperpolarizing prepulse clearly magnified the presence of this second, faster component. (Bottom) The results of the subtraction of the -10 mV pre-pulse family from the -90 mV pre-pulse family. The difference between these two current profiles is the presence of a quickly activating and inactivating current when the fiber is exposed to the hyperpolarizing prepulse.





between 130-140 ms after the application of the test pulse (Figure 11). The capacitance of these fibers was 5.6 ± 1.2 pF, yielding an average of 74 pA/pF.

The fast current was isolated from the slow current in the manner described above, by subtracting a family of test potentials with a -10 mV prepulse from the same family of test potentials with a -90 mV prepulse. After such a protocol, the fibers displayed an outward current of 165 ± 88 pA (n=10) at +50 mV in the time period 3-8 ms after the application of the test pulse (Figure 12). The capacitance of these fibers was 6.1 ± 1.2 pF and an average of 27 pA/pF.

FIGURE 11. The larger voltage-dependent outward current activates slowly and inactivates very slowly. (Top) An example of a typical profile and (bottom) the current vs. voltage relationship for the slow current. The values for the I-V relationship are the average of the current levels from 130-140 ms after the application of the 150 ms test pulse. The current elicited with a test pulse to +50 mV was 413 \pm 158 pA (n=21).

FIGURE 11

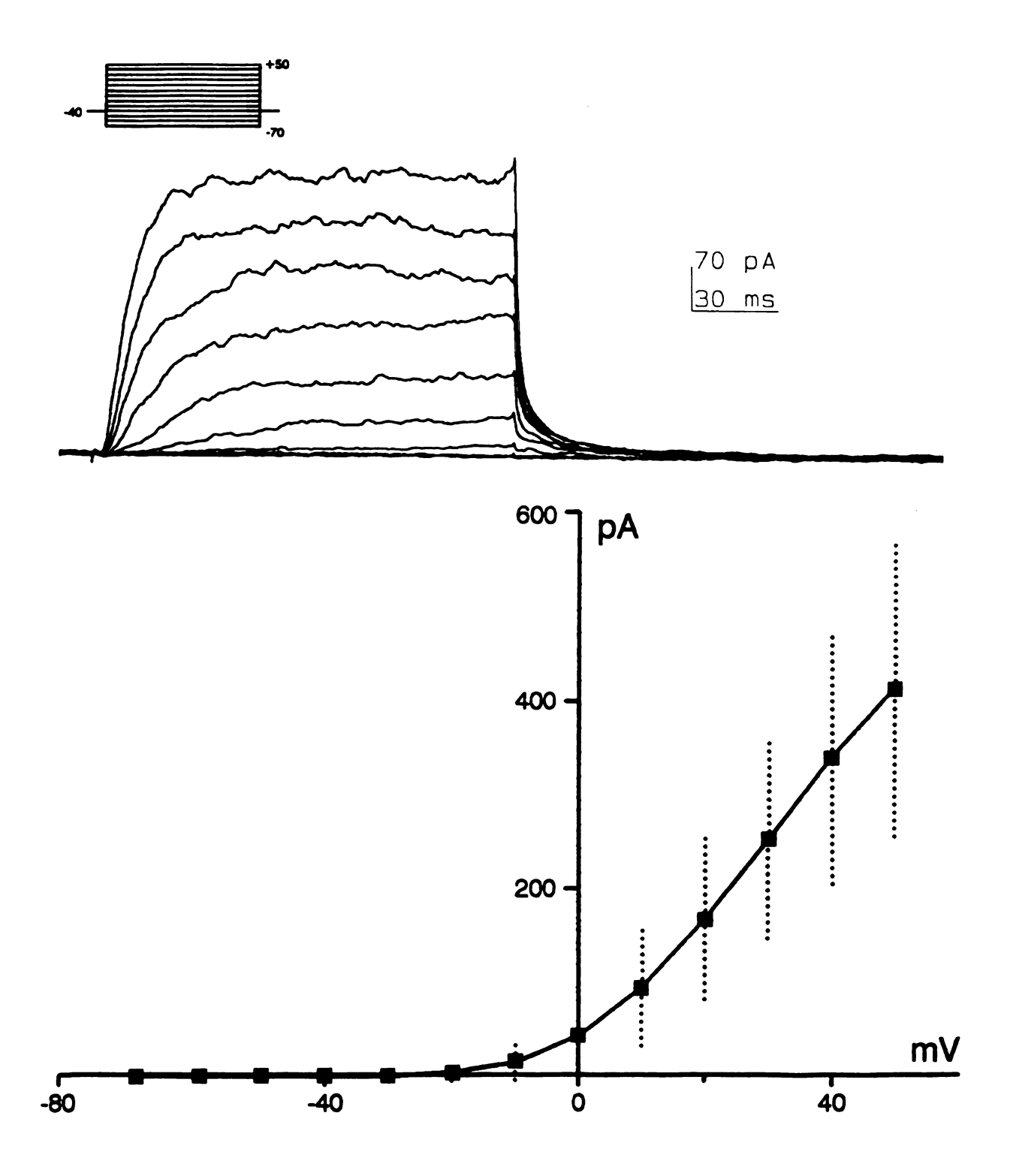
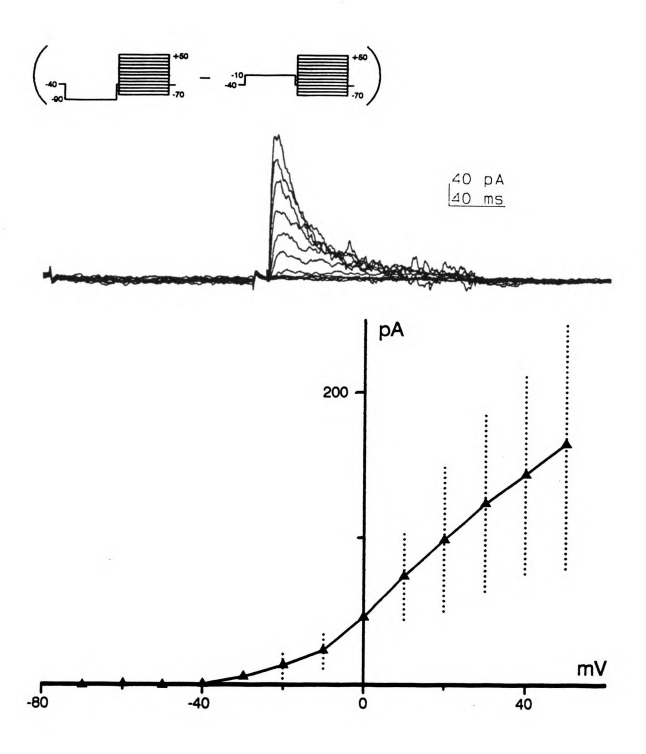


FIGURE 12. The smaller voltage-dependent outward current activates rapidly and inactivates rapidly. An example of a typical current profile and the current vs. voltage relationship for the fast current. Values for the I-V relationship are the average of the current levels from 3-8 ms after the initiation of the test pulse, from current families isolated as described in this section (n=10). The current elicited with a test pulse to + 50 mV was 165 ± 87 pA (n=10).

FIGURE 12



B. BOTH OUTWARD CURRENTS ARE K*-SELECTIVE

Both the slow and the fast voltage-dependent outward currents are carried selectively by K⁺, as determined by examination of the reversal potential of each. If a current is activated by a sufficient depolarizing test pulse, tail currents can be observed upon repolarization as the channels mediating the current close. Inspection of these tail currents makes it possible to measure the direction of current flow at potentials at which the current would not be activated and, therefore to determine the potential at which the current reverses direction.

easily isolated by maintaining the test pulse for 150 ms, insuring no interference from the fast current due to its' complete inactivation. Under the standard recording conditions, where the equilibrium potential for K+ was -82 mV (130 mM K+ and 5.4 mM K+ out), the reversal potential of the slow current was -70 mV (Figures 13 & 14). Any alteration in the [K+] out resulted in a corresponding change in the reversal potential of the current. This current showed a shift in reversal potential of 59 mV per 10-fold change in [K+] out, while the nernst equation predicts a 58 mV shift in reversal potential per 10-fold change in [K+] out for a K+-selective current (Figure 14).

In order to isolate tail currents attributable to the fast current, it was necessary to test fibers in which the

FIGURE 13. The reversal potential of the slow outward current depends on extracellular [K+]. (Left) Examples of the tail currents generated in (from top) 5 mM, 25 mM and 50 mM extracellular K+. These individual records are not all from the same cell. The current traces show only the end of a 150 ms test pulse to +50 mV from a -40 mV holding potential. In each example, there is a line that denotes the zero current level. (Right) The corresponding current vs. voltage relationship for each example. The values for the current vs. voltage relationship were obtained by averaging the current level between 2.5 and 3.5 ms after cessation of the test pulse and the beginning of the variable after-pulse potential. The line drawn is a regression through those points, and the x-intercept of the regression is the reversal potential shown in Figure 14.

FIGURE 13

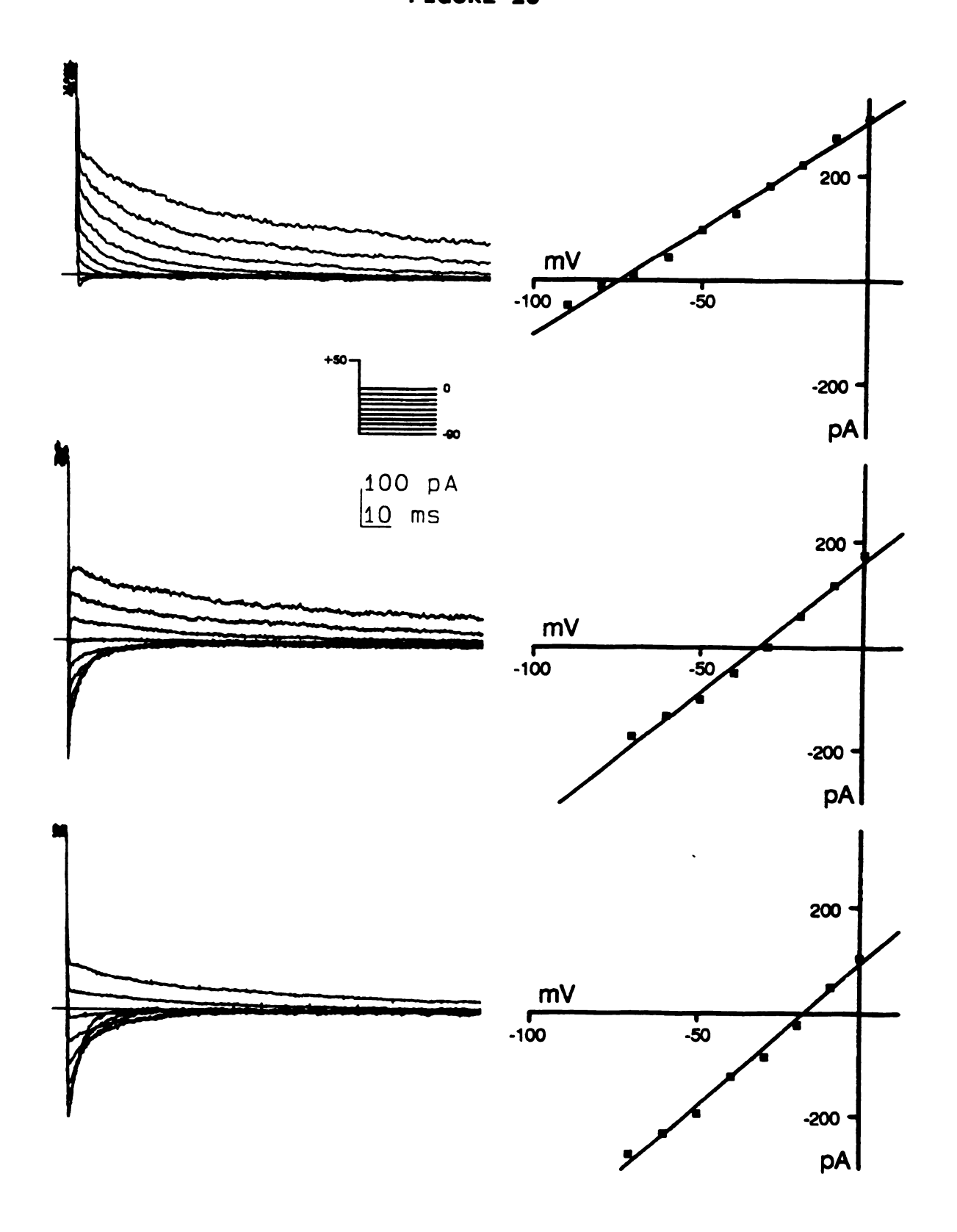
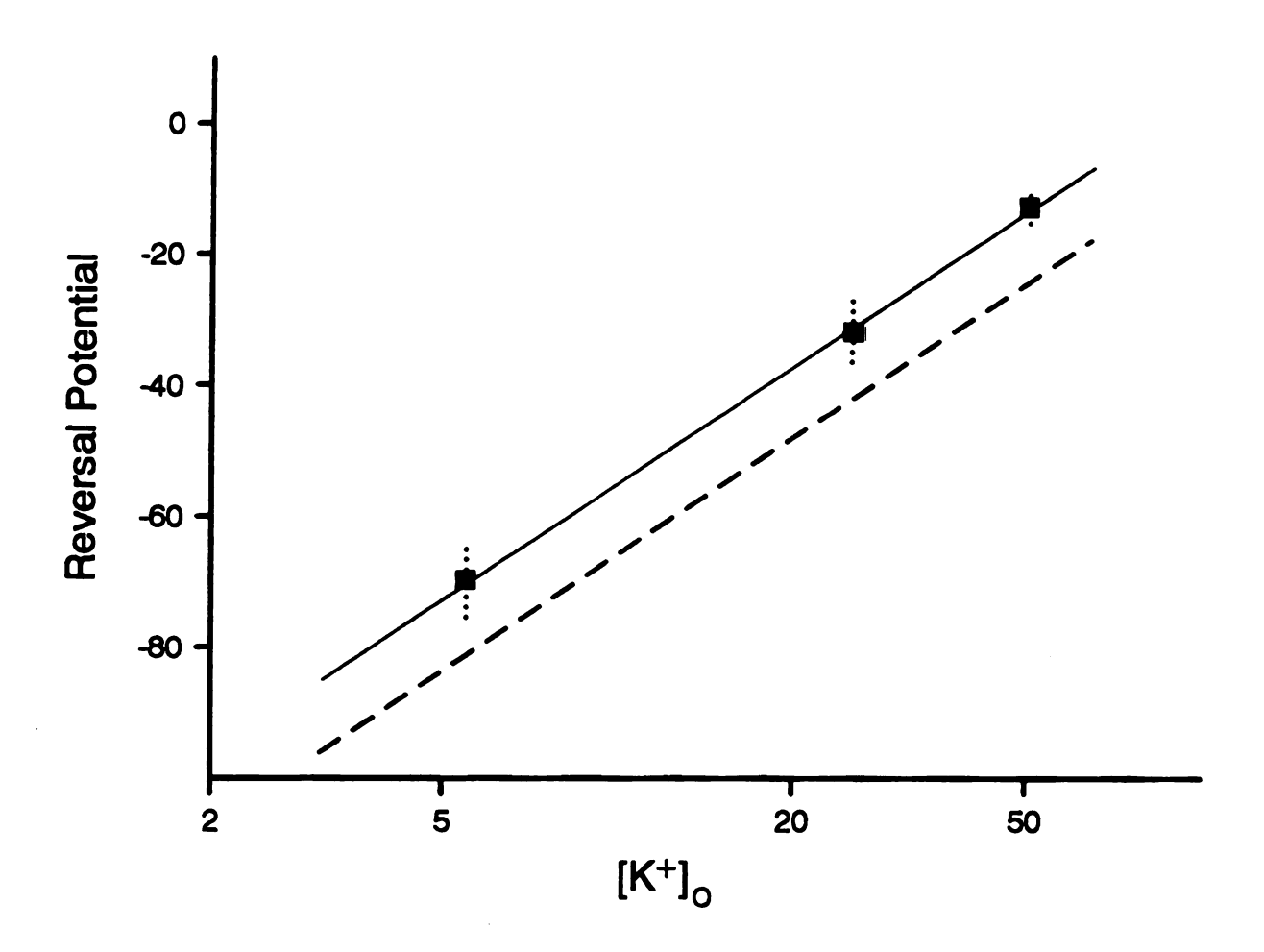


FIGURE 14. The slow outward current is K⁺-selective. The relationship between reversal potential of slow current tails and $[K^+]_{\circ}$. The values for reversal potential were taken from the x-intercept of the regression line through current vs. voltage relationships like those demonstrated in Figure 13. Each point is the average of at least five trials. The dashed line represents the predicted reversal potential for K⁺, slope of -58 mV/10-fold $[K^+]_{\circ}$, and the line formed by the data has a slope of -59 mV/10-fold $[K^+]_{\circ}$.

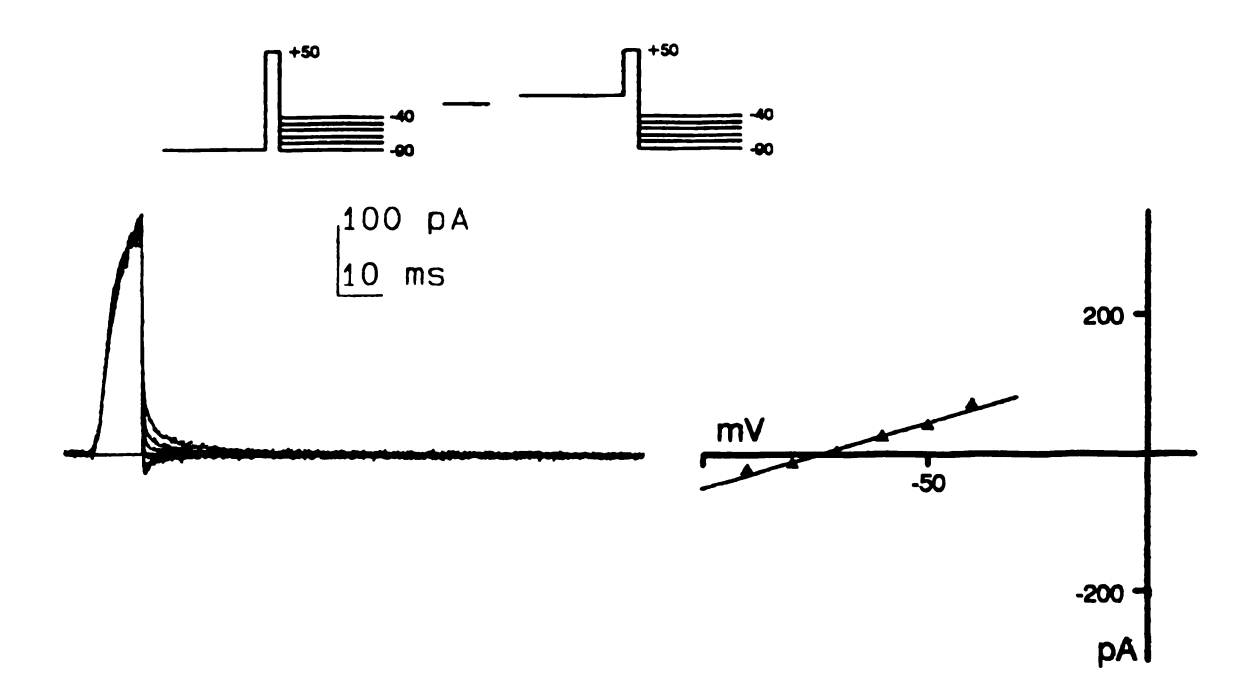
FIGURE 14



fast current was relatively large. Further, due to the transient nature of the fast current, it was necessary to limit the duration of the test potential to approximately 8 ms, in order to insure that the shift to the post-pulse potential was made before the fast current inactivated. In order to protect against interference from the slow current, a -10 mV prepulsed protocol was subtracted from a protocol prepulsed to -90 mV (Figure 15). With the equilibrium potential for K⁺ at -82 mV, the reversal potential of the fast current was -72 mV (Figure 15). Due to the relatively small size and fast kinetics of these tail currents, determination of reversal potential after media exchange provided erratic, dubious results that are not provided here.

FIGURE 15. The reversal potential of the fast outward current coincides with the equilibrium potential for K+. (Left) An example of tail currents attributable to the fast current. In order to augment the fast current and subtract out the influence of the slow current, a subtraction of prepulsed protocols was used. The duration of the test pulse is only 9 ms in this example, long enough to ensure fast current activation without allowing significant The length of the test pulse was varied for inactivation. each fiber in order to correlate with the peak of the fast current. The straight line denotes the zero current level. (Right) The current vs. voltage relationship for the tail currents in this example. The current values were obtained by averaging the current level between 2 and 2.5 ms after the cessation of the test pulse and the beginning of the variable after-pulse potential. The line drawn is a regression through the points and the x-intercept of the regression is -76 mV in this example. The reversal of the tails averaged -72 ± 9 mV (n=5) under these conditions in which the reversal potential of K+ is -82 mV.

FIGURE 15



C. Vol

(The

1

depend voltad

was e

poten
K⁺-se

The c

drawn

volt

at t

at t

mV 1

the cur

Pot the

дe

C. VOLTAGE-DEPENDENCE OF THE OUTWARD CURRENTS

(The data from this section are summarized in Table 2 on page 73.)

1. VOLTAGE-DEPENDENCE OF ACTIVATION

The conductance of both of these outward currents was dependent on the amplitude of the test potential. The voltage-dependence of activation for each of the currents was examined by comparing the conductance at each test potential. Since both currents had been determined to be K^+ -selective, the conductance of each could be calculated. The conductance at any potential is the slope of a line drawn between the following two points on a current vs. voltage relationship: 1) the observed amplitude of current at that potential and 2) the hypothesized zero current flow at the conducting ion's reversal potential, in this case -82 mV for K^+ . At a test potential of +50 mV, conductance of the slow current was 3.13 ± 1.20 nS (n=21) and the fast current was 1.32 ± 0.71 nS (n=10).

The relative conductance, the conductance at a given potential compared to that at +50 mV, was plotted against the amplitude of the test potential and the relationship was described by the Boltzmann equation in the form:

$$X = (1 - A)/[1 + e^{v-v50/k}] + A$$

EQUATION 1

where .
y-axis
potent:
the slo
of the
deviat:

T 19 mV

in the

more o

curren

also that

stead

exam:

rela

hold hold

Plot

the

(Ed.

where X is the relative conductance, A is the portion of the y-axis that is not fit by the curve, V is the test potential, V_{50} is the voltage of half activation and k is the slope factor. The slope factor indicates the steepness of the voltage-dependence about the midpoint, such that a deviation of k mV from V_{50} results in a change of 1/(1+e) in the level of activation.

The voltage of half-activation for the slow current is 19 mV with a slope factor of -10.6 (Figure 16). The fast current has a lower voltage of half-activation, 3 mV, and a more gradual slope factor of -12.4 (Figure 17).

2. VOLTAGE-DEPENDENCE OF INACTIVATION

The conductance of both of these outward currents is also dependent on the amplitude of the holding potential that preceeds the test pulse. The voltage-dependence of steady-state inactivation of each of the currents was examined by comparing the conductance generated by a test pulse to +50 mV from various holding potentials. The relative conductance, the conductance generated from a given holding potential divided by that generated from the most hyperpolarized holding potential utilized (-100 mV), was plotted against the amplitude of the holding potential and the relationship was described by the Boltzmann equation (Equation 1).

FIGURE 16. The conductance of the slow outward current is dependent on the amplitude of the test potential and the holding potential. The activation and inactivation curves for the slow outward current. The parameters describing the voltage-dependence of activation were determined by fitting the relationship between relative conductance and test potential to Equation 1 (a). For each fiber, the conductance at each potential was determined by dividing the value of the average current from 130-140 ms after the initiation of the test potential by the difference between the test potential and the reversal potential for K+ (Ex+=-82 mV); the relative conductance was determined by dividing the conductance at each test potential by that at +50 mV. The parameters describing the voltage-dependence of inactivation were determined by fitting the relationship between the relative conductance and holding potential to The holding potential was imposed on the Equation 1 (**a**). fiber for 20 s before a +50 mV test potential and the current averaged from 130-140 ms after the initiation of the test pulse. That current value was used to determine the conductance at +50 mV from that holding potential, which was compared to the conductance at +50 mV from a -100 mV holding potential.

FIGURE 16

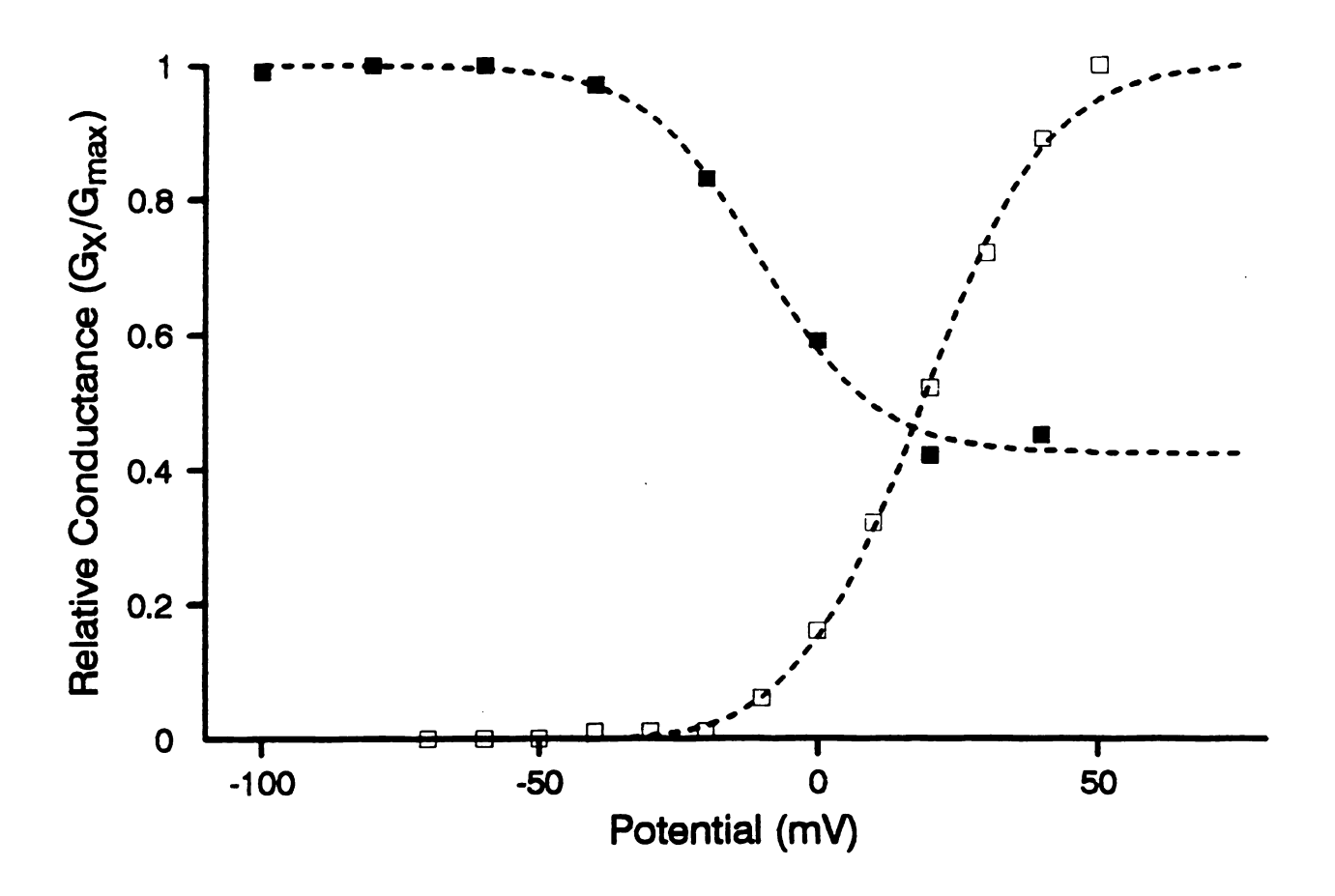
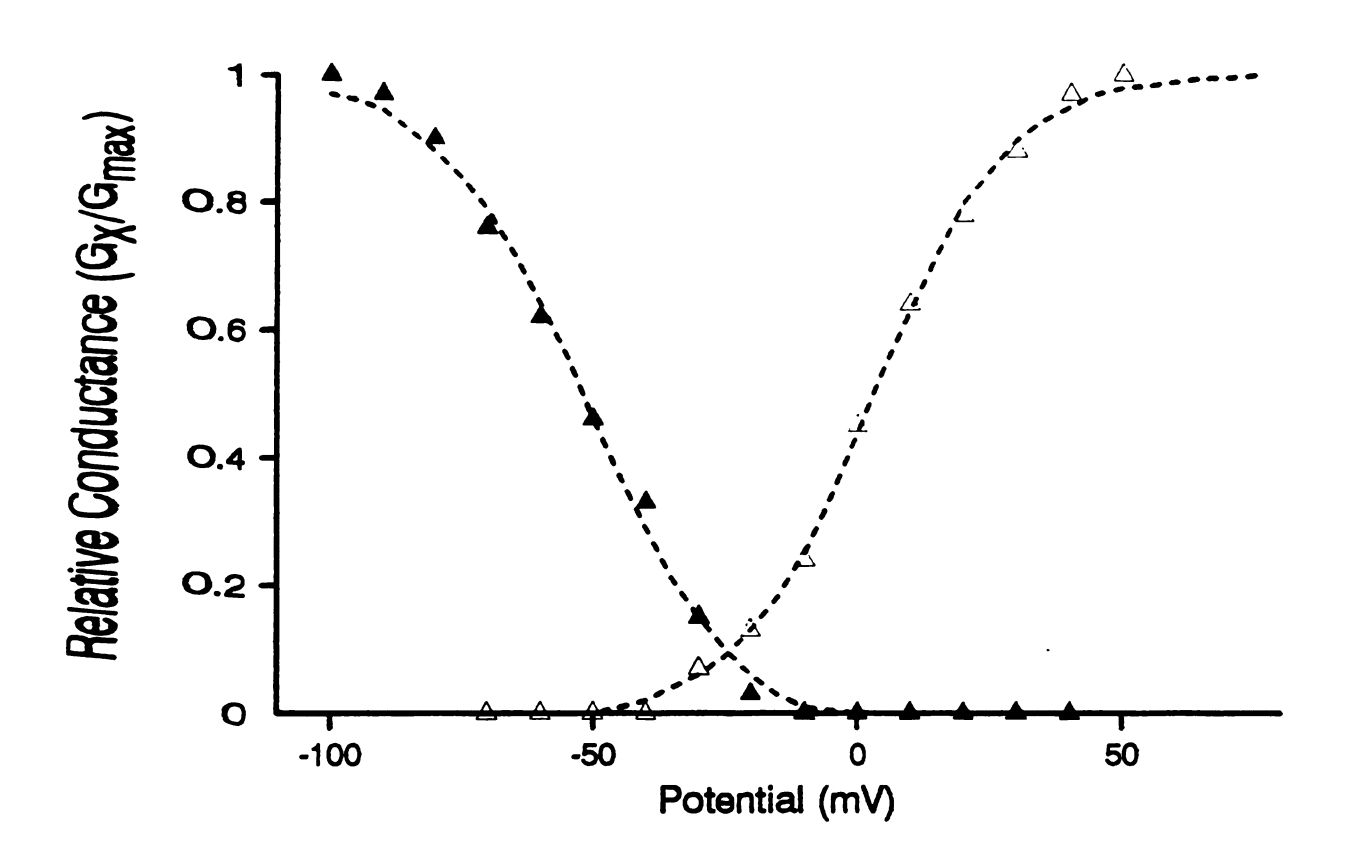


FIGURE 17. The conductance of the fast outward current is dependent on the amplitude of the test potential and the holding potential. The activation and inactivation curves for the fast outward current. This graph was derived in the same manner as Figure 16 except: 1) the inactivating holding potential was only applied for 150 ms, and 2) the current values used were those averaged from 3-8 ms after the initiation of the pulse from records of isolated fast currents. The relationship between relative conductance and test potential describes activation (Δ) and the relationship between relative conductance and holding potential describes inactivation (Δ).

FIGURE 17



The two K⁺ currents varied dramatically in their steady-state inactivation characteristics. The steady-state inactivation of the slow current required a very long period of time. There was clearly more inactivation after 10 s than after 5 s in every instance, and some fibers required more than 15 s to maximize steady-state inactivation of the slow current. Conversely, the steady-state inactivation of the fast current required only a very short time, easily reaching maximum effect by 150 ms.

A large portion, 42%, of the slow current was not Subject to steady-state inactivation and did not inactivate even after being held at +40 mV for 20 s. All of the fast current was subject to steady-state inactivation, even after Only 150 ms at -10 mV.

Ninety-seven per cent of the slow current was

Unaffected by steady-state inactivation at the standard

holding potential of -40 mV, while only 33% of the fast

Current was intact at this potential. The V₅₀ of

inactivation for the slow current is -10 mV (Figure 16),

While that of the fast current is -51 mV (Figure 17). The

slope of the inactivation of the slow current is steeper

than that of the fast current (slope factor of 10.3 vs.

1 4 .1).

All of the parameters listed above were determined in the presence of 0.4, 4 or

25 mM Ca²⁺ in the extracellular medium had no effect on these descriptors of voltage-dependence.

D. KINETICS OF THE OUTWARD CURRENTS

(The data from this section are summarized in Table 2 on page 73.)

1. ACTIVATION KINETICS

The rate of activation for the fast and the slow outward current are voltage dependent, with greater depolarizing steps producing a faster activation of the currents (Figure 18). The time course of activation for both currents was fit with Hodgkin-Huxley-type kinetics, using the equation:

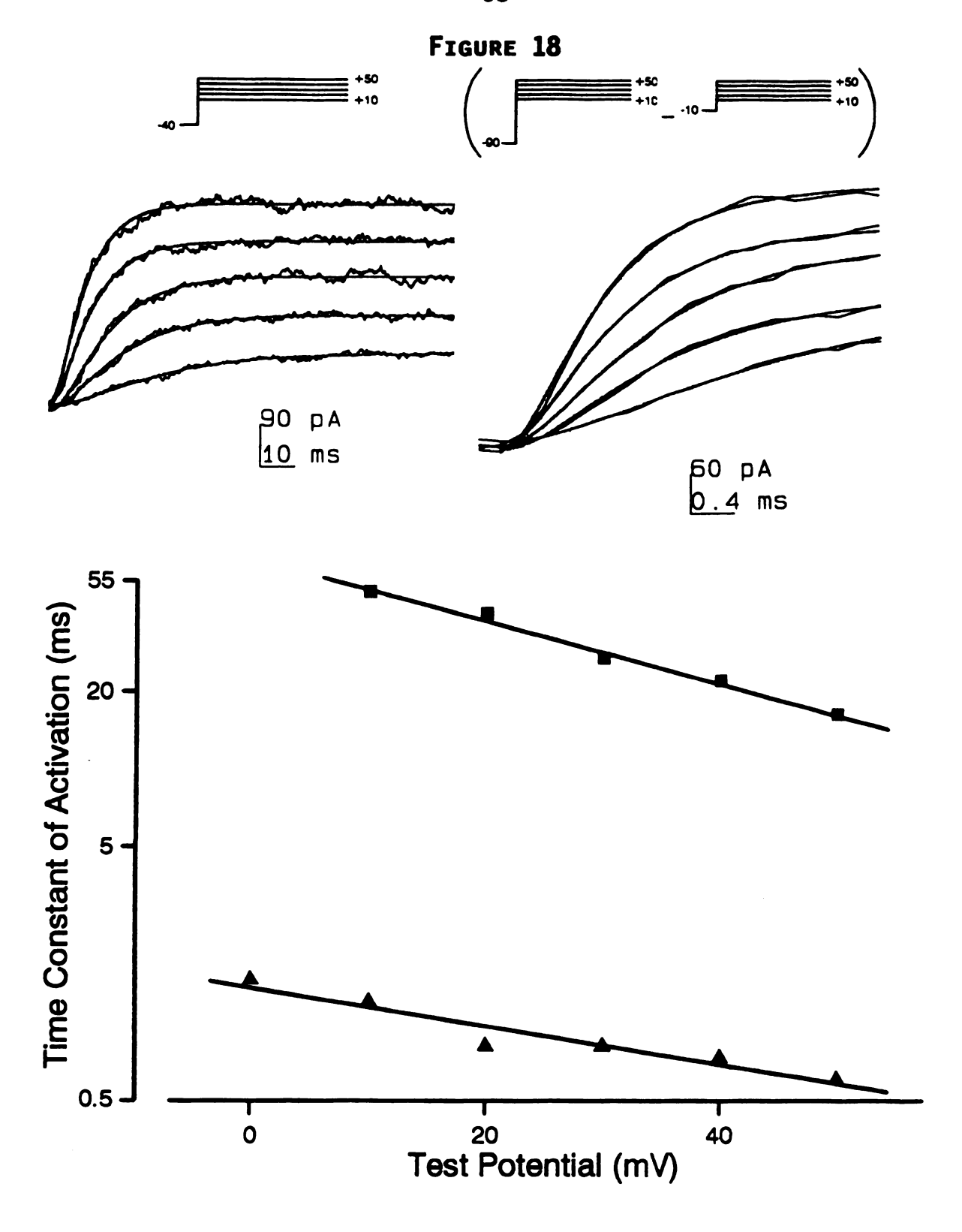
$$I = A + A_{z} (1 - e^{-\varepsilon/\tau})^{n}$$

EQUATION 2

where τ is the time constant of activation, A_{I} is the amplitude of the current fit by the equation and A is the amplitude of the offset from zero of the current fit by the curve. Both currents were described best when the exponent n=2.

The slow current was fit utilizing records produced from the standard -40 mV holding potential in which the fast current was not evident. The slow current displayed a τ_{act} 16.8 \pm 4.2 ms (n=10) for a test pulse to +50 mV and an e-1d change for every 36 mV change in pulse potential igure 18). The τ_{act} was not significantly altered when

FIGURE 18. The rate of activation is voltage-dependent for both the slow and the fast outward currents. (Top) Examples of activating slow currents (left) and fast currents (right) with superimposed mathematical approximations. The time constants of activation of the slow current were determined by fitting the current values from the region 1-135 ms after the initiation of the test potential to Equation 2 with n=2. For the fast current, the same equation was used and the beginning of the fitting region was always 1 ms, but the end ranged from 4 ms (at +50 mv test potential) to 7 ms (at 0 mV), depending on the location of the peak outward current. In both cases, the fitting region began at 1 ms after the pulse in order to avoid interference from capacitive transients. (Bottom) The relationship between the time constants of activation and the test potential for the slow current (■) and the fast current (▲).



slow current activation was fit utilizing records in which the fast current was noticeable. This is due to the fact that the fitting region for the slow current activation was 135 ms long and the fast current interfered for only a small fraction of this time.

The fast current was fit by utilizing subtractions of traces with a 150 ms, -10 mV prepulse from those with a 150 ms, -90 mV prepulse. From a -90 mV holding potential, the fast current had a τ_{act} of 0.6 ± 0.1 ms (n=5) for a test pulse to +50 mV and an e-fold change for every 60 mV change in pulse potential (Figure 18). Activation of the fast current could also be fit by utilizing the initial region of fast activation in records produced from the standard -40 mV holding potential in which the fast current was clearly evident. This analysis showed that, from a -40 mV holding potential, the current had a τ_{act} of 1.1 \pm 0.4 ms (n=5) for a test pulse to +50 mV. The activation was slower at any potential from the -40 mV holding potential as opposed to the -90 mV holding potential, but the slope factor describing the change in τ_{act} per change in mV of test potential was equal.

The activation kinetics of these currents were not altered by the presence of normal (0.4 mM) or high (4 mM) extracellular Ca²⁺, nor by the presence of 2 mM intracellular adenosine triphosphate (ATP).

2. INACTIVATION KINETICS

The rate of inactivation for the fast current is voltage dependent, but the inactivation rate of the slow current is relatively independent of voltage (Figure 19). In both instances, the inactivation of the current was fit best by a single exponential, utilizing the equation:

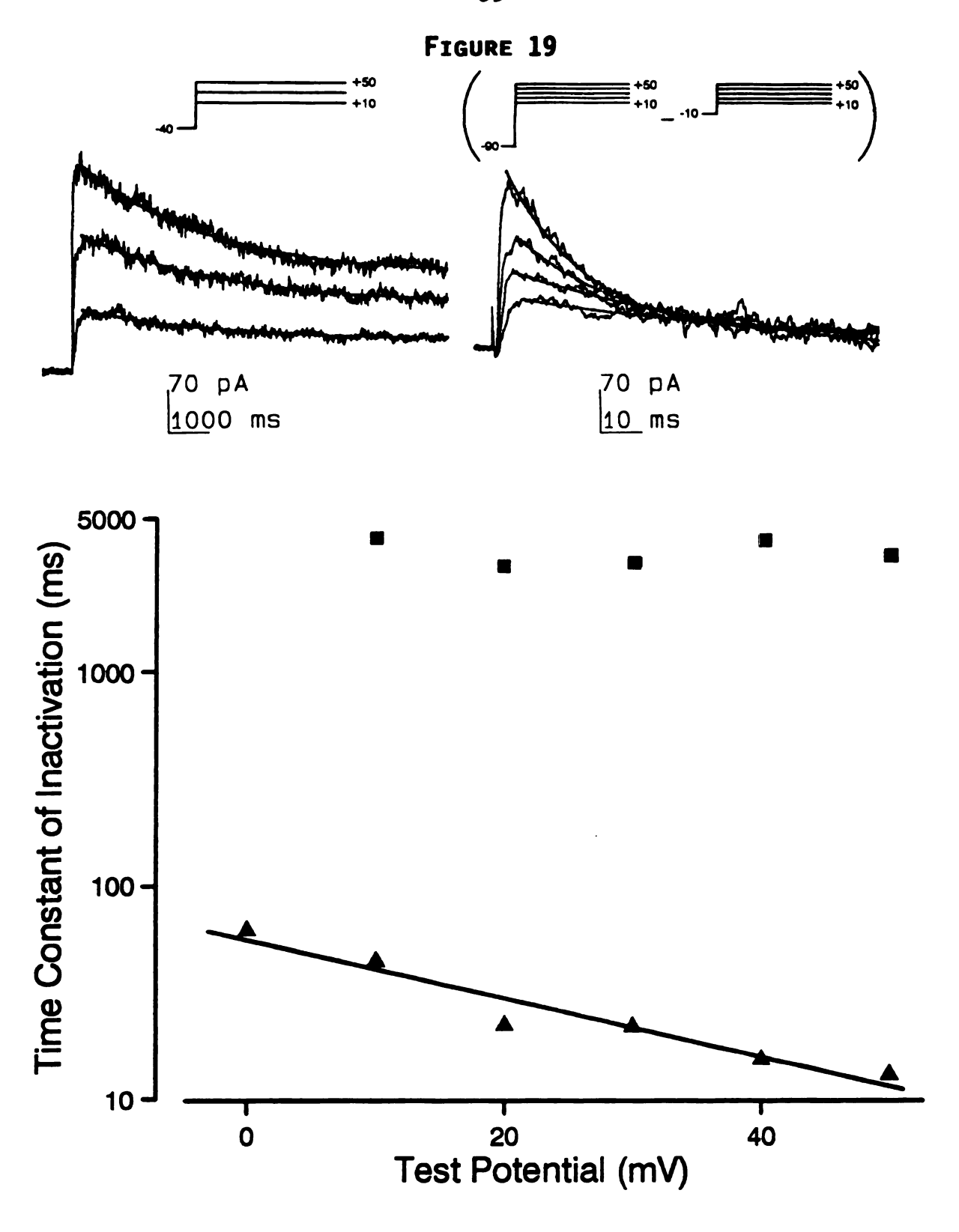
$$I = A + A_1 e^{-t/\tau}$$

EQUATION 3

where A is the amplitude of the non-inactivating current, A_I is the amplitude of the inactivating current and τ is the single time constant of activation.

The slow current had a τ_{inact} of 3423 \pm 782 ms (n=5) when pulsed to +50 mV and did show a trend of slower inactivation at lower potentials, but the correlation was weak (Figure 19). Inactivation of the slow current was fit utilizing the net outward current from fibers in which the fast current was not very prominent. Even so, it might be expected that the presence of the fast current could make the description of net inactivation a biexponential function, but this was not the case. The first signs of inactivation of the net outward current, and therefore the beginning of the fitting region for inactivation, did not occur until over 150 ms after the initiation of the test

FIGURE 19. The rate of inactivation is voltage-independent for the slow outward current, but voltage-dependent for the fast outward current. (Top) Examples of inactivating slow currents (left) and fast currents (right) with superimposed mathematical approximations. The time constants of inactivation of the slow current were determined by fitting the region that spanned from the peak of the net outward current (between 200-400 ms after the application of the test potential, depending on its value) to 9000 ms to Equation 3. For the fast current, the beginning of the fitting region was dictated by the location of the peak of the outward current in subtraction-isolated traces, which usually occurred between 4-7 ms after the application of the test potential, and the end was set at 100 ms. (Bottom) The relationship between the time constants of inactivation and the test potential for the slow current () and the fast current (▲).



pulse. This is more than 10 times the ≈ 13 ms τ_{inact} of the fast current, insuring that the inactivation of the fast current would not interfere with the inactivation of the slow current, providing it a misleading biphasic form.

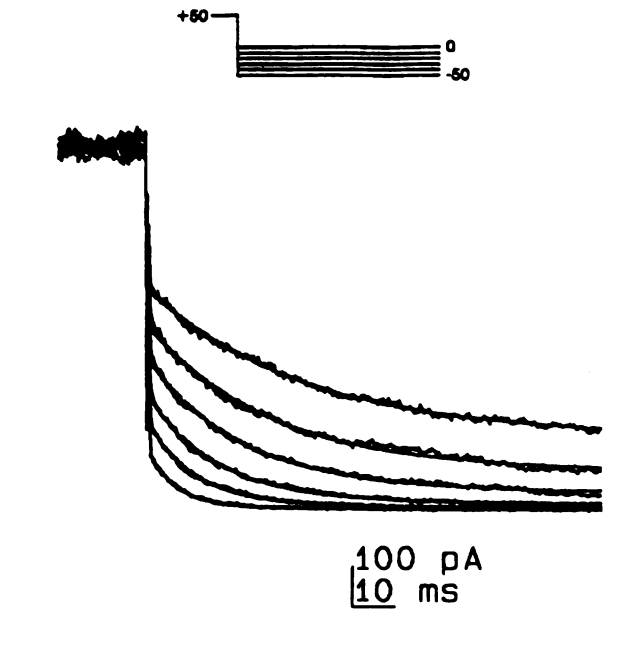
The fast current had a τ_{inact} of 13 ± 6 ms (n=5) when pulsed to +50 mV and was e-fold slower for every 37 mV drop in the test potential (Figure 19). The inactivation of the fast current was fit utilizing records of the isolated fast current as derived from the subtraction of protocols previously discussed.

3. RELAXATION KINETICS

Relaxation, sometimes referred to as deactivation, of the slow current is very strongly voltage-dependent. The relaxation of the slow current was fit by the same single exponential equation as was the inactivation (Equation 3). When the fully activated current was returned to the holding potential of -40 mV, the current relaxed with a τ of 15 \pm 3 ms (n=7) and was e-fold faster per -39 mV (Figure 20). Relaxation of the fast current was difficult to discern in any reliable quantitative way and did not fit any kinetic model.

FIGURE 20. The rate of relaxation is voltage-dependent for the slow outward current. (Top) Examples of inactivating slow currents with superimposed mathematical approximations. The time constants of relaxation were determined by fitting the region from 1-80 ms after cessation of a +50 mV test potential to Equation 3. (Bottom) The relationship between the time constant of relaxation and the test potential.

FIGURE 20



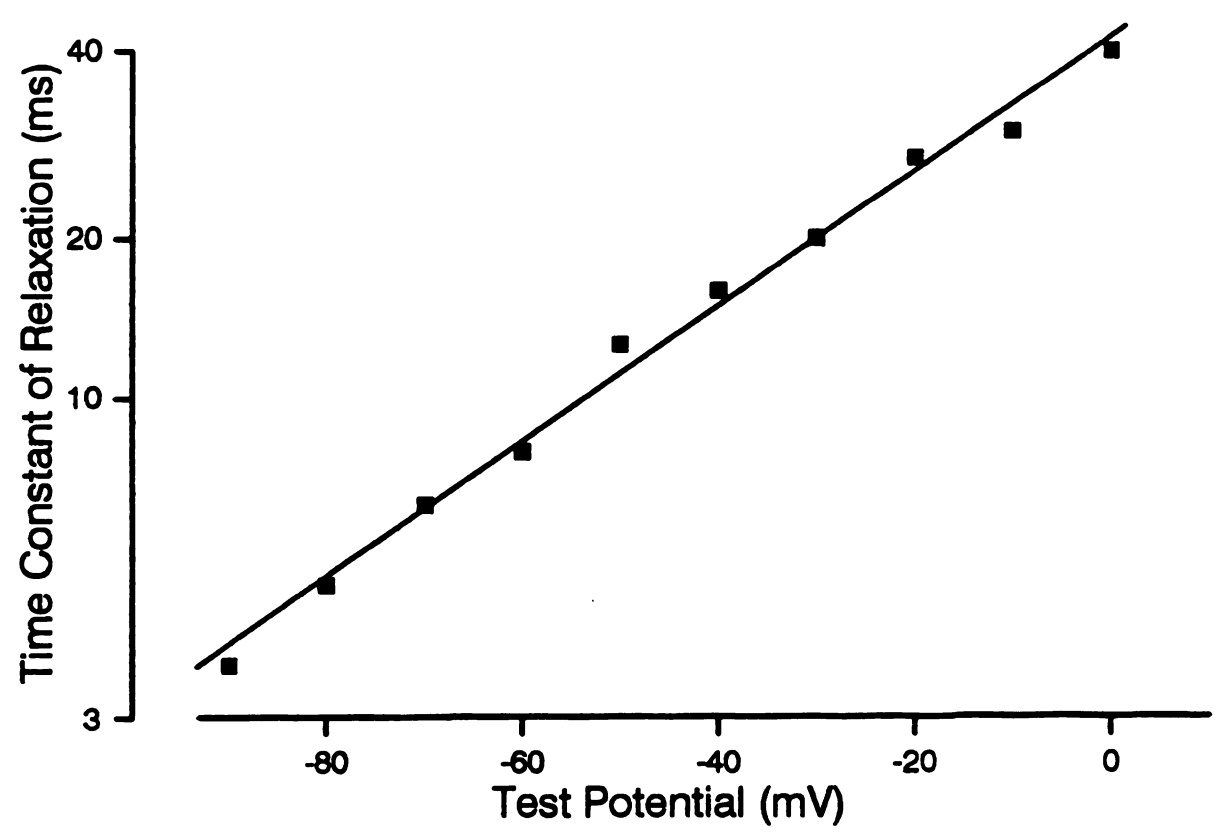


TABLE 2.

Properties of the Two Voltage-Dependent K+ Currents of Schistosome Frayed Muscle Fibers.

DELAYED RECTIFIER CURRENT	
I _{max} , +50	413 ± 158 pA
G _{max} , +50	$3.13 \pm 1.20 \text{ nS}$
Voltage-Dependence	
activation	
threshold	≈-10 mV
V _{so}	19 mV
slope factor (k)	-10.6 mV
inactivation	
V ₅₀	-10 mV
slope factor (k)	10.3 mV
% non-inactivating	42%
Kinetics	
activation	
Tact, +50	$16.8 \pm 4.2 \text{ ms}$
e-fold change per	36 mV
inactivation	
finact, +50	$3423 \pm 782 \text{ ms}$
e-fold change per volt	tage-independent
relaxation	
Trelax, -40	$15.4 \pm 2.5 \text{ ms}$
e-fold change per	39 mV
"A" CURRENT	
I _{max. +50}	$165 \pm 87 pA$
G _{max} , +50	$1.32 \pm 0.71 \text{ nS}$
Voltage-Dependence	
activation	
threshold	≈-40 m.V
V ₅₀	3 mV
slope factor (k)	-12.4 mV
inactivation	
V ₅₀	-51 mV
slope factor (k)	14.1 mV
Kinetics	
activation	
Tact, +50	1.1 ± 0.4 ms
e-fold change per	60 mV
inactivation	
71nact, +50	$13 \pm 6 \text{ ms}$
e-fold change per	37 mV
•	

E. PHARMACOLOGY OF THE OUTWARD CURRENTS

1. TETRAETHYLAMMONIUM (TEA+)

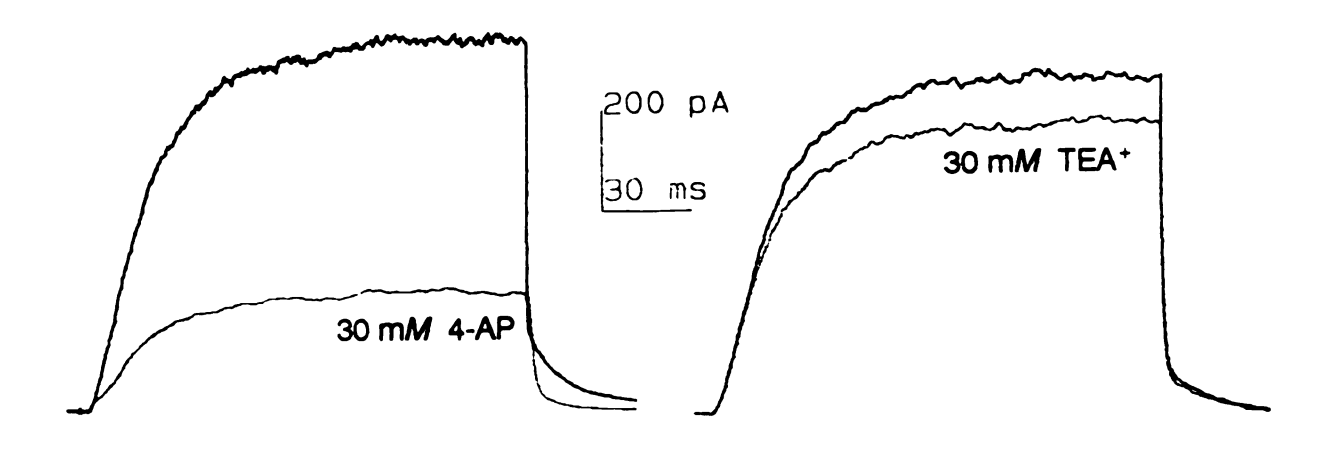
Both the slow and the fast currents are relatively insensitive to extracellular TEA⁺. After external application of 30 mM TEA⁺, the slow current was reduced to 88% of control values (Figure 21). Further, a significant slow current could be measured in fibers even when the 110 mM extracellular Na⁺ was completely replaced with TEA⁺. The fast current was slightly more sensitive to the TEA⁺ application, with only 69% of the control current remaining in the presence of 30 mM TEA⁺ (Figure 22).

2. 4-AMINOPYRIDINE (4-AP)

Both the slow and the fast currents can be blocked by 4-AP, but only at relatively high concentrations. Half-blockade of the slow current was accomplished by approximately 10 mM 4-AP, as the external application of 10 mM 4-AP reduced the current to 48% of control values (Figure 21). Half-blockade of the fast current required less than 3 mM 4-AP, as that concentration reduced the fast current to 45% of control values (Figure 22).

FIGURE 21. The slow outward current is partially blocked by tetraethylammonium or 4-aminopyridine. (Top) Current traces demonstrating the response of the slow current to 30 mm 4-AP (left) and to 30 mm TEA+ (right). The darker trace is the control current and the lighter trace is current in the presence of the treatment. (Bottom) The dose-response relationship of both compounds on the current. A control current response was obtained by averaging the last seven of 15 consecutive 150 ms voltage pulses to +50 mV. The procedure was repeated five minutes after the addition of the desired concentration of the test compound to the extracellular bath. Each point on the graph below represents an n≥4.

FIGURE 21



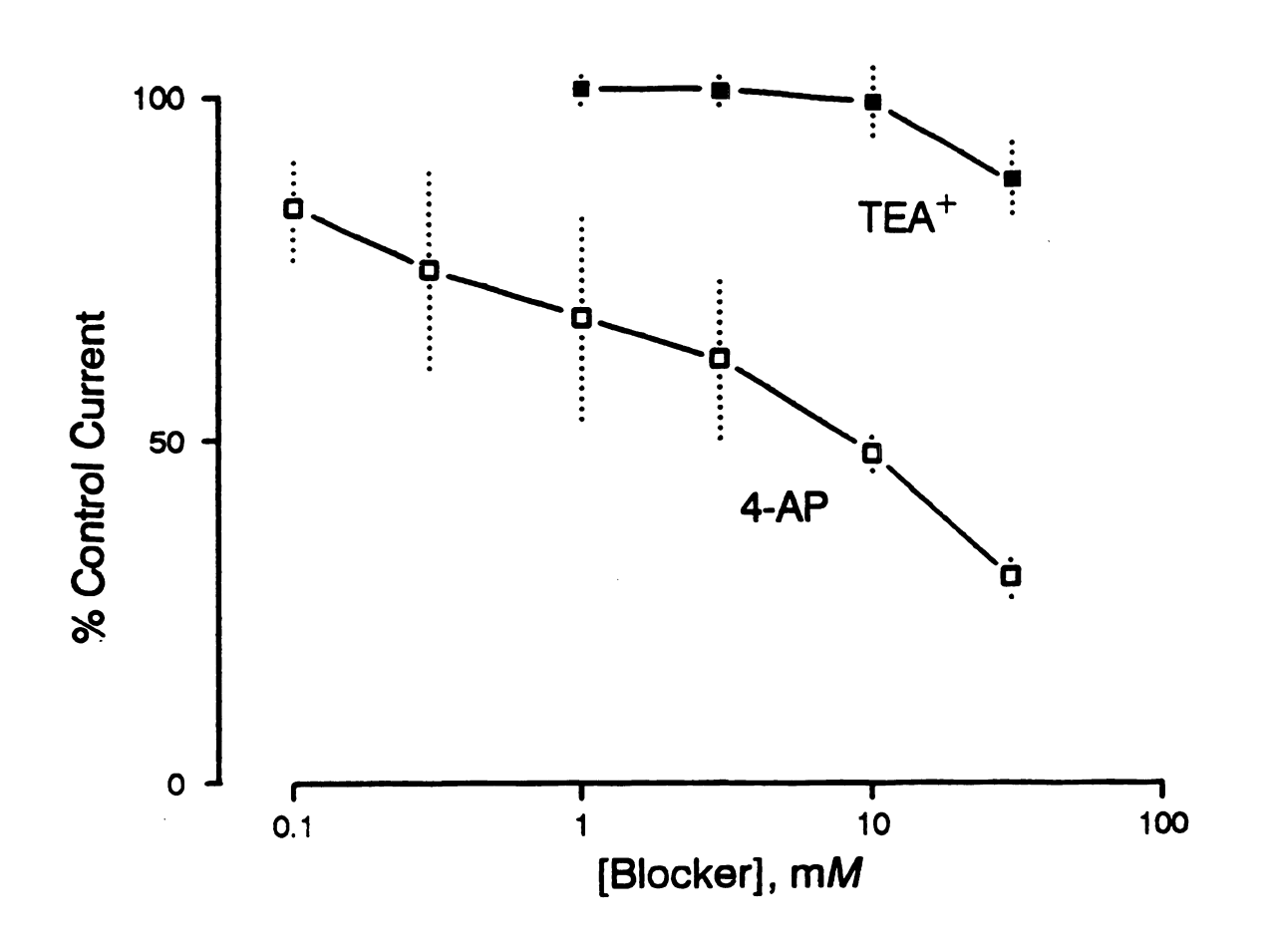
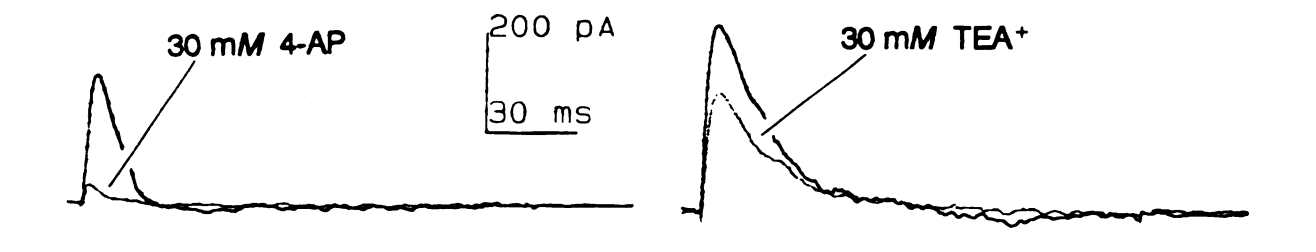
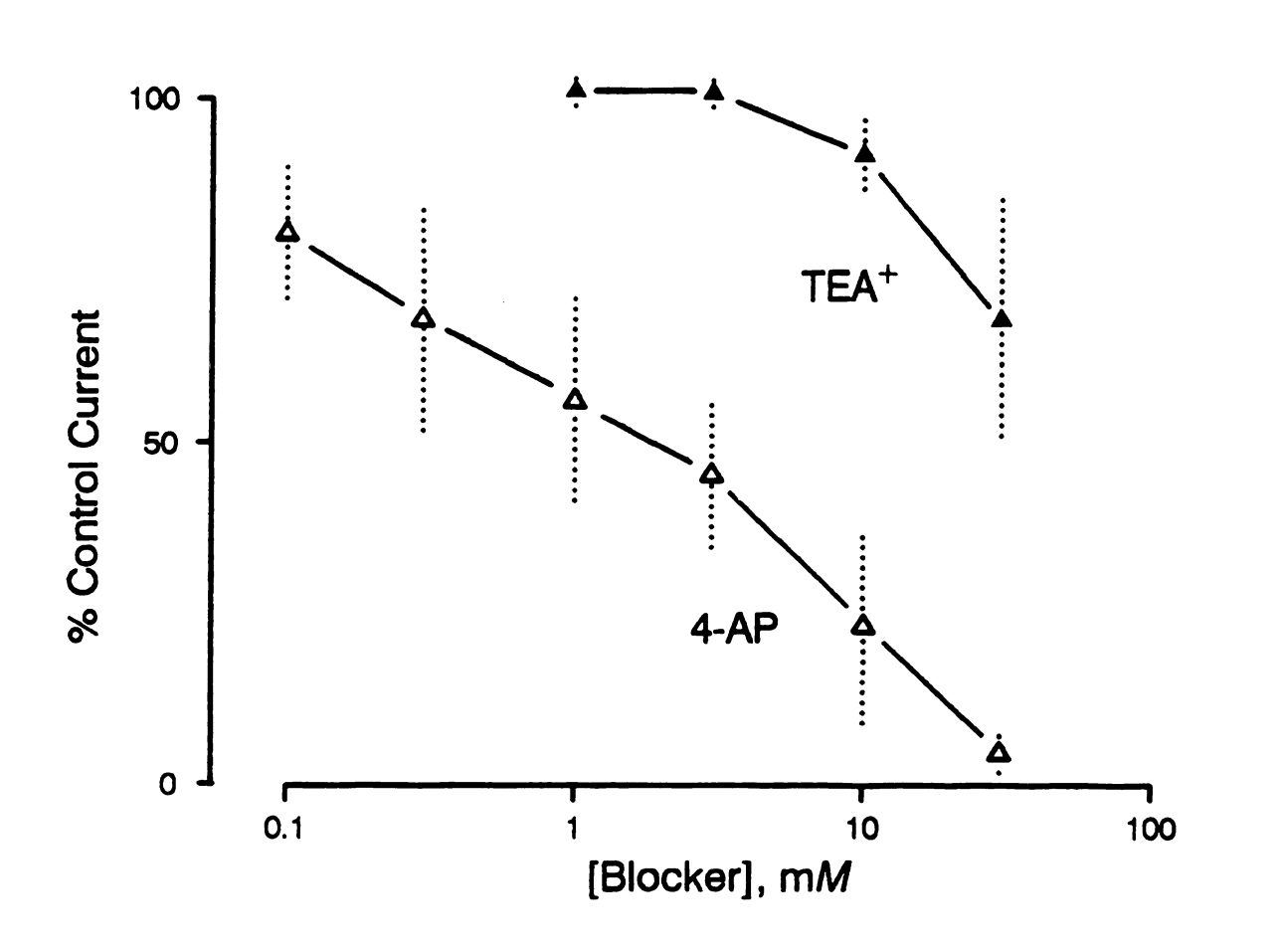


FIGURE 22. The fast outward current is partially blocked by tetraethylammonium and is completely blocked by high concentrations of 4-aminopyridine. (Top) Current traces demonstrating the response of the fast current to 30 mm 4-AP (left) and to 30 mm TEA $^+$ (right). The darker trace is the control current and the lighter trace is the current in the presence of the treatment. (Bottom) The dose-response relationship of both compounds on the current. The experiments were performed as described in Figure 21, except that the fast current had to be isolated via the subtraction method described earlier. Each point on the graph below represents an $n \ge 4$.

FIGURE 22





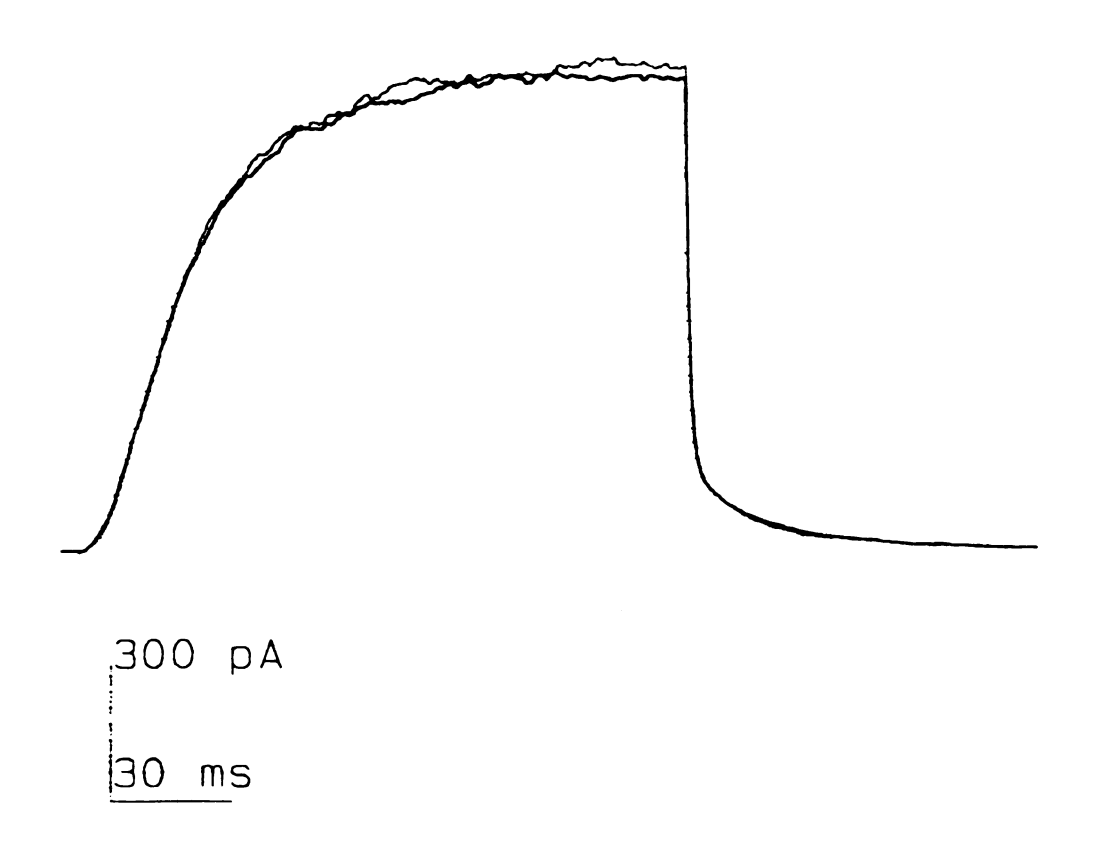
3. DENDROTOXIN (DTX)

Both the slow and the fast currents are insensitive to the potassium channel toxin DTX, the neurotoxic peptide isolated from the venom of the African green mamba snake.

DTX in concentrations as high as 200 nM had no measurable effect on either current (Figure 23).

FIGURE 23. The slow and the fast outward currents are both insensitive to dendrotoxin. Current traces demonstrating the insensitivity of both the slow (above) and the fast (below) outward currents to 200 nM DTX. In both cases, the experiments were performed as described for the previous two figures and the darker trace is the current trace and the lighter trace is five minutes after the application of DTX.

FIGURE 23





100 pA 30 ms

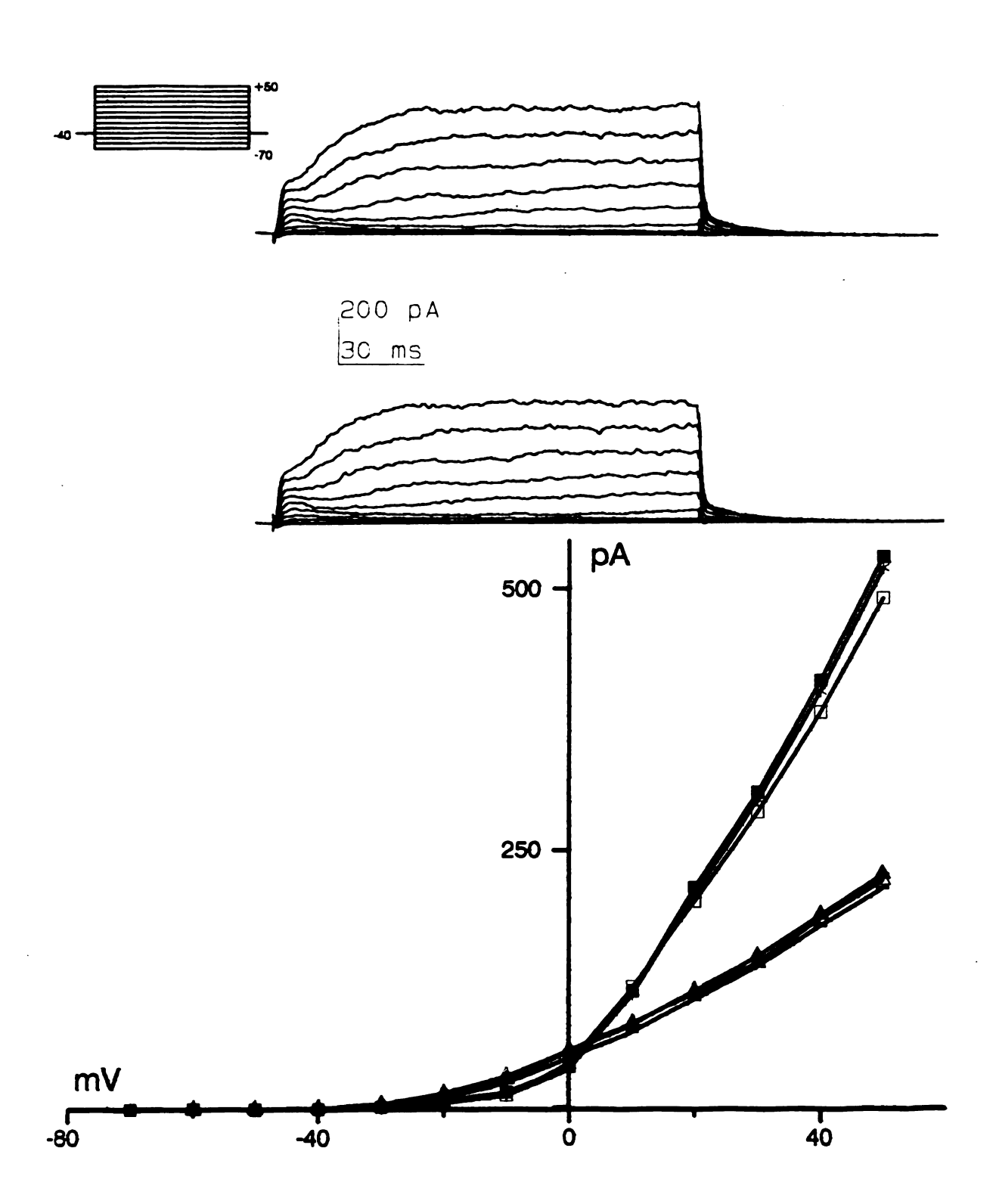
IV. VOLTAGE-DEPENDENT INWARD CURRENTS

As detailed earlier in this section, none of these fibers ever displayed action potentials in response to depolarizing current injections under any of these experimental conditions. The possible presence of voltage-dependent inward currents was further explored in the whole-cell voltage clamp mode. Because concurrent studies in our laboratory suggested that the frayed fibers were more contractile when cultured in the supplemented DMEM, this was used as the extracellular medium for these experiments (see Appendix I for more detail on this matter).

The first step toward detecting voltage-dependent Ca2+ currents was to raise the level of extracellular Ca2+. Voltage-dependent Ca2+ channel activity could potentially be detected in two different ways from these conditions. Most obviously, the increased [Ca2+] could provide enough charge carrier to produce noticable inward currents, even in the presence of the relatively fast outward currents. Secondly, even if the fast outward current obscured an inward current, voltage-dependent Ca2+ influx could be detected due to an increased outward current, since the presence of Ca2+dependent K+ channels in these fibers has been established (Blair et al., 1991). However, when the [Ca2+] was varied between nominally Ca²⁺-free (i.e., no added Ca²⁺, no EGTA) and 20 mM, there was no sign of an inward current and no change in the macroscopic outward current (Figure 24).

FIGURE 24. Increased extracellular [Ca2+] does not expose a voltage-dependent inward current nor does it alter the macroscopic outward current. Examples of typical currents recorded from a single cell that was exposed to (top) nominally Ca2+ free and (middle) 20 mM Ca2+ in the extracellular medium. The current responses appear essentially identical, with no evidence of an inward current in the high extracellular Ca2+. (Bottom) The current vs. voltage relationship for the slow and the fast outward currents of this cell in three different extracellular [Ca²⁺]. The slow current in nominally Ca²⁺-free (■), 4 mM Ca^{2+} (\Box) and 20 mM Ca^{2+} (*) and same data for the fast current (A , A , and -). Even though the presence of Ca^{2+} dependent K+ channels has been established in these fibers, there is no Ca²⁺-dependent component of the macroscopic outward current, supporting the indication that voltagedependent Ca2+ entry is not occurring under these conditions. Similar tests were performed on five other cells with like results.

FIGURE 24

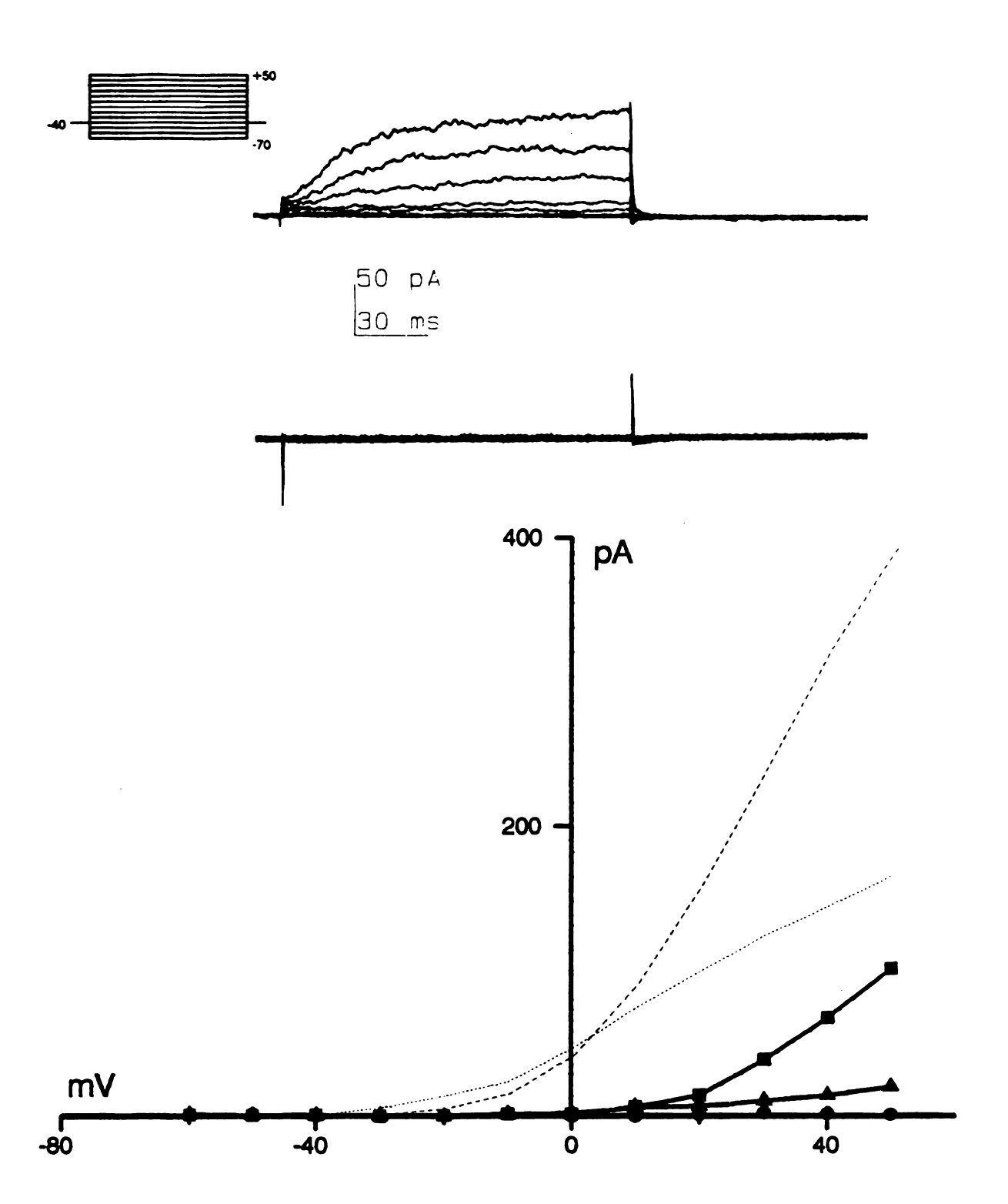


Further attempts to directly measure inward currents required the blockade of the the relatively large voltagedependent outward currents that have already been described. A substantial outward current persisted even after complete replacement of the 110 mM Na⁺ in the extracellular solution with 110 mM TEA+ (Figure 25). However, when the replacement of the extracellular Na+ with TEA+ was coupled with the complete replacement of the 120 mM K+ in the intracellular solution with 120 mm Cs+, the outward currents were completely abolished. With the outward currents blocked in this fashion and extracellular Ca2+ (or the alternate charge carrier Ba2+) raised as high as 50 mM, no voltage-dependent inward currents were evident in response to the standard voltage protocol applied from a -40 mV holding potential (Figure 25). Hyperpolarizing prepulses to as much as -90 mV were added to the protocol in attempts to overcome any steady-state inactivation but, still, no inward currents were detected. Also unsuccessful in conjunction with these protocols were various additions made to the intracellular solution: 2-10 mm ATP, 2 mm cAMP, 2-5 mm GTP, 2 mm cGMP, 0.5 mM GTP- γ -S, 20 mM glucose.

In some instances, I was successful in obtaining a high-resistance seal and subsequent whole-cell access in spontaneously contracting fibers. Even in these instances, inward currents could not be detected.

FIGURE 25. No voltage-dependent inward currents are evident when the outward currents are partially blocked by extracellular tetraethylammonium or completely attenuated by intracellular Cs+. (Top) An example of typical currents obtained with the extracellular Na+ entirely replaced with The experiments described here were performed using an inorganic extracellular medium based on the supplemented Both the fast current and the slow current are still evident in the presence of such high concentrations of extracellular TEA+, and there are no signs of any inward currents. (Middle) An example of typical currents obtained with the 110 mm extracellular Na+ replaced with 50 mm Ca2+ and 60 mM TEA+ as well as the intracellular K+ replaced completely with Cs⁺. The outward currents are abolished when the intracellular K+ is replaced with Cs+, but even in this example where there is 50 mM extracellular Ca2+, no inward currents are evident. (Bottom) The current vs. voltage relationship for trials in the conditions shown Shown are the average amplitudes of the fast and the slow currents in normal conditions (dashed line and dotted line, repectively), the average fast and slow current with 110 mM extracellular TEA⁺ (■ and ▲, n=3) and the average current with extracellular TEA+/Ca2+ and intracellular Cs+ (♠, n=3). The same results were obtained when the extracellular cations were 50 mm Ba2+ and 60 mm TEA+ (n=5).

FIGURE 25



DISCUSSION

I. MATHEMATICAL MODELING

The two voltage-dependent K^+ currents of the schistosome muscle fibers are described well by the classical equations typically used to fit the individual kinetic parameters of K^+ currents. For example, Hodgkin-Huxley-type kinetics describe the onset of either the delayed rectifier current or the "A" current very satisfactorily, with the best fit in both instances being with n=2 (Equation 2). As has been determined with other K^+ currents, inactivation of both currents fits a single exponential function (Equation 3).

In each of these instances, however, the aspects in question were fit isolated from other aspects of the macroscopic current. The macroscopic current is affected simultaneously by all processes: activation and inactivation of both the delayed rectifier current and the "A" current. In order to determine how well the combination of these equations described the complete current elicited from a test pulse, the equations describing activation and inactivation of both currents were combined.

The summed equation describing the activation and inactivation of both currents at any given potential is:

$$I = [A_{dr} * (1 - e^{-t/rdr \cdot act})^{2} * (e^{-t/rdr \cdot inact})] + [A_{a} (1 - e^{-t/ra \cdot act})^{2} * (e^{-t/ra \cdot inact})]$$

EQUATION 4

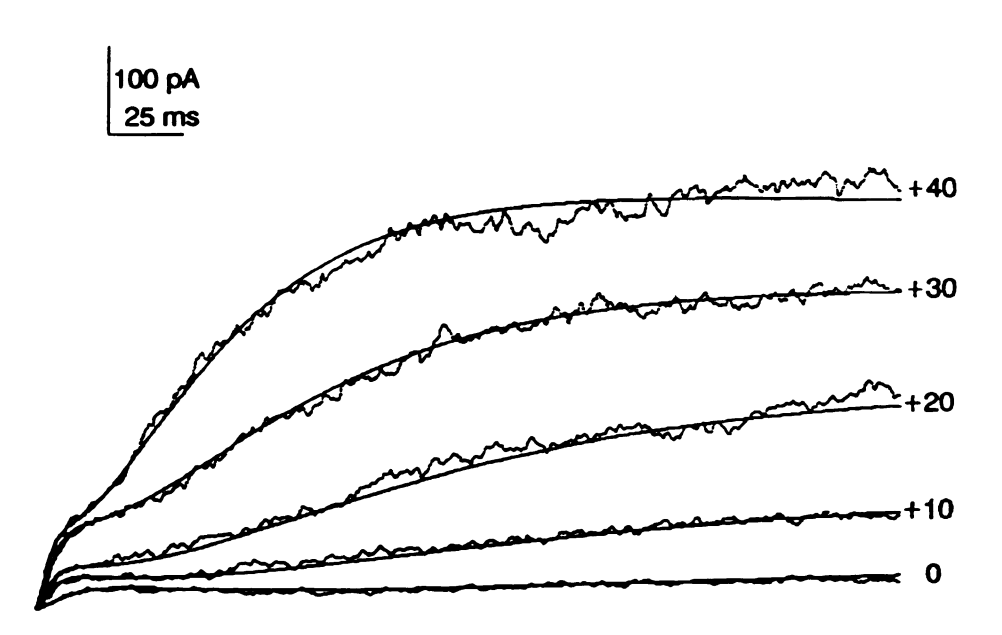
where A is the amplitude of the respective currents, t is the time after the initiation of the test pulse and τ 's the various time constants.

In order to test the ability of this combined equation to describe the macroscopic current of specific fibers, the individual amplitudes and time constants of both currents were determined for an individual fiber as described in the Results section (Table 3). Then, the variables were placed in Equation 4 and the results were superimposed on the original data traces (Figure 25). The results confirm the accuracy of these previously-established mathematical models and show that the combined equation is sufficient to describe the entire current response of a fiber. This affirms that the combined activity of delayed rectifier and "A" currents as described are sufficient to account for the entirety of the current response, i.e., that no other significant currents are present.

TABLE 3. Variables for the Mathematical Model in Figure 25.							
+40	+30	+20	+10	0			
	306	271	1/.6	65			
20.6 3670	30.8 3670	48.8 3670	64.9 3670	95.7 3670			
128 1.82 10.1	101 2.01 19.8	65 2.30 25.9	45 3.13 33.8	31 4.48 44.1			
	+40 +40 rrent 489 20.6 3670	+40 +30 rrent 489 386 20.6 30.8 3670 3670 128 101 1.82 2.01	+40 +30 +20 rrent 489 386 271 20.6 30.8 48.8 3670 3670 3670 128 101 65 1.82 2.01 2.30	+40 +30 +20 +10 +40 +30 +20 +10 rrent 489 386 271 146 20.6 30.8 48.8 64.9 3670 3670 3670 3670 128 101 65 45 1.82 2.01 2.30 3.13			

FIGURE 26. The combined equation describing delayed rectifier and "A" current activation and inactivation is sufficient to model the macroscopic current of the fibers. The voltage responses of a fiber and the mathematical model of those responses generated from the combined equation for the delayed rectifier and "A" currents (Equation 4). The amplitude and kinetic parameters used in the equation were calculated for this example exactly as the parameters reported in the Results section.

FIGURE 26



II. CLASSIFICATION OF THE TWO SCHISTOSOME K* CURRENTS A. DELAYED RECTIFIER CURRENT

A delayed, slow, voltage-dependent outward K+ current was first identified in the squid giant axon (Hodgkin & Huxley, 1952a, 1952b). Since the current was activated after a delay upon membrane depolarization and it provided rectification in response to the depolarization, it has classically been referred to as a delayed rectifier current. The criteria used to identify a K+ current as a delayed rectifier current are not completely agreed upon, but in general two criteria are used (Rudy, 1988). First, the kinetic behavior of the current must be similar to that described by Hodgkin and Huxley, i.e., it must be described by Hodgkin-Huxley kinetic models. Second, the current must be neither a Ca2+-dependent current (activated by internal [Ca2+]) nor an "A" current (quickly inactivating and heavily subject to steady-state inactivation). As would be expected, this definition yields a fairly diverse class of currents that often display very different kinetic properties, voltage-dependent properties and pharmacological profiles that can be mediated by very different channels. The slow current of the schistosome muscle fibers is, by this definition, a delayed rectifier current.

B. "A" CURRENT

A fast, transient, voltage-dependent outward K⁺ current that was extremely susceptible to steady-state inactivation was first identified in the nerve somata of a sea slug (Connor & Stevens, 1971). The criteria typically used to identify a K⁺ current as an "A" current have been: 1) activation must be fast compared to other voltage-dependent K⁺ currents, 2) inactivation must be fast and complete, 3) the current must be sensitive to steady-state inactivation, and 4) threshold of activation must be low compared to other K⁺ currents. The fast current of the schistosome fibers is an "A" current by this definition.

III. ABSENCE OF VOLTAGE-DEPENDENT INWARD CURRENTS

Although the electrophysiological studies produced no direct evidence for the presence of voltage-gated Ca²⁺ channels in these fibers, concurrent studies in our laboratory provided some indirect evidence of their presence.

Spontaneous contractile activity was not uncommon amongst frayed fibers produced by the dispersion procedure listed in the Materials and Methods and the fibers were incubated in the supplemented DMEM or the inorganic version of the supplemented DMEM (see Appendix I for more detail). The spontaneous activity varied from full contraction-

relaxation cycles every few seconds to barely detectable twitching of the extremities of the fibers.

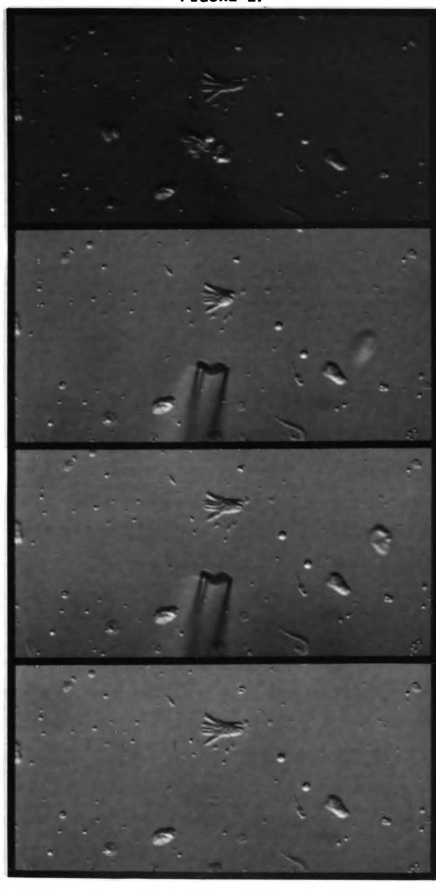
Exposure of individual fibers to an extracellular solution with 25 mM K⁺ induced contractions in quiescent fibers about 80% of the time (Figure 27). The high K⁺-induced contractions were generally similar to the spontaneous contractions, that is, they consisted of a series of quick twitches or more complete contraction-relaxation cycles that continued for as long as the high K⁺ was applied. In other instances, the contractions were sustained and relaxation would not occur until high K⁺ application was halted.

These high K⁺-induced contractions were dependent on extracellular Ca²⁺. The K⁺-induced contractions were abolished if the 3.6 mM Ca²⁺ was omitted and 0.5 mM EGTA was added to both the extracellular medium in which the fibers were bathing and the high K⁺ medium with which the fibers were depolarized. Further, the high K⁺-induced contractions are blocked by the presence of classical voltage-gated calcium channel blockers such as 10 µM nicardipine or 5 mM Co²⁺.

So, it is clear that depolarization by high K⁺ causes contraction of individual schistosome muscle fibers. This suggests the presence of some mechanism for depolarization-induced Ca²⁺ entry into these fibers, possibly through voltage-gated Ca²⁺-selective channels. This idea is

FIGURE 27. The frayed fibers contract in response to depolarization by high K^+ . A sequential series of micrographs showing the depolarization-induced contraction of a frayed fiber. The top panel shows the fiber at rest and the next panel shows the fiber in a contracted state moments after being exposed to a small amount of high K^+ -containing version of the culture medium via the pipet. In the third panel, the fiber is relaxing though still being perfused with the high K^+ medium and the bottom panel is after removal of the perfusing pipet.

FIGURE 27



supported by the fact that these depolarization-induced contractions are inhibited by the voltage-dependent Ca²⁺ channel blocker nicardipine. However, neither voltage or current clamp studies provided any direct evidence for the presence of such channels. It is possible that these fibers do not have voltage-gated Ca²⁺ channels and high K⁺-induced contractions are mediated by some other mechanism. However, I think it more likely that voltage-gated Ca²⁺ channels are present but are not detectable under the conditions of these studies.

One possible explanation for this could be that the Ca2+ channels are rendered non-functional due to the omission of critical molecules from the experimental intracellular solution. However, voltage-dependent Ca2+ currents have been recorded from many smooth muscle types utilizing simple extracellular solutions composed of inorganic ions with glucose and intracellular solutions composed completely of inorganic ions (Bolton et al., 1986; Bean et al., 1986; Ohya, Kitamura & Kuriyama, 1988). example, the conditions under which voltage-dependent Ca2+ currents can be measured in rabbit portal vein smooth muscle, (Beech & Bolton, 1989a), toad stomach smooth muscle (Walsh & Singer, 1987), or ctenophore smooth muscle (Dubas, Stein & Anderson, 1988) do not produce measurable inward currents in schistosome muscle. In some muscle types, the addition of 2-5 mm ATP to the intracellular solution

provided a dramatic improvement in the amplitude or the persistence of the Ca²⁺ currents (Yatani *et al.*, 1987;

Matsuda, Volk & Shibata, 1990; Kotlikoff, 1988), but the presence of ATP had no effect on the current of schistosome muscle.

One difference that exists between these other muscle types and schistosome muscle is that the schistosome fibers are much smaller, such that the intracellular contents may be dialyzed much more rapidly. Evidence of how fast the dialysis of cell contents occurs in the schistosome fibers is that the outward K⁺ currents were attenuated immediately when Cs⁺ was used to replace K⁺ in the pipet. In larger cells, similar attenuation of K⁺ currents can require up to 30 seconds.

Another possibility is that the Ca²⁺ currents are present but are simply too small to be measured by these techniques. The small size of the schistosome muscle fibers grants that even a modest Ca²⁺ influx may be sufficient to control intracellular events. Inward currents less than about 25 pA could be difficult to discern under these recording conditions.

IV.

rec

hai

pro

of

ha

an

re

(F

(M

De es

bo

ha

P:

t

е

N t

Ţ

C

IV. COMPARATIVE SIGNIFICANCE

This is the first direct demonstration of delayed rectifier and "A" currents in the platyhelminths. presence of these currents with no novel properties is in harmony with the continuity that is observed in viewing the properties of the voltage-dependent K+ currents across the phyla. In organisms as primitive as protozoa, a wide range of voltage-dependent outward K+ and inward Ca2+ currents have been identified which are strikingly similar to the K+ and Ca²⁺ currents of many mammalian cells. Delayed rectifier currents have been identified in sarcomastigotes (Febvre-Chevalier et al., 1986, 1989) and in ciliates (Machemer & Ogura, 1979; Satow & Kung, 1980; Wood, 1982; Deitmer, 1984). The presence of "A" currents have also been established in ciliates (Deitmer, 1984, 1989). Further, both transient and sustained voltage-dependent Ca2+ currents have been found in the protozoa (Deitmer, 1984, 1986, 1989). Present in a heliozoan is a single voltage-dependent current that mediates action potentials which can be supported by either Ca2+ or Na+, and is sensitive to the classical Ca2+ channel blocker D-600 (Febvre-Chevalier, 1986, 1989). Notably absent from this phylum, however, is the tetrodotoxin-sensitive voltage-dependent Na+ current that is responsible for the propagation of signals in a variety of cell types in higher animals.

Ctenophore muscle has a voltage-dependent inward Ca²⁺/Na⁺ current similar to that of the heliozoan. This current can be supported by either Ca²⁺ or Na⁺, is sensitive to verapamil and is not sensitive to TTX (Dubas, Stein & Anderson, 1988). Jellyfish nerve has a voltage-dependent inward current that is Na⁺-selective, yet is sensitive to verapamil and insensitive to TTX and a separate Ca²⁺-selective current that is much smaller and somewhat slower (Anderson, 1987). The muscle and nerve of ctenophore both have "typical" delayed rectifier and "A" currents, with the exception being that the macroscopic delayed outward current appears to have a notable Cl⁻ component. It is unclear if this is due to Cl⁻ flow through K⁺ channels or due to the contribution of a separate voltage-dependent Cl⁻ component.

Evidence for the presence of a TTX-sensitive voltage-dependent Na+ current first appears in platyhelminth neurons (Blair & Anderson, 1991). This research is the first published description of voltage-dependent currents from any platyhelminth muscle and the first description of voltage-dependent K+ channels in the phylum. The results reinforce the continuity of the general properties of the voltage-dependent K+ currents across the phyla. Unfortunately, the results shed little light on the presence or nature of the voltage-dependent inward currents of platyhelminth muscle.

V. FUNCTIONS OF THE DELAYED RECTIFIER CURRENT

A. GENERAL DELAYED RECTIFIER CURRENT FUNCTIONS

As demonstrated in the schistosome fibers, delayed rectifier currents are the source of outward rectification. They stabilize the membrane by protecting against drastic steady-state voltage responses to depolarizing currents, although they usually activate too slowly to inhibit action potential generation via fast, voltage-dependent inward currents. Specifically, it has been shown that delayed rectifier currents are responsible for tempering the amplitude of depolarizing slow waves. Delayed rectifier currents have also been shown to affect repolarization of the membrane after action potentials.

1. SLOW RECTIFICATION: CREATING PLATEAUS IN SLOW-WAVE DEPOLARIZATIONS

Some cells exhibit slow oscillations of membrane potential, which may or may not have action potentials superimposed. Canine colonic smooth muscle exhibits such slow wave activity and the depolarizing phase plateaus when the delayed rectifier current is activated to offset the inward current being mediated by voltage-gated Ca²⁺ channels (Cole & Sanders, 1989). The delayed rectifier current can provide a useful rectification in response to such slow depolarizing currents because of its inactivation characteristics. Although the delayed rectifier current is

often not able to offset fast depolarizations because of relatively slow activation, it is able to offset slower, sustained depolarizations because of relatively slow inactivation. Further, in some instances, a portion of the current is not subject to inactivation and is therefore available to provide long-term outward rectification even in response to a slow depolarization which might cause the steady-state inactivation of other currents (Okabe, Kitamura & Kuriyama, 1987; Numann, Wadman & Wong, 1987; Beech & Bolton, 1989b).

2. REPOLARIZATION AFTER ACTION POTENTIAL: CONTROLLING SPIKE DURATION

In some cell types, delayed rectifiers provide the driving force that repolarizes the membrane after action potentials (Barish, 1986; Cole & Sanders, 1989; Beech & Bolton, 1989a), and it has been directly demonstrated that altering the activation kinetics of the delayed rectifier current will alter the duration of the action potential (Suzuki, Nishiyama & Inomata, 1963; Osa, 1974). In these cells, the activation kinetics of the delayed rectifier current determines the length of the action potential. For example, the delayed rectifiers are slow (\$\tau_{act} \approx 1000 ms)\$ and the action potentials are long (duration \approx 1000 ms) in amphibian cardiac muscle (Hume & Giles, 1983; Simmons, Creazzo & Hartzell, 1986), while in the smooth muscle of

rabbit portal vein (Beech & Bolton, 1989b), delayed rectifiers are faster (\$\tau_{act}\$\approx 100 ms)\$ and the action potentials shorter (duration \approx 100 ms). In many neurons, very fast delayed rectifier currents (\$\tau_{act}\$ from 1-10 ms) are responsible for keeping action potentials very short (duration from 1-10 ms)(for example, Connor, 1975; Galvan & Sedlmeir, 1984; Belluzzi, Sacchi & Wanke, 1985).

B. CONSIDERATION OF THE FUNCTION OF THE DELAYED RECTIFIER CURRENT IN THE SCHISTOSOME MUSCLE

Delayed rectifier currents have been identified in a huge variety of cells, including most nerve and muscle cells investigated and both excitable and non-excitable cell types. The demonstrated functions of these currents are in some cases related to modulation of slow wave electrical activity and in other cases related to the modulation of action potentials.

until the presence or absence of electrical excitability or slow wave electrical activity is determined in these fibers, discussion of the function of the delayed rectifier current in the schistosome muscle is only conjecture. However, a look at the properties of the current might provide some clues to its function. The properties of the schistosome delayed rectifier current would allow it to perform either of the functions that delayed rectifiers have been directly demonstrated to

fulfill, either in the modulation of slow wave activity or in the control of spike duration.

1. INACTIVATION CHARACTERISTICS: THE ABILITY TO PROVIDE MAINTAINED RECTIFICATION

The delayed rectifier current described here is among the slowest and least completely inactivating described, with a τ_{inact} in the 5 s range and over 40% non-inactivating. In response to either a maintained depolarizing current or a slow depolarizing current, the delayed rectifier current of these fibers could provide a maintained rectification. For example, even after 20 seconds of a sustained or slow depolarization, almost half of the maximal current mediated by these channels would still be flowing.

2. ACTIVATION RATE: THE ABILITY TO CONTROL SPIKE DURATION

If the schistosome delayed rectifier current is the agent of action potential repolarization, the action potentials would be limited to between 10-20 ms, as deduced from the correlation that exists between the τ_{act} and the duration of action potentials in other such cells.

VI. FUNCTIONS OF THE "A" CURRENT

A. GENERAL "A" CURRENT FUNCTIONS

"A" currents have been demonstrated to delay or inhibit the initiation of an action potential in response to a depolarization, to lengthen the interval between action potentials, and to shorten the duration of the action potential. If they are available from the resting potential and fast enough, they can delay or inhibit the initiation of an action potential in response to a depolarization from rest. An "A" current can also lengthen the interval between action potentials, if it is recruited by the hyperpolarization that follows action potentials. Lastly, if they inactivate slowly enough, they can play a role in action potential repolarization.

1. FAST RECTIFICATION: DELAYING THE INITIATION OF ACTION POTENTIALS

It has been demonstrated that by supplying a fast and transient rectification, the "A" current can create a latency between the onset of depolarization and the initiation of an action potential mediated by voltage-gated inward currents (Getting, 1983; Segal, Rogawski & Barker, 1984). With membrane depolarization, the "A" current quickly activates, slowing the rate of depolarization and, therefore, increasing the time required for the

depolarization to reach threshold and initiate an action potential.

Fulfilling a similar function, fast inward currents have been described in crustacean coxal receptors which have fast voltage-gated Na⁺ channels but do not fire action potentials in physiological conditions (Mirolli, 1981).

Normally, the formation of action potentials is inhibited by the fast hyperpolarizing current that is activated in response to any depolarization, but if these fast K⁺ currents are blocked, action potentials can be elicited.

The role of "A" currents in controlling the rate or the extent of the initial depolarization (i.e., the latency period) depends on: 1) the kinetics of their activation and 2) the voltage-dependence of their inactivation. To provide such a shunting depolarization, the channels mediating the "A" current must activate at least as quickly, if not more quickly, than the channels mediating the inward current. is also necessary that the channels mediating the "A" current not be completely steady-state inactivated at the resting potential, so that a significant portion of the current is available. Indeed, in each of the systems where the "A" current has been demonstrated to fulfill such a role the current has a very fast τ_{act} (<1 ms in Mirolli, 1981; <5 ms in Getting, 1983; <5 ms in Segal, Rogawski & Barker, 1984) and the relationship between the cell's resting potential and the V_{50} of inactivation predicts near 50%

activation. Also, the extent of the delay that they create will depend on the rate of their inactivation. As long as the "A" current is activated, it will inhibit action potential formation, but as it inactivates, the depolarizing current will be unopposed (Segal, Rogawski & Barker, 1984). Therefore, a more quickly inactivating "A" current will delay the initiation of action potentials for only a short period, while a more slowly inactivating current can provide a longer delay.

2. AFTER-SPIKE RECTIFICATION: LENGTHENING THE INTERSPIKE INTERVAL

It has also been demonstrated that the "A" current can lengthen the duration of the interval between successive action potentials (Getting, 1983; Segal, Rogawski & Barker, 1984). When the "A" current is active, the interspike interval is longer; When the "A" current is inactive the interspike interval is shorter.

The role of the "A" current in controlling the interspike interval is again dependent on fast activation, but is not as dependent on the voltage-dependence of inactivation. This function does not require activation at the resting potential, since the channels may be activated by the hyperpolarization that often follows action potentials. The speed, as well as the extent of activation, is enhanced by the after-spike hyperpolarization, since the

time constant of activation is faster from more hyperpolarized potentials. Therefore, an "A" current that may activate too slowly from the resting potential or may be too inactivated at the resting potential to inhibit the formation of an action potential in response to an initial depolarization could still lengthen the interspike interval because the hyperpolarization following the first action potential would speed the activation kinetics and recruit a greater portion of the current.

3. REPOLARIZATION AFTER ACTION POTENTIAL: SHORTENING SPIKE DURATION

It has been demonstrated that the "A" current can play a key role in mediating the repolarizing phase of an action potential (Galvan & Sedlmeir, 1984; Giles & Van Ginneken, 1985). Although this function is typically assigned to delayed rectifier currents, the selective blockade of the "A" current in some cells results in a substantial lengthening of the action potential.

The critical parameter in determining an "A" current's ability to serve such a function is the time course of its inactivation. For example, "A" currents with a τ_{inact} of 5 ms could not be involved in action potential repolarization in a cell with an action potential 100 ms in duration. This function has only been demonstrated in cells with relatively

slowly inactivating "A" currents ($\tau_{inact} \approx 100$ ms in Galvan & Sedlmeir, 1984; ≈ 100 ms in Giles & Van Ginneken, 1985).

B. CONSIDERATION OF THE FUNCTION OF THE "A" CURRENT IN THE SCHISTOSOME MUSCLE

This consideration of their function demonstrates why
"A" currents have typically been associated with
excitability and are thought of as a practically ubiquitous
feature of excitable cells—all of the demonstrated
functions of the "A" current are related to modulation of
action potentials. Until the presence or absence of
electrical excitability is confirmed in these fibers,
discussion of the function of the "A" current in the
schistosome muscle is only conjecture. However, a
consideration of the properties of the current might provide
some clues to its possible function.

The schistosome muscle "A" current is among the fastest activating "A" currents with a τ_{act} in the 1 ms range, certainly fast enough to provide significant fast rectification under conditions in which the current is activated. The fast rate of inactivation of this current dictates that it could have little effect on the repolarization phase of an action potential, unless that action potential is atypically short for a smooth muscle fiber.

This consideration only takes into account the functions of "A" currents that have actually been demonstrated in various cells, all of which are associated with excitability and only eliminates some of those functions as unlikely on the basis of measured parameters of the schistosome "A" current. It is certainly possible that the "A" current in schistosome performs an as-yet-undemonstrated function that may or may not be associated with excitability.

1. RELATIONSHIP BETWEEN RESTING POTENTIAL AND V_{50} : THE ABILITY TO PROVIDE RECTIFICATION FROM THE RESTING POTENTIAL

As mentioned, critical to the function of the "A" current, or any current for that matter, is the normal relationship between the resting potential of the cell and the voltage-dependence of inactivation for the current. This points out the fact that the resting potential of the cell is important in determining how these inactivating currents will function in the cell. There is evidence that the resting potential of the schistosome muscle fibers in situ may be in the -30 mV range. Studies on intact schistosomes attribute a resting potential near -30 mV to the muscle in situ (Bricker, Pax & Bennett, 1982), and these studies of the isolated fibers yielded a potential of -22 mV. Further, many other invertebrate muscle types display less drastic membrane potentials than typical neurons. In

relationship to the membrane potential, the V_{50} for inactivation of the "A" current is near -50 mV. If the resting membrane potential of these cells is really near -30 mV, then only a very small portion, less than 20%, of the channels would be available for activation in a resting situation.

It has been shown that divalent cations can affect some of the voltage-dependent characteristics of "A" currents in smooth muscle (Beech & Bolton, 1989a) and in neurons (Galvan & Sedlmeir, 1984; Numann, Wadmann & Wang, 1987), altering the V_{30} of inactivation. These effects of divalent cations are not attributable to a Ca2+- or divalent cationdependence of the current, since the current is still present in the absence of all divalent cations and Cd2+ is more efficacious at producing the effects than is Ca²⁺. Instead, the alterations in the voltage-dependence of the "A" currents are ascribed to the effect that divalent cations can have on local surface potentials (Beech & Bolton, 1989a). Although I designed no experiments to specifically investigate the effects of divalent cations on the voltage-dependence of the "A" currents in schistosome muscle, the presence of extracellular Ca2+ in physiological ranges (0.4 to 4 mm) caused no measurable alteration in voltage-dependence as compared to those in the absence of Ca²⁺.

The lack of divalent effects on the schistosome "A" current can be explained by the relatively gentle slope of its voltage-dependency relationship (k for inactivation = 14 mV). It has been hypothesized that the stronger voltagedependence makes such currents more sensitive to alterations in surface potentials caused by divalent cations (Beech & Bolton, 1989a). "A" currents generally show steep voltage dependence, with typical inactivation k's ranging between 4-6 mV (Hagiwara, Yoshida & Yoshi, 1981; Galvan & Sedlmeir, 1984; Zbicz & Weight, 1985; Wu & Haugland, 1985), and only the steepest of these have been demonstrated to be affected in this way by divalent cations (Beech & Bolton, 1989a). Delayed rectifier currents generally show more shallow voltage-dependence, with typical inactivation k's ranging between 7-9 mV (Adrian, Chandler & Hodgkin, 1970; Cahalan et al., 1985; Gustin et al., 1986; Yamamoto, Hu & Kao, 1989; Kotlikoff, 1990), with the steepest example being 6 mV (Marchetti, Premont & Brown, 1988). As predicted, the voltage-dependent characteristics of delayed rectifiers have never been shown to be affected by divalent cations and have been shown in many instances to be unaffected (Beech & Bolton, 1989a; Mayer & Sugiyama, 1988).

If, in fact, the resting potential of these cells in the animal is in the -30 mV range and physiologically relevant concentrations of divalent cations do not affect the voltage-dependence of the "A" current, the relative

unavailability of the current from rest would not allow it to play a significant role in fast rectification in response to depolarizing currents from the resting potential. could not be expected to shunt or dampen the voltage response to depolarizing current and control the initial rate of depolarization (read, "interval to first action potential" if, in fact, this cell discharges action potentials). So, hyperpolarization from resting potential would be required for significant availability of this "A" current. As mentioned previously, such currents can be recruited by the hyperpolarization following an action potential and, so, lengthen the interval between spikes. The time and voltage-dependent parameters of the schistosome "A" current are such that it could fulfill this function. However, since it is not clear if these muscles do, in fact, fire any action potentials, it is untenable to speculate that their function is such. Even if these fibers do not fire action potentials, it is worthwhile to consider that any stimulus causing activation of the delayed rectifier channels would lead to hyperpolarization of the fiber and increase the amount of "A" current available in the event of any subsequent depolarization.

2. RATE OF INACTIVATION: THE ABILITY TO CONTROL SPIKE DURATION

The "A" current described here inactivates fairly quickly with a \(\tau_{inact}\) in the 10 ms range. This means that this current could only be involved in action potential repolarization for a fairly fast action potential, certainly not contributing much to repolarization of an action potential lasting longer than 20 ms. Since the action potentials of smooth muscle are typically much longer than this, the fast inactivation of the schistosome "A" current would make it very ineffective for the purpose of action potential repolarization.

SUMMARY

- 1) Individual frayed contractile fibers dispersed from adult schistosomes have a resting membrane potential of \approx -22 mV.
- 2) The fibers display a marked time-dependent outward rectification in response to injected current which is attenuated by the replacement of intracellular K⁺ with Cs⁺. Under these conditions, the fibers do not produce action potentials in response to depolarizing current injections, even if the outward rectification is blocked.
- 3) The fibers have at least two distinct voltage-dependent K+ currents; a slow current which is in the delayed rectifier class and a fast current which is in the "A" class. The properties of these two currents are summarized in Table 2 on page 73.
- 4) The fibers do not show any voltage-dependent inward currents, even with the outward currents blocked, high extracellular Ca²⁺ or Ba²⁺, hyperpolarizing prepulses and a variety of intracellular additives.
- 5) Individual fibers contract in response to exposure to high K^+ if Ca^{2+} is present in the extracellular medium. The K^+ -induced contractions are blocked by 10 μM

nicardipine. This suggests the presence of voltage-gated calcium channels in the fibers, despite the failure to measure voltage-dependent inward currents with in voltage clamp.



APPENDIX I

PREPARATION OF DISPERSED MUSCLE FIBERS FROM THE SCHISTOSOME

The procedure for the preparation of dispersed muscle fibers from schistosomes provided in the Materials and Methods is actually the culmination of a fairly long development process. Throughout the development of this procedure, the parasites were the Puerto Rican strain of <u>S. mansoni</u>, removed 45-60 days after infection from the portal and mesenteric veins of Swiss Webster mice. Before papain was discovered to be an effective enzyme for the procedure, various combinations of collagenase, elastase, pronase, dispase, trypsin and chymotrypsin were also tested, but they yielded few intact cells.

The earliest version of the procedure which produced intact, contractile fibers suitable for electrophysiological studies primarily utilized the culture medium RPMI-1640 (Gibco, Grand Island, NY, USA), which had proven to be a very suitable medium for the in vitro maintenance of the whole worms. After removal from the host, 15-25 paired adult parasites were placed directly into supplemented RPMI (Table 4) at 37.C and allowed to incubate for 15 min. The

worms were rinsed several times, placed on a glass slide and chopped coarsely with a razor blade, approximately 40 strokes with the razor. The resultant pieces were incubated for 15 min in the supplemented RPMI to which was added 0.1% bovine serum albumin (BSA), at which point the medium was drawn off and replaced with 5 ml of the same medium to which had been added 6 mg/ml papain (Sigma Co.). This preparation was incubated for 30 min, then gently drawn back and forth through the tip of a Pasteur pipet approximately 20 times. After settling had occurred, 4 ml of the supernatant fraction was removed and replaced with 2 ml of the supplemented RPMI with BSA but without papain, thus reducing the papain concentration by %. This preparation was then incubated for 90 min and then once again agitated by passage through the tip of a pasteur pipet 20-40 times. Approximately 100 μ l of this suspension was placed in the middle of the 500 µl culture dishes and given 15 min to settle, at which point the dish was rinsed 10 times the dish volume of supplemented RPMI. The plated cells were then incubated in the supplemented RPMI at 37.C in an air atmosphere until used, usually within 6 hr. This form of the preparation yielded fibers that contracted reliably in response to osmotic stimulus, but rather unreliably in response to exposure to high extracellular K+.

A large reduction in the amount of papain and some slight alterations in the same basic procedure yielded a

larger number of dispersed fibers that were noticeably more extended. The worms were picked and chopped as per the last procedure, but the pieces were placed in 1 ml of the supplemented RPMI to which had been added 0.1% BSA. 1 mm EGTA, 1 mm EDTA and 2 mm DTT as well as 1 mg/ml papain, pipetted 20 times then incubated at 37°C. At 15 min, this incubation medium was drawn off and replaced with 1 ml of the same medium and the worm parts were passed back and forth through a pasteur pipet 20 times, which usually caused a fairly significant dispersion. After 15 more minutes at 37°C, the cells were pipetted again and the incubation medium diluted 10 times with the same medium without papain. This suspension was then plated like before and, after 15-30 min for attachment of the fibers, the cells were rinsed 10 times in supplemented RPMI with 2 mm DTT, which was used as the culture medium.

The primary differences between the preparation yielded from this procedure and the one listed before it were that the resultant fibers were, on the average, longer and that the preparation was cleaner in terms of the amount of non-cellular or extracellular debris. In general, the morphological classes of contractile fibers described above were not altered, except that the frayed fibers and crescents were often longer. As a result of the decreased extracellular matrix, the fibers were generally easier to work with in electrophysiological experiments. The fibers

prepared in this manner displayed contractile responses like those prepared with earlier procedures: consistent contraction to osmotic stimulus, but apparently inconsistent contraction to high K^+ stimulus.

Eventually, it was discovered that the apparent high K+ contractions were, in fact, osmotically-induced. If the [K⁺] outside of a cell is altered while the [Cl⁻] remains constant, the resultant alteration in the K+ X Cl- product will result in ion and water fluxes across the cell membrane which can cause cell swelling and be very analogous to exposure of that cell to hypo-osmotic medium. In order to independently assess the effect of depolarization without fluxes of Cl and water, it is necessary to keep the K X Cl product constant in the control and the experimental When the K⁺ X Cl⁻ product was controlled, the fibers no longer responded to the high K+ stimulation, suggesting that the apparent high K+ responses had in fact been osmotically-induced. None of the preparation procedures using supplemented RPMI as the base medium yielded fibers that contracted consistently to the high K+ stimulation when the K X Cl product was controlled.

The next major modification in the procedure was the substitution of a DMEM-based medium for the RPMI-based medium. After a few other minor modifications, the procedure yielded fibers that contracted regularly in

response to high K^+ stimulation with the K x Cl product constant.

In this procedure, the one which is listed in the Materials and Methods, the parasites were removed and chopped in the same fashion as in the proceeding protocols, except that these steps were carried out using an culture medium of supplemented DMEM. After chopping, the pieces were incubated with gentle agitation on a shaker table for 45 min at 37 · C in the supplemented DMEM to which was added: 1 mm (EGTA), 1 mm (EDTA), 1 mm DTT, 0.1% BSA and 1 mg/ml papain. After 45 min, the enzymatic medium was removed and the worm pieces washed with three exchanges of enzyme-free incubation medium and then incubated for an additional 10 min in the enzyme-free supplemented DMEM. The worm pieces, still intact for the most part, were then broken up by forcing them back and forth through the orifice of a pasteur pipet 75 to 100 times. The resultant suspension was then plated, allowed to settle and rinsed with supplemented DMEM which was used as the incubation medium.

One of the focal differences of this procedure, besides the substitution of DMEM for RPMI, is the fact that the worm pieces are not pipetted, and therefore not substantially broken up, until after the enzyme containing medium has been replaced, when the incubation medium is relatively enzymefree. Theoretically, with this procedure the individual dispersed fibers have a drastically reduced exposure to

enzyme than with any previous method. This method yielded fibers which were much like those from the RPMI-based procedure in shape and size, but the fibers contracted reliably in response to high K⁺ stimulation when the K⁺ X Cl⁻ product was controlled.

Tight-seal, whole-cell recordings have been made on fibers with supplemented RPMI, supplemented DMEM, inorganic versions of RPMI and DMEM, and several other variations of each serving as the extracellular medium. The K+ currents showed no detectable differences regardless of the extracellular medium, and the lack of measurable inward currents was also uniform in all of these extracellular media, with all of these slightly varied dispersion protocols.

TABLE 4. Primary Media Used in Various Isolation Procedures.

	Supplemented RPMI	Supplemented DMEM
K+	5.4	4.1
Na ⁺	114.0	82.6
Ca ²⁺	0.4	3.6
Mg ²⁺	0.4	3.3
cī -	108.0	93.7
so ₄ -	0.4	3.3
PO	5.6	0.04
NO3-	0.9	
5-HT		0.01
Glucose	11.1	79.9
HEPES	20.0	15.0
L-Asparagine	0.4	
L-Arginine	1.2	0.3
L-Aspartic Acid	2.2	
L-Aspartic Acid L-Cystine	0.2	0.2
L-Cystine L-Glutamic Acid	0.1	
L-Glutamine	2.0	3.0
	0.1	0.5
Glycine	0.1	0.2
L-Histidine		0.2
L-Hydroxyproline	0.2	0.6
L-Isoleucine	0.4	
L-Leucine	0.4	0.6
L-Lysine	0.2	0.8
L-Methionine	0.1	0.2
L-Phenylalanine	0.1	0.3
L-Proline	0.2	
L-Serine	0.2	0.3
L-Threonine	0.2	0.6
L-Tryptophan	0.02	0.1
L-Tyrosine	0.01	0.4
L-Valine	0.2	0.6
Biotin	0.2 mg/ml	
D-Ca-Pantothenate	0.3 mg/ml	3.0 mg/ml
Choline Chloride	3.0 mg/ml	3.0 mg/ml
Folic Acid	1.0 mg/ml	3.0 mg/ml
Myo-Inositol	35.0 mg/ml	5.4 mg/ml
Niacinamide	1.0 mg/ml	3.0 mg/ml
Orotic Acid		37.5 mg/ml
PABA	1.0 mg/ml	
Pyroxidine-HCl	1.0 mg/ml	3.0 mg/ml
Riboflavin	0.2 mg/ml	0.3 mg/ml
Thiamine	1.0 mg/ml	3.0 mg/ml
Vitamine	$5.0 \mu \text{g/ml}$	
ATCHMIN D15	2.0 WR/ mT	

APPENDIX II

COMPARISON OF VOLTAGE-DEPENDENT K+ CURRENT PROPERTIES

This appendix is built around two tables, each of which furnish some of the quantitative properties of voltage—dependent K+ currents; Table 5 details delayed rectifier currents and Table 6 enumerates "A" currents. The tables are not intended to be exhaustive, but they are intended to supply examples from a fairly wide range of the animal phyla. Further, the tables are not intended to be precise, rather their purpose is to be accurate in depicting the relative physiological characteristics. In many cases, the data were not available to provide a complete entry for a given cell type, but the presence of a cell type in the table reflects that there is fairly conclusive evidence for a current of this class in that cell type.

The values given are not precise values, but rather indexes that strive to standardize for the varied conditions as described below:

tau is the standard concept of time constant (τ).

The τ 's were rounded to values of 1 ms, 5 ms, 10

ms, 50 ms, 100 ms, etc... All τ 's are standardized to approximate the expected value at 25°C, assuming a Q_{10} of 3. The various τ 's are also intended to reflect the time constant at a given test potential: 1) +50 mV for delayed rectifier activation and inactivation, 2) +10 mV for "A" activation and inactivation and 3) -50 mV for delayed rectifier relaxation. Although these experiments may reflect the use of various holding potentials, no compensation is made for this variance.

t'ld is the threshold of activation.

- V_{50} is the voltage of half activation or half inactivation as determined by a Boltzmann distribution (see Equation 1).
 - k is the slope factor for the voltage-dependence of activation or inactivation as determined by the Boltzmann distribution.
- % non is the percentage of the delayed rectifier current that does not inactivate.

4-AP and TEA are values reflecting the sensitivity of the currents to these compounds. The value represents the mM concentration of the compound that produces a block of 40-60% of the current. If the value is preceded by "NB" it represents the highest concentration that was tested that had no significant effect on the current.

			Ant ivet	at ion			Thert	Tractivation	5	_	Valad			
	Specific	tau	t'ld V50	450 V50	٧.	tau	tau2	V50	. ×	•	tau	4-AP	TEA	
Animal	Cell Type	(ms)	(mV)	(MV)	(mV)	(BB)	(ms)	(mV)	(mV)	non	(ms)	(mm)	(mM)	reference
	Saccharomyces												20	Gustin et al. 1986; Kung 1989
Sarcodina	Actinocoryne											10	10	Febvre-Chevalier et al. 1986, 1989
Ciliate	Stentor													Wood 1982
Ciliate	Paramecium	S												Satow et al. 1980; Machemer 1979
Ciliate	Stylonychia	10	-30											Deitmer 1984, 1989
Jellyfish	Nerve													Meech 1989
Jellyfish	Nerve		-20											Anderson 1987, 1989
Jellyfish	Cnidocyte													Anderson et al. 1987; Anderson 1989
Comb jelly	Smooth muscle	100	-20									5	s	Anderson 1984; Dubas et al. 1988
Comb jelly	Radial Muscle	20											20	Bilbaut et al. 1988, 1989
comb jelly	Egg cell	20	-10								_	NB 1		Hagiwara et al. 1981
Flatworm	Somatic Muscle	10	-10	20	11	2000		-10	10.3	42	10	10	NB 10	
Polycheat	Giant axon	S	-30	-10										Binstock et al. 1967; Goldman 1973
Sea slug	Nerve somata	100	-20			2000		-50		25				Connor et al. 1971b
Sea hare	Bag cell neuron	10				200					10		9	Strong et al. 1975; Kaczmarek 1984
Sea hare	Bag cell neuron	20				1000					20		9	Strong et al. 1975; Kaczmarek 1984
Sea hare	Ink cell neuron	10	-20			200		-25					25	Byrne 1980a, 1980b
	Ganglion	10	-30	0							_	NB 3	20	Neher 1971; Thompson 1977
	Photoreceptors										_	NB 1		Lisman et al. 1978
	Giant axon	-	-50					-40				01		Connor 1975; Quinta-Ferreira 1982
	Flight muscle	20	-30			10000					_	NB 10		Salkoff et al. 1983
	Body muscle	100	-20	01	9	2000		-20	œ		20		10	Wu et al. 1985
	Retinal h'zntl	100	-20										20	Tachibana 1983
	Hepatocyte	S	-10			1000		-45	9.6		10	-		Marchetti et al. 1988
Axolotl	Merve	-									s			Barish 1986
	Striated muscle	10	-50	-10		1000		-40	7.5		100			Adrian et al. 1970a, 1970b
	Cardiac muscle	1000	-30	-10		10000					1000			Simmons et al. 1986
	Cardiac muscle	1000	-40	-15	11.4									Hume & Giles 1983; Hume et al. 1986
	Macrophage	ß	-50	-20		200					100	S		Ypey et al. 1984
	SNS neuron	'n	9	-5										Galvan et al. 1984; Belluzzi 1985
	H'camp neuron	100	-50	-35		2000		09-			_	NB 5	25	Segal & Barker 1984; Segal 1984
Guinea pig			-20					-35	0					Klockner at al. 1985
Guinea pig	H'camp neuron	100	0			2000		-90		20			10	Numann et al. 1987
Guinea pig	Taenia coli	S	-10	20		100	1000	-50	6	10	10			Yamamoto et al. 1989
Rabbit	SA node p'maker		-50	-25	7.4	200					100			Shibaski 1987

								IAE	TABLE 5, cont'd	2	ביב					
	Comparison	ris		of t	he	Prope	rties	3 of	Var	ion	s De	laye	d Re	ctifier	of the Properties of Various Delayed Rectifier Currents.	
			Acti	Activation	ū		Inact	Inactivation	lon		Relax					
	Specific	tau	t'1d	V50	t'ld V50 k	tau		V50	×	•	tau	tau2 V50 k % tau 4-AP TEA	TEA			
Animal	Cell Type	(ms)	(MV)	(BV)	(mV)	(me)	(ms)	(MV)	(mV)	non	(ms)	(mH)	(mm)	(ms) (mV) (mV) (mV) (ms) (ms) (mV) (mV) non (ms) (mH) (mH) reference		
Rabbit	Ileum muscle		-20									NB 1	10	NB 1 10 Ohya et al. 1986	1986	
Rabbit	Artery muscle	20				2000		-20		Q		7	100	100 Okabe et al. 1987	. 1987	
Rabbit	Vein muscle	10	9			1000	0009	-30	7	25		S	NB 5	Beech et al	NB 5 Beech et al. 1989a, 1989b	д
Cat	Artery muscle	ĸ	-20			2000						10	100	10 100 Bonnet et al. 1991	11. 1991	
bod	Colonic myocyte	20	-15			2000						NB 20		10 Cole et al. 1989	1989	
Dog	Airway muscle	₩	-20			100	100 1000 -5 7.5 15	-5	7.5	15				Kotlikoff 1990	066	
Bunan	T-lymphocyte	2	-55	-35	-35 5.2	100		-65	-65 7.5		20			Cahalan et al. 1895	al. 1895	

	Comparison of the	risc	o uc)f t		Properties	tie	s of	Var	Various	"A" Currents.
			Acti	Activation	e o	Inac	Inactivation	lon			
	Specific	tau	t'1d	1 V50	, k	tau	V50	×	4-AP	TEA	
Animal	Cell Type	(ms)	(mV)	(BV)) (mV)	(ms)	(mV)	(mV)	(mM)	(mM)	reference
Ciliate	Stylonichia		-35								Deitmer 1984, 1989
Jellyfish	Cnidocyte	1	-10			2			7		Anderson & McKay 1987; Anderson 198
Jellyfish	Nerve										Anderson 1987; Anderson 1989
Jellyfish	Cnidocyte	-	-10								Anderson & McKay 1987; Anderson 198
Jellyfish	Merve										Hagiwara et al. 1961; Meech 1989
Comb jelly	Long. muscle										Bilbaut et al. 1988, 1989
Comb jelly	Radial muscle	3	-30			10	-50		7	NB 50	Bilbaut et
Comb jelly	Smooth muscle	10	9			100					al. 19
Comb jelly	Egg cell	S	-20			10	-40	•	s		Hagiwara et al. 1981
Flatworm	Somatic muscle	-	-40		0 12.4	10	-50	14.1	-	KB 10	
Sea slug	Nerve somata	10	-50			100	-75		100		Connor & Stevens 1971b
Sea hare	Ink cell neuron	S	-50			20	-55		10		Byrne 1980a, 1980b
Sea hare	Bag cell neuron		-55				-70				Kaczmarek et al. 1984; Strong 1985
Snail	Interneuron	10	09-			100	-65				Getting 1983
Snail	Ganglion	10	-50	-40	_	200	-70		2	NB	Thompson 1977
Crab	Photorecetors								-		Lisman et al. 1978
Crab	Giant axon	1	-60			S	-65		70		Connor 1975; Quinta-Ferreira 1982
Crab	Coxal receptors	7	-65			2			S	NB	Mirolli 1981
Fly	Flight muscle	10	-50			100			10		Salkoff et al. 1983
Fly	Larval muscle	10	-30			20	-40	4.5			Wu et al. 1985
Fly	Myotubes	-	-30			10	-30	4.9	S		Solc et al. 1987
Fly	Neurons					100	-75	9.4	S		Solc et al. 1987
Fish	Retinal h'zntl	2	-25			200	-35		10	NB	Tachibana 1983
Frog	Stomach muscle										Walsh et al. 1987
Frog	Sympathetic	2	-60			20	-65				Adams et al. 1982
Frog	Aud. hair cell	S	-50			20			10	NB	Lewis et al. 1983
Rabbit	Myocytes	S	-20	-5	5 5	100	-30	7.8	m		Giles et al. 1985
Rabbit	Vein muscle	10	-65			100	-80	5.1	S	NB	Beech et al. 1989a, 1989b
Guinea pig	H'camp neuron	S	-50			200	-60	3.2	0.5	NB 10	Sbicz et al. 1985
Guinea pig		1	-60	-35	5 11.3	2	-85	7.5	7	NB 10	Halliwell et al. 1986; Numann 1987
Guinea pig		ß	-60	-30	•	100	-75		S		Kasai et al. 1986
Rat	H'camp neuron	S	-60	-30	_	20	-70		S	NB	Seagl & Barker 1984; Segal 1984
Rat	SNS neuron	1	-60	-30	_	20	-80	7.3	-	NB	Galvan et al. 1984; Belluzzi 1985
Rat	Locus coeruleus		-60			100	-60		-		Williams et al. 1984
Rat	Ventr. myocyte	S	-30			10			7		Josephson et al. 1984
Dat	Nodose ganglia	10				20					Coner et al. 1985

BIBLIOGRAPHY

BIBLIOGRAPHY

- Adams, P.R., Brown, D.A. & Constanti, A. (1982). M-currents and other currents in bullfrog sympathetic neurons.

 <u>Journal of Physiology</u> 330:537-572.
- Adrian, R.H., Chandler, W.K. & Hodgkin, A.L. (1970a). Slow changes in potassium permeability in skeletal muscle.

 <u>Journal of Physiology</u> 208:645-668.
- Adrian, R.H., Chandler, W.K. & Hodgkin, A.L. (1970b).

 Voltage clamp experiments in striated muscle fibers.

 Journal of Physiology 208:607-644.
- Anderson, P.A.V. (1984). The electrophysiology of single smooth muscle cells isolated from the ctenophore Mnemiopsis. Journal of Comparative Physiology 154:257-268.
- Anderson, P.A.V. (1987). Properties and pharmacology of a TTX-insensitive sodium current in neurones of the jellyfish Cyanea capillata. Journal of Experimental Biology 133:231-248.
- Anderson, P.A.V. (1989). Ionic Currents of the Scyphozoa. In: <u>Evolution of the First Nervous Sysytems</u>, Ed: P.A.V. Anderson, Plenum Press, New York, NY, pp. 267-280.
- Anderson, P.A.V. & McKay, M.C. (1987). The electrophysiology of cnidocytes. <u>Journal of Experimental Biology</u> 133:215-230.
- Barish, M.E. (1986). Differentiation of voltage-gated potassium current and modulation of excitability in cultured amphibian spinal neurons. <u>Journal of Physiology</u> 375:229-250.
- Barker, L.R., Bueding, E. & Timms, A.R. (1966). Possible role of acetylcholine in <u>Schistosoma mansoni</u>. <u>British Journal of Pharmacology</u> 26:656-665.
- Barnes, R.S.K., Calow, P. & Olive, P.J.W. (Eds.) (1988): The Invertebrates: A New Synthesis. Blackwell Scientific Publications, Oxford, England.

- Bean, B.P., Sturek, M., Puga, A. & Hermsmeyer, K. (1986). Calcium channels in muscle cells isolated from rat mesenteric arteries: Modulation by dihydropyridine drugs. <u>Circulation Research</u> 59:229-235.
- Beech, D.J. & Bolton, T.B. (1989a). Two components of potassium current activated by depolarization of single smooth muscle cells from the rabbit portal vein. <u>Journal of Physiology</u> 418:293-309.
- Beech, D.J. & Bolton, T.B. (1989b). A voltage-dependent outward current with fast kinetics in single smooth muscle cells isolated from rabbit portal vein. <u>Journal of Physiology</u> 412:397-414.
- Belluzzi, O., Sacchi, O. & Wanke, E. (1985a). A fast transient outward current in the rat sympathetic neurone studied under voltage clamp conditions.

 <u>Journal of Physiology</u> 358:91-108.
- Belluzzi, O., Sacchi, O. & Wanke, E. (1985b). Identification of a delayed potassium and calcium currents in the rat sympathetic neurone under voltage clamp. <u>Journal of Physiology</u> 358:109-130.
- Bennett, J.L. & Bueding, E. (1971). Biogenic amines in Schistosoma mansoni. Comparative Biochemistry and Physiology 39:A859-A867.
- Bennett, J.L. & Bueding, E. (1973). Uptake of 5-HT by Schistosoma mansoni. Molecular Pharmacology 5:542-545.
- Bilbaut, A., Hernandez-Nicaise, M.L., Leech, C.A. & Meech, RW (1988). Membrane currents that govern smooth muscle contraction in a ctenophore. Nature 331:533-535.
- Bilbaut, A., Hernandez-Nicaise, M.L. & Meech, R.W. (1989).
 Ionic Currents in Ctenophore Muscle Cells. In:
 Evolution of the First Nervous Systems, Ed: P.A.V.
 Anderson, Plenum Press, New York, NY, pp. 299-314.
- Binstock, L. & Goldman, L. (1967). Giant axon of <u>Myxicola</u>: some membrane propeties as observed under voltage clamp. <u>Science</u> 158:1467-1469.
- Blair, K.L. & Anderson, P.A.V. (1991). Tetrodotoxinsensitive sodium currents in flatworm neurons. <u>Society</u> for <u>Neuroscience Abstracts</u> 17:956.

- Blair, K.L., Day, T.A., Lewis, M.C., Bennett, J.L. & Pax, R.A. (1991). Studies on muscle cells isolated from Schistosoma mansoni: a calcium-dependent potassium channel. Parasitology 102:251-258.
- Bolton, T.B., Lang, R.J., Takewaki, T. & Benham, C.D. (1986). Patch and whole-cell voltage clamp studies on single smooth muscle cells. <u>Journal of Cardiovascular Pharmacology</u> 8:S20-S24.
- Bonnet, P., Rusch, N.J. & Harder, D.R. (1991).
 Characterization of an outward K+ current in freshly dispersed cerebral arterial muscle cells. <u>Pfluger's Archives</u> 418:292-296.
- Bricker, C.S., Pax, R.A. & Bennett, J.L. (1982).

 Microelectrode studies of the tegument and subtegumental compartments of male <u>Schistosoma mansoni</u>: anatomical location of sources of electrical potentials. <u>Parasitology</u> 85:149-161.
- Bullock, T.H. & Horridge, G.A. (1965): Structure and Function in the Nervous System of Invertebrates. W.H. Freeman and Company, London, England.
- Byrne, J.H. (1980a). Analysis of ionic conductance mechanisms in motor cells mediating inking behavior in <a href="https://doi.org/10.103/phi/doi.
- Byrne, J.H. (1980b). Quantitative aspects of ionic conductance mechanisms contributing to firing pattern of motor cells mediating inking behavior in <u>Aplysia</u> californica. Journal of Neurophysiology 43:651-668.
- Cahalan, M.D., Chandy, K.G., DeCoursey, T.E. & Gupta, S. (1985). A voltage-gated potassium channel in human T lymphocytes. <u>Journal of Physiology</u> 358:197-237.
- Cole, W.C. & Sanders, K.M. (1989). Characterization of macroscopic outward currents of canine colonic myocytes. American Journal of Physiology 257:C461-C469.
- Connor, J.A. (1975). Neural repetitive firing: a comparative study of membrane properties of crustacean walking leg axons. <u>Journal of Neurophysiology</u> 38:922-932.
- Connor, J.A. & Stevens, C.F. (1971a). Inward and delayed outward membrane currents in isolated neural somata under voltage clamp. <u>Journal of Physiology</u> 213:1-20.

- Connor, J.A. & Stevens, C.F. (1971b). Voltage clamp studies of a transient outward current in gastropod neural somata. <u>Journal of Physiology</u> 213:21-30.
- Cooper, E. & Shrier, A. (1985). Single channel analysis of fast transient potassium currents from rat nodose neurons. <u>Journal of Physiology</u> 369:199-208.
- Day, T.A., Orr, N., Bennett, J.L. & Pax, R.A. (1993).

 Voltage-gated currents in muscle cells of <u>Schistosoma</u>

 <u>mansoni</u>. <u>Parasitology</u>, in press.
- Deitmer, J.W. (1984). Evidence for two voltage-dependent calcium currents in the membrane of the ciliate Stylonychia. Journal of Physiology 355:137-159.
- Deitmer, J.W. (1986). Voltage dependence of two inward currents carried by calcium and barium in the ciliate Stylonychia mytilus. Journal of Physiology 380:551-574.
- Deitmer, J.W. (1989). Ion Channels and the Cellular Behavior of Stylonychia. In: Evolution of the First Nervous

 Systems, Ed: P.A.V. Anderson, Plenum Press, New York,
 NY, pp. 255-265.
- Dubas, F., Stein, P.G. & Anderson, P.A.V. (1988). Ionic currents of smooth muscle cells isolated from the ctenophore <u>Mnemiopsis</u>. <u>Proceedings of the Royal</u> Society of London 233:99-121.
- Fatt, P. & Katz, B. (1953). The electrical properties of crustacean muscle fibers. <u>Journal of Physiology</u> 120:171-204.
- Febvre-Chevalier, C., Bilbaut, A., Bone, Q. & Febvre, J. (1986). Sodium-calcium action potetnial associated with contraction in the heliozoan <u>Actinocoryne contractilis</u>. <u>Journal of Experimental Biology</u> 122:177-192.
- Febvre-Chevealier, C., Bilbaut, A., Febvre, J. & Bone, Q. (1989). Membrane Excitability and Motile Responses in the Protozoa, with Particular Attention to the Heliozoan <u>Actinocoryne contractilis</u>. In: <u>Evolution of the First Nervous Systems</u>, Ed: P.A.V. Anderson, Plenum Press, New York, NY, pp. 237-253.
- Fetterer, R.H., Pax, R.A. & Bennett, J.L. (1977).

 <u>Schistosoma mansoni</u>: Direct method for simultaneous recordings of electrical and motor activity.

 <u>Experimental Parasitology</u> 43:286-294.

- Fetterer, R.H., Pax, R.A. & Bennett, J.L. (1980).
 Praziquantel, potassium, and 2,4-dinitrophenol:
 Analysis of their action on the musculature of
 Schistosoma mansoni. European Journal of Pharmacology
 64:31-38.
- Galvan, M. & Sedlmeir, C. (1984). Outward currents in voltage clamped rat sympathetic neurones. <u>Journal of Physiology</u> 356:115-133.
- Getting, P.A. (1983). Mechanisms of pattern generation underlying swimming in <u>Tritonia</u>. III. Intrinsic and synaptic mechanisms for delayed excitation. <u>Journal of Neurophysiology</u> 49:1036-1051.
- Giles, W.R. & Van Ginneken, A.C.G. (1985). A transient outward current in isolated cells from the crista terminalis of rabbit heart. <u>Journal of Physiology</u> 368:265-292.
- Goldman, L. & Schauf, C.L. (1973). Quantitative description of sodium and potassium currents and computed action potentials in Myxicola giant axons. Journal of General Physiology 61:361-384.
- Gustin, M.C., Martinac, B., Saimi, Y., Culberston, M.R. & Kung, C. (1986). Ion channels in yeast. <u>Science</u> 233:1195-1197.
- Hagiwara, S., Kusano, K. & Saito, N. (1961). Membrane changes of <u>Onchidium</u> nerve cell in potassium-rich media. <u>Journal of Physiology</u> 155:470-489.
- Hagiwara, S., Yoshida, S. & Yoshii, M. (1981). Transient and delayed potassium currents in the egg cell membrane of the coelenterate, <u>Renilla koellikeri</u>. <u>Journal of Physiology</u> 318:123-141.
- Halliwell, J.V., Othman, L.B., Pelchen-Matthews, A. & Dolly, J.O. (1986). Central action of dendrotoxin selective reduction of a transient K⁺-conductance in hippocampus and binding to localized acceptors. <u>Proceedings of the National Academy of Science, USA</u> 83:493-497.
- Hamill, O.P., Marty, A., Neher, E., Sakmann, B. & Sigworth, F.J. (1981). Improved patch-clamp techniques for high-resolution current recording from cells and cell-free membrane patches. <u>Pfluger's Archives</u> 391:85-100.
- Hillman, G.R. (1983). The neuropharmacology of schistosomes.

 Pharmacological Therapeutics 22:103-115.

- Hodgkin, A.L. & Huxley, A.F. (1952a). The components of membrane conductance in the giant axon of Loligo.

 Journal of Physiology 116:473-496.
- Hodgkin, A.L. & Huxley, A.F. (1952b). A quantitative description of membrane currents and its application to conduction and excitation in nerve. <u>Journal of Physiology</u> 117:500-544.
- Holy, J.M., O'Leary, K.A., Oaks, J.A. & Tracy, J.W. (1989). Immunocytochemical localization of the major glutathione s-transferases in adult <u>Schistosoma mansoni</u>. <u>Journal of Parasitology</u> 75:181-190.
- Hume, J.R. & Giles, W. (1983). Ionic currents in single isolated bullfrog atrial cells. <u>Journal of General Physiology</u> 81:153-194.
- Hume, J.R., Giles, W., Robinson, K., Shibata, E.F., Nathan, R.D., Kanai, K. & Rasmusson, R. (1986). A time- and voltage-dependent K+ current in single cardiac cells from bullfrog atrium. <u>Journal of General Physiology</u> 88:777-798.
- Josephson, I.R., Sanchez-Chapula, J. & Brown, A.M. (1984).

 Early outward current in rat single ventricular cells.

 <u>Circulation Research</u> 54:157-162.
- Kaczmarek, L.K. & Strumwasser, R. (1984). A voltage clamp analysis of current underlying cAMP-induced membrane modulation in isolated peptidergic neurons of <u>Aplysia</u>. <u>Journal of Neurophysiology</u> 52:340-349.
- Kasai, H., Kameyam, D., Yamaguchi, K. & Fukuda, J. (1986). Single transient K⁺ channels in mammary sensory neurons. <u>Biophysical Journal</u> 49:1243-1247.
- Klockner, U. & Isenberg, G. (1985). Action potentials and net membrane currents of isolated smooth muscle cells (urinary bladder of the guinea pig). Pfluger/s Archives 405:329-339.
- Kotlikoff, M.I. (1988). Calcium currents in isolated canine airway smooth muscle cells. <u>American Journal of Physiology</u> 254:C793-C801.
- Kotlikoff, M.I. (1990). Potassium currents in canine airway smooth muscle cells. <u>American Journal of Physiology</u> 259:L384-L395.

- Kung, C. (1989). Ion Channels of Unicellular Microbes. In: <u>Evolution of the First Nervous Systems</u>, Ed: P.A.V. Anderson, Plenum Press, New York, NY, pp. 203-214.
- Lewis, R.S. & Hudspeth, A.J. (1983). Voltage- and iondependent conductances in solitary vertebrate hair cells. <u>Nature</u> 304:538-541.
- Lisman, J., Fain, G. & Swan, M. (1978). Voltage-dependent conductance in <u>Limulus</u> ventral photoreceptors.

 <u>Biological Bulletin</u> 155:453-454.
- Machemer, H. & Ogura, A. (1979). Ionic conductances of membranes in ciliated and deciliated <u>Paramecium</u>. <u>Journal of Physiology</u> 296:49-60.
- Marchetti, C., Premont, R.T. & Brown, A.M. (1988). A whole-cell and single-channel study of the voltage-dependent outward potassium current in avian hepatocytes.

 Journal of General Physiology 91:255-274.
- Matsuda, J.J., Volk, K.A. & Shibata, E.F. (1990). Calcium currents in isolated rabbit coronary arterial smooth muscle myocytes. <u>Journal of Physiology</u> 427:657-680.
- Mayer, M.L. & Sugiyama, K. (1988). A modulatory action of divalent cations on transient outward current in cultured sensory neurons. <u>Journal of Physiology</u> 396:417-433.
- Meech, R.W. (1989). The Electrophysiology of Swimming in the Jellyfish <u>Aglantha digitale</u>. In: <u>Evolution of the First Nervous Systems</u>, Ed: P.A.V. Anderson, Plenum Press, New York, NY, pp. 281-298.
- Mirolli, M. (1981). Fast inward and outward current channels in a non-spiking neurone. Nature 292:251-253.
- Neher, E. (1971). Two transient current components during voltage clamp in snail neurons. <u>Journal of General Physiology</u> 61:385-399.
- Numann, R.E., Wadman, W.J. & Wong, R.K.S. (1987). Outward currents of single hippocampal cells obtained from the adult quinea-pig. <u>Journal of Physiology</u> 393:331-353.
- Ohya, Y., Kitamura, K. & Kuriyama, H. (1988). Regulation of calcium current by intracellular calcium in smooth muscle cells of rabbit portal vein. <u>Circulation</u>
 <u>Research</u> 62:375-383.

- Ohya, Y., Terada, K., Kitamura, K. & Kuriyama, H. (1986).

 Membrane currents recorded from a fragment of rabbit intestinal smooth muscle cell. American Journal of Physiology 251:C335-C346.
- Okabe, K., Kitamura, K. & Kuriyama, H. (1987). Features of a 4-aminopyridine sensitive outward current observed in single smooth muscle cells from the rabbit pulmonary artery. Pfluger's Archives 409:561-568.
- Osa, T. (1974). Effects of tetraethylammonium on the electrical activity of pregnant mouse mymetrium and the interaction with manganese and cadmium. <u>Japanese Journal of Physiology</u> 24:119-133.
- Pax, R.A. & Bennett, J.L. (1992). Neurobiology of parasitic flatworms: How much "neuro" in the biology? <u>Journal of Parasitology</u> 78:194-205.
- Pax, R.A., Siefker, C., Hickox, T. & Bennett, J.L. (1981).

 <u>Schistosoma mansoni</u>: Neurotransmitters, longitudinal musculature and effects of electrical stimulation.

 <u>Experimental Parasitology</u> 52:346-355.
- Pax, R.A., Bricker, C.S., Thompson, D.P., Semeyn, D.R. & Bennett, J.L. (1983). Neurophysiology of adult male Schistosoma mansoni. Pharmacology and Therapeutics 22:117-125.
- Quinta-Ferreira, M.E., Rojas, N. & Arispe, N. (1982).

 Potassium currents in the giant axon of the crab

 <u>Carcinus maenus</u>. <u>Journal of Membrane Biology</u> 66:171181.
- Rudy, B. (1988). Diversity and ubiquity of K+ channels. Neuroscience 25:729-749.
- Salkoff, L.B. & Wyman, R.J. (1983). Ion currents in <u>Drosophila</u> flight muscles. <u>Journal of Physiology</u> 337:687-709.
- Satow, Y. & Kung, C. (1980). Membrane currents of pawn mutants of the PWA group in <u>Paramecium tetraurelia</u>. <u>Journal of Experimental Biology</u> 84:57-71.
- Segal, M. & Barker, J.L. (1984). Rat hippocampal neurones in culture potassium conductances. <u>Journal of Neurophysiology</u> 51:1409-1433.

- Segal, M., Rogawski, M.A. & Barker, J.L. (1984). A transient potassium conductance regulates the excitability of cultured hippocampal and spinal neurons. <u>The Journal of Neuroscience</u> 4:604-609.
- Shibaski, T. (1987). Conductance and kinetics of delayed rectifier potassium channels in nodal cells of the heart. <u>Journal of Physiology</u> 387:227-250.
- Silk, M.H. & Spence, I.M. (1969a). Ultrastructural studies of the blood fluke <u>Schistosoma mansoni</u>. II. The musculature. <u>South African Journal of Medical Science</u> 34:11-20.
- Silk, M.H. & Spence, I.M. (1969b). Ultrastructural studies of the blood fluke <u>Schistosoma mansoni</u>. III. The nerve tissue and sensory structures. <u>South African Journal of Medical Science</u> 34:93-104.
- Simmons, M.A., Creazzo, T. & Hartzell, H.C. (1986). A time-dependent and voltage-sensitive K+ current in single cells from frog atrium. <u>Journal of General Physiology</u> 88:739-755.
- Singer, J.J. & Walsh, J.V. (1980). PAssive properties of the membrane of single freshly isolated smooth muscle cells. American Journal of Physiology 239:C153-C161.
- Solc, C.K., Zagotta, W.N. & Aldrich, R.W. (1987). Single channel and genetic analyses reveal two distinct Atype potassium channels in <u>Drosophila</u>. <u>Science</u> 236:1094-1098.
- Stein, P. & Palade, P. (1989). Patch clamp of sarcolemmal spheres from stretched skeletal muscle fibers.

 <u>American Journal of Physiology</u> 256:C434-440.
- Strong, J.A. & Kaczmarek, L.K. (1985). Multiple components of delayed potassium current in peptidergic neurons of <a href="https://doi.org/10.1001/nj.nc.1
- Sukhdeo, M. (1992). The behavior of parasitic flatworms in vivo: What is the role of the brain? <u>Journal of Parasitology</u> 78:231-242.
- Sukhdeo, M. & Mettrick, D.F. (1987). Parasite behavior: Understanding platyhelminth responses. <u>Advances in Parasitology</u> 26:73-144.

- Suzuki, H., Nishiyama, A. & Inomata, H. (1963). Effect of tetraethylammonium ion on the electrical activity of smooth muscle cells. Nature 197:908-909.
- Tachibana, M. (1983). Ionic currents of solitary horizontal cells isolated from goldfish retina. <u>Journal of Physiology</u> 345:329-351.
- Thompson, D.P., Pax, R.A. & Bennett, J.L. (1982).

 Microelectrode studies of the tegument and subtegumental compartments of male <u>Schistosoma mansoni</u>: an analysis of electrophysiological properties.

 Parasitology 85:163-178.
- Thompson, S.H. (1977). Three pharmacologically distinct potassium channels in molluscan neurones. <u>Journal of Physiology</u> 265:465-488.
- Tomosky, T., Bennett, J.L. & Bueding, E. (1974).
 Tryptaminergic and dopaminergic responses of
 Schistosoma mansoni. The Journal of Pharmacology and
 Experimental Therapeutics 190:260-271.
- Utroska, J.A., Chen, M.G., Dixon, H., Yoon, S., Helling-Borda, M., Hogerzeil, H.V. & Mott, K.E. (1989). An estimate of global needs for praziquantel within schistosomiasis control programmes. World Health Organization document WHO/SCHISTO/89.102.
- Walsh, J.V. & Singer, J.J. (1987). Identification and characterization of major ionic currents in isolated smooth muscle cells using the voltage-clamp technique. Pfluger's Archives 408:83-97.
- Webb, R.A. (1987). Innervation of muscle in the cestode <u>Hymenolpis</u> <u>microstoma</u>. <u>Canadian Journal of Zoology</u> 65:928-935.
- Williams, J.T., North, R.A., Shefner, S.A., Nishi, S. & Egan, T.M. (1984). Membrane properties of rat locus coeruleus neurons. Neuroscience 13:137-156.
- Wood, D.C. (1982). Membrane permeabilities during resting, action and mechanoreceptor potentials in <u>Stentor</u> coeruleus. <u>Journal of Comparative Physiology</u> 146:537-540.
- Wu, C.F. & Haugland, F.N. (1985). Voltage-clamp analysis of membrane currents in larval muscle fibers of Drosophila: Alteration of potassium currents in Shaker mutants. The Journal of Neuroscience 5:2626-2640.

- Yamamoto, Y., Hu, S.L. & Kao, C.Y. (1989). Outward current in single smooth muscle cells of the guinea pig taenia coli. <u>Journal of General Physiology</u> 93:551-564.
- Yatani, A., Seidel, C.L., Allen, J. & Brown, A.M. (1987). Whole-cell and single-channel calcium currents of isolated smooth muscle cells from saphenous vein. Circulation Research 60:523-533.
- Ypey, D.L. & Clapham, D.E. (1984). Development of a delayed outward-rectifying K⁺ conductance in cultured mouse peritoneal macrophages. <u>Proceedings of the National</u> Academy of Science, USA 81:3083-3087.
- Zbicz, K.L. & Weight, F.F. (1985). Transient voltage and calcium-dependent outward currents in hippocampal CA3 pyramidal neurons. <u>Journal of Neurophysiology</u> 53:1038-1058.